1985

Electric Choremaster I : Test Procedures and Results

Bryan P. Thoreson

ELECTRIC CHOREMASTER I:

TEST PROCEDURES AND RESULTS

BY

BRYAN P. THORESON

A thesis submitted
in partial fulfillment of the requirements for the
degree Master of Science, Major in Agricultural
Engineering, South Dakota State University
1985

ELECTRIC CHOREMASTER I:

TEST PROCEDURES AND RESULTS

This thesis is approved as a creditable and independent investigation by a candidate for the degree, Master of Science, and is acceptable for meeting the thesis requirements for this degree. Acceptance of this thesis does not imply that the conclusions reached by the candidate are necessarily the conclusions of the major department.

Thesis Advisor Date

Major Advisor Date

Head of Major Department Date

ACKNOWLEDGEMENTS

The author wishes to thank Dr. Les Christianson, Mr. Ralph Alcock, and Dr. Don Froehlich for their technical assistance, advice, and encouragement during this study. Appreciation is extended to Dr. Mylo Hellickson, department head, the entire Agricultural Engineering Department, and fellow graduate students for their assistance and cooperation during this research.

The National Rural Electric Cooperative Association and the South Dakota State University Experiment Station support and funding for this project is greatly appreciated. Special thanks go to Dr. Lee Tucker for his help with the statistical analysis of results, and Mr. Wayne Knabach for his help with instrumentation for the capacity and charger tests. The assistance provided by Terry Healy during testing was appreciated.

Finally, gratitude is expressed to the author's family and friends for their support, patience, and encouragement throughout this candidacy.

BPT

TABLE OF CONTENTS

LIST OF TABLES

LIST OF ILLUSTRATIONS

INTRODUCTION

Development of test procedures and the accumulation of test data are essential for the proper design of agricultural electric vehicles (EVs). Electric Chore-master I (EC-I) is a research prototype that applies the advantages of EV technology to farm chore tasks. Design and construction of this tractor were completed in June 1984 (Vik, 1985). Life-cycle economic savings plus demonstrated EV advantages of low noise, absence of noxious fumes and ease of starting were expected to favor EVs for farm chore tasks.

Many battery-powered vehicles were in use at the beginning of this century. However, due to their limited range, they were replaced by internal-combustion engine vehicles for all but specialized applications. The energy crisis in the 1970s rekindled public interest in general-purpose EVs. Although that public interest has waned in the wake of the present "oil glut", the quantity and diversity of EVs sold has grown as industries capitalize on the advantages of such vehicles for specialty applications. Continued expansion of EV use would help reduce the vulnerability of the United States to another

energy crisis. Similarly, electric tractor development would help reduce the vulnerability of agriculture to a sudden slowdown or interruption of oil supplies.

The Department of Energy sponsored studies at several land-grant universities to determine the feasibility of battery-powered tractors. The results of a study at South Dakota State University (SDSU) indicated that an electric tractor could do many chore tasks on North Central United States farms (Resen, et al., 1981). Low battery energy densities relative to liquid fuel energy densities limit EVs for field work, but these researchers determined that this would not be a limiting factor for specialized chore work. Less noise, no fumes and lower repair cost were cited as advantages.

The National Rural Electric Cooperative Association (NRECA) and the SDSU Agricultural Experiment Station financed the conversion of a four-wheel drive, articulated diesel tractor to battery-power, which resulted in the EC-I. The first prototype was designed and built, but the limited availability of design information to size the EV components meant that testing was crucial to evaluate component sizing. Extensive testing of the prototype was, therefore, necessary to obtain important information to help design future electric tractors. Testing provided a more exact method of predicting energy use to help size

batteries and motors for specific agricultural tasks. The main goal of testing was to determine the operating characteristics of the prototype EC-I, thereby, providing information for design improvements and for design of future agricultural EVs. The following four objectives were defined to achieve this goal:

1. Devise a test procedure to quantify battery-powered farm tractor performance.

2. Determine power take-off (pto) and drawbar power maximums and related operating characteristics.

3. Develop a model that calculates EC-I energy use for farm chore tasks by summing the predicted energy requirements for standard task segments, and evaluate the model using an independent data set.

4. Recommend design improvements for the EC-I prototype.

LITERATURE REVIEW

Electric Vehicle Feasibiltiy

Nonagricultural Feasibility

Electric vehicles have existed in specialized applications throughout this century in both the United States and Europe. Examples of these specialized applications include: forklifts, mine vehicles, aircraft tow vehicles, delivery vans and trucks, golf carts, personnel carriers, lawn and garden tractors and feed carts. Electric vehicles have flourished in these applications due to their lower life-cycle cost and lack of noise and toxic fumes (Christianson, et al., 1985).

Most manufacturers have directed their efforts to specialty applications for EVs, since limited range, sluggish performance and high purchase price restrict acceptance of electric road vehicles. EVs have been used as delivery vans and in commercial fleets in Europe, and research examining these EV applications is being conducted in the United States. Due to the limited daily travel required, these applications are within present EV capabilities. Berg, et al., (1984) surveyed commercial fleet operators and found that 3.3 million vehicles were

driven less than 60 miles per day. These vehicles could be replaced by electric vans designed with technology available today and be economically competitive on a life-cycle basis (Hamilton and Bevilacqua, 1985). The Electric Power Research Institute (EPRI) and the Electric Vehicle Development Corporation (EVDC) have assessed commercial fleet EV applications and are developing an EV introduction strategy (Kalhammer, et al., 1984). Past research and field data demonstrate that EVs can be technically and economically competitive with internal-combustion engine vehicles for specialty applications.

Agricultural Feasibility

Agricultural chore and utility work are specialized applications with duty cycles similar to other successful EV applications and, therefore, could be technically and economically suitable for EVs. The Department of Energy funded regional feasibility studies to determine, if electric tractors could substitute for petroleum powered vehicles in agricultural applications. Alcock, et al. (1981) determined that an electric tractor could be used in existing farm patterns in New Jersey to reduce on-farm energy use. The same study demonstrated that electric tractors could assume light field and

hauling tasks on Virginia farms and reduce tractor energy consumption by 13 percent. Resen, et al. (1981) concluded that: (1) battery-powered vehicles are technically feasible for farm use in the North Central region, (2) electric tractors are more feasible on 200 to 1000 acre farms than on larger farms and (3) electric tractor potential use is affected by farm operation type. Alcock (1983) developed a computer model to study the design and field performance of a battery-powered tractor and found this tractor to be best suited for materials carrying and light cultivation tasks. Available battery energy densities of 0.03 kilowatt/kilogram (kW/kg) limited the range of the tractor, thereby, limiting its potential for heavy field work.

Studies have indicated that EVs are economically competitive with diesel tractors for farm applications. Considering battery replacement as an energy cost, a battery-powered tractor saved 11 percent as compared to a diesel tractor (Table 1). Christianson, et al. (1985) estimated the annual cost of electric tractors to be 11 percent less than diesel tractors by assuming vehicle life and maintenance cost differences to be comparable to those documented for diesel and electric forklifts (Table 2).

Table 1. Energy cost comparison between electric farm tractors and equivalent-sized diesel tractors (Christianson, et al., 1985).

	Electric		Diesel
	Direct[1]	Battery-powered	
Energy cost/unit	$.10/kWh[2]	$.05/kWh[2]	$.30/liter
Efficiency at part-load, stop-and-go conditions	77%	33%	10%
Energy cost/useful output at vehicle axles	$.13/kWh	$.15/kWh	$.28/kWh
Battery replacement cost/useful output at vehicle axles ($150/kWh initial cost and 1500 cycle life)		$.10/kWh	
Vehicle energy operating cost/unit useful output at vehicle axles	$.13/kWh	$.25/kWh	$.28/kWh

[1]Direct-power EVs have the electrical energy transmitted through some type of cord arrangement to the motor while the vehicle is moving. Examples include cord-type electric lawnmowers, electric trains, electric rail-type buses and electrically driven center-pivot irrigators.

[2]These electric energy costs assume that the direct-powered vehicle is operated using on-peak electrical energy at $.10/kWh while the battery-powered vehicle is charged using off-peak electrical energy at $.05/kWh.

Table 2. Life-cycle analysis of electric versus conventional farm tractors (Christianson, et al., 1985).

	Electric		Diesel
	Direct[1]	Battery-powered	
Initial costs of a 60 kW, 4 WD equivalent tractor (1984 in United States)	$40,000	$50,000[2]	$40,000
Expected vehicle life	10 years	10 years	7 years
Annual ownership costs at 10% interest	$ 6,525	$ 8,150	$ 8,290
Annual energy costs with 7500 kWh energy available at axles	$ 975	$ 1,875	$ 2,100
Annual maintenance and repair costs	$ 6,000	$ 4,500	$ 6,000
Total annual costs	$13,500	$14,525	$16,390

[1]Direct-power EVs have the electrical energy transmitted through some type of cord arrangement to the motor while the vehicle is moving. Examples include cord-type electric lawnmowers, electric trains, electric rail-type buses and electrically driven center-pivot irrigators.

[2]The battery costs associated with this vehicle are included in the energy costs (table 1) because batteries are a replaceable item with an expected life less than that of the tractor.

These studies indicate that an electric tractor is technically and economically feasible for specialized chore and utility agricultural tasks. This vehicle could do limited duration field work in emergencies, but would not be suited for continuous heavy field work with currently available industrial, lead-acid batteries.

Electric Choremaster I Design

A battery-powered tractor was designed and built at SDSU with funding from NRECA and the SDSU Agricultural Experiment Station. A four-wheel drive, articulated frame, diesel tractor was converted to battery power. An industrial, lead-acid storage battery powers a 36-kW direct current (dc) motor that drives the wheels, and a 17-kW dc motor that drives the pto and hydraulic pump. EC-I utilizes the original diesel tractor power train and hydraulic system.

Initial comparative testing indicated 57 to 67 percent energy savings for the electric version (Vik, 1985). EC-I performance of farm chores demonstrated a need for better speed control of the pto and hydraulics motor (Helder, 1985). The noise level of the electric version was 62 decibels contrasted with 80 to 90 decibels

for typical diesel tractors (Latif, 1985). These studies describe vehicle advantages and note some design problems for further investigation.

Electric Vehicle Testing

Electric vehicle testing can be divided into two main areas: (1) component testing and (2) vehicle testing. Many researchers (Carter and Todd, 1983; Blickwedel and Hand, 1983; Popeck, et al., 1983; Bish and Tietmeyer, 1983 and Fenton and Olsen, 1983) used periodic component tests as part of a vehicle testing program to help explain changes in vehicle performance. A comprehensive test plan which included safety evaluations, charger tests, battery capacity tests and vehicle performance dynamometer, track and road tests was developed by EPRI and the Tennessee Valley Authority (TVA) (Carter and Todd, 1983).

Component Testing

"Propulsion battery performance is the single largest variable in EV testing", according to Marte and Bryant (1983) from the Jet Propulsion Laboratory (JPL). Capacity tests at a constant rate of discharge and life-cycle tests are the two main types of battery tests.

EPRI/TVA discharged batteries at a constant current of 50 or 75 amperes (A) until the battery pack voltage dropped below 1.75 volts per cell to determine capacity (Carter and Todd, 1983). Fenton and Olsen (1983) from Detroit Edison determined battery capacity by discharging at a constant current of 75 A until any group of six cells reached a voltage of 1.75 volts per cell. These researchers measured load current, battery terminal voltage, voltage of groups of four to six cells, electrolyte temperature and time of discharge. The National Electrical Manufacturers Association (NEMA) Standard IB-2 (1974) recommends a discharge rate in amperes (held within one percent) equal to one-sixth of the battery six-hour capacity rating, which is terminated when the battery pack voltage reaches 1.70 volts per cell. The National Battery Testing Laboratory (NBTL) at Argonne National Laboratory (ANL) discharged lead-acid batteries at the rate recommended by the manufacturer until an endpoint of 1.75 volts per cell was reached (Hornstra and Yao, 1982). The average capacity from three discharges was reported as the battery capacity.

The EC-I battery capacity test results should show a capacity near the published specifications of 340

ampere-hours (Ah)[1] and 42 kilowatt-hours (kWh). Data provided by General Battery Corporation (GBC, 1980) illustrated the accelerating decline in terminal voltage and linear declines in specific gravity and ampere-hours discharged over time for the capacity test. Vincent, et al. (1984), and Unnewehr and Nasar (1982), conducted discharge tests that showed similar accelerating declines in terminal voltage over time of discharge. Marsh (1981) discussed results that showed the electrolyte temperature would slowly rise about seven degrees Celsius (C) over a complete discharge, which began at ambient temperature.

Vivian and Bryant (1984) conducted tests to evaluate charger performance at different initial battery depth-of-discharge (DOD) and electrolyte temperature. They recommended that charge algorithms for lead-acid batteries compensate for battery temperature to prevent over- or under-charging. Battery terminal voltage, charging current and temperature were measured at three locations during tests and charger operation time and alternating current (ac) power required were recorded. Power and energy input to the charger were measured by Reese (1983). Additionally, the root mean square (rms) value, the rms

---

[1] An ampere-hour is a measure of the volume of electricity, equal to one ampere for one hour, or 3600 coulombs. It is used to express battery capacity (GBC, 1980).

value of the first 25 harmonics, the phase angle of the harmonics and the waveform of ac voltage and current were measured. Average and waveform values of voltage, current, ampere-hours, power and energy output by the charger were also recorded.

Researchers have documented the change in some battery parameters while the battery is on-charge. Results from Hornstra (1985) and GBC (1980) showed an increase in battery terminal voltage and specific gravity and a linear increase of electrolyte temperature and ampere-hours returned to the battery with time. Typical battery energy efficiencies reported were 75 percent (Marsh, 1981 and GBC, 1980). The charger manufacturer indicated the charger would be about 85 to 90 percent efficient (Schober, 1984). Reese (1983) reported data that showed 25 harmonics were behind the ac voltage and current waveforms for a Philips charger, and that an ac ripple was behind the dc current and voltage to the battery. Little information is available in the literature on the ferro-resonant type of charger used to charge the EC-I battery.

Battery life-cycle test results were needed to accurately predict the life-cycle cost of EC-I and determine if capacity changes during cycling for these tests would affect test results. Conducting a life-cycle test on the EC-I battery was impractical due to time

considerations and the demise of the battery at the end of the test, consequently battery life was estimated from the literature. Industrial storage batteries are designed to last about 2000 operation/charge cycles (GBC, 1980). The battery in EC-I has a three year guarantee for one cycle per 24 hours, or 1095 cycles (Miller, 1984).

The battery manufacturer determines cycle life by randomly selecting a few cells from production, and discharging at the four-hour rate for a series of cycles (NEMA, 1983). Every 100 cycles, the battery capacity is checked (NEMA, 1974), and if the battery fails to reach 80 percent of rated capacity in one of two tests the number of this discharge cycle is recorded as the battery life (NEMA, 1983). Little information is available in the literature about industrial storage batteries (examples include forklift and mining vehicle batteries), because attention has been focused on traction batteries (examples include golf cart and electric car batteries) for EV application. Ponsford (1979) and Vincent (1984) indicated that industrial batteries have more life cycles (about 1500) but a lower energy density compared to EV traction batteries. Ponsford (1979), Ewashinka (1984) and Perone and Spindler (1984) have all conducted life cycle tests on EV traction batteries. It is difficult to compare the results of these tests because each researcher cycled

different batteries in a slightly different manner and used different end of life criteria. Based on this information, one thousand cycles for EC-I battery life would be a conservative estimate. Since approximately 35 cycles immediately following the battery break-in cycles were envisioned for this testing, capacity changes during testing were assumed to be negliglible.

Vehicle Testing

Bryant (1983) from JPL recommended two test types for EVs: (1) engineering and (2) "how people drive". Engineering tests can be subdivided into dynamometer and track tests (Marte and Bryant, 1983). Marte and Bryant (1983) believe dynamometer testing is best because of its repeatability and have developed a method of correlating dynamometer test results to track test results. Fenton and Olsen (1983) also conducted their vehicle tests on a dynamometer. Carter and Todd (1983) from EPRI/TVA conducted most of their vehicle testing on an oval test track. The Society of Automotive Engineers (SAE, 1976) Recommended Practice J227a specifies road tests for EVs. Nowak (1981) and Menga, et al. (1981) used road tests to determine EV performance.

The main advantage of dynamometer and track tests is their repeatability under controlled test conditions, compared to the advantage of road tests, which is obtaining vehicle performance results under actual operating conditions. Although these researchers disagreed on the best test method, they all measured vehicle speed, battery current, battery voltage and battery energy discharged as functions of time.

These researchers used either a digital data acquisition system or strip chart recorders to record data during tests. Menga, et al. (1981) and Blom, et al. (1981) powered the instrumentation system with a 12-volt (V) deep-cycle battery. Blom, et al. (1981) sampled data every second during tests, while Marte and Bryant (1981) from JPL sampled data as fast as the system capability allowed for a short time interval during tests and at a slower rate for the remainder of the test. Instrumentation used included shunts, voltage dividers and strain gages (Menga, et al., 1981), Hall-effect transducers (Carter and Todd, 1983 and Blom, et al., 1981) and a fifth wheel (Carter and Todd, 1983 and SAE, 1976). To obtain a certain percent battery DOD, the following equation was used (SAE, 1976):

$$DOD=(ED/EA)*100$$

where: DOD=depth-of-discharge, percent
ED=energy discharged at a specified rate, kWh
EA=total energy available (capacity) at a specified rate, kWh

Other methods used to define DOD include cell voltage and specific gravity measurements (GBC, 1980). The effects of DOD are investigated with the batteries 0, 40 and 80 percent discharged (SAE, 1976). Fenton and Olsen (1983) conducted acceleration tests at 0, 20, 40, 60 and 80 percent battery DOD to determine the effect of DOD on acceleration. The SAE J227a C and D cycles are the predominant test cycles used, but the Federal Urban Driving Schedule (FUDS) has been used as a cycle by some researchers (Fenton and Olsen, 1983). Military Standard MIL-STD-268C (USDOD, 1963) has been used to test electric forklifts. Although this information was helpful in designing an instrumentation system, choosing what parameters to measure and developing test cycles; these tests were not developed to quantify and evaluate tractor performance.

Agricultural tractor testing differs from EV testing because the maximum pto and drawbar power is as

important as the vehicle range. The American Society of Agricultural Engineers (ASAE) Standard 209.5 (1985) provides a standardized, repeatable method of measuring the performance of conventional tractors. This standard also describes test procedures to determine fuel consumption at maximum and varying pto and drawbar power. Pto power tests are conducted at the standard pto speed of 540 revolutions per minute (r/min), and drawbar power tests are conducted at selected speeds for each tractor. A concrete or bituminous surface, a minimum of 91 meters (m) in length with an approach of 15 m, is recommended for drawbar power tests.

Tests following this procedure are performed at the Nebraska tractor test facility in Lincoln, Nebraska. This facility uses the engine of a specially modified tractor as a compressor to provide the load for draft tests (Leviticus, 1985). Firestone uses a large tractor throttled back as the load during traction tests, in other words, the load is the braking power of the engine (Brodbeck, 1985).

Stange, et al. (1982); Grevis-James, et al. (1983); Tompkins and Wilhelm (1982) and Green, et al. (1983) are a few of the many researchers that have developed tractor instrumentation systems. These systems were tailored to meet each researcher's specific

objectives and used data acquisition equipment to record data and either a 12-volt battery or a portable generator to power the instrumentation. Drawbar pull was measured by a strain gage dynamometer, and speed was measured by a radar transducer or by counting revolutions of either the front wheel or a fifth wheel. Tompkins, et al. (1985) compared the performance of these three speed measurement techniques and concluded that radar was the most accurate for all speeds and surfaces, except vegetative cover. Other parameters were measured as required by each researcher.

Stange, et al. (1982) described the basic instrumentation package used to record pto and drawbar power data for these tests. Modifications and additions to the basic package will be noted and described in the test procedure section.

Some trends for the results can be described based on the EV and tractor testing other researchers have completed. Due to the current limit set by the motor controls (Helder, 1985), EC-I was expected to have a reduced maximum power output at low state-of-charge (SoC) (or high DOD) because of lower battery terminal voltage. EV acceleration, or maximum power available, was reduced at low SoC (Fenton and Olsen, 1983). However, at low power levels, performance was not affected by SoC (JPL, 1981 and

Von Courbiere and Klein, 1983). This was supported by initial EC-I test results (Vik, 1985). EC-I was expected to provide maximum power for short durations above the rated power of the vehicle because of series-wound dc electric motor operating characteristics. During constant draft tests on asphalt, the draft was expected to vary plus or minus one percent from the average (Sampson, 1985), compared to plus or minus 50 to 100 percent from the average on dirt (Stange, et al., 1982 and Bandy, et al., 1985). These results highlight some of the inherent differences between an electric tractor and a diesel tractor, such as higher than rated power for short durations and lower maximum power at low SoC.

Agriculture Electric Vehicle Energy Use Model

Researchers have developed EV range and performance models based on: (1) measured test data and (2) theoretical concepts. Many EV models have been developed using analytical methods to predict on-road performance (Unnewehr and Nasar, 1982). Most models of this type were developed by combining analytical models of individual components to predict range or acceleration. Other models used component test data rather than analytical methods to predict performance.

Alcock (1983) developed a model that predicted energy requirements for battery-powered vehicles to perform field tasks. This computer model was based on traction theory, and the results suggested that a battery-powered vehicle would be unsuitable for heavy field work.

Booth (1977) recommended that models be partitioned into subsystems and asserted that it is essential that the model be evaluated with data other than that used to develop it. A model that predicts energy use by dividing each task into standard segments such as accelerating a load to a constant speed, pulling a load at a constant speed and deccelerating a load, has not been developed for agricultural work. The proposed model will utilize test results to develop empirical equations to predict energy use for each segment of a task. Predicted energy use for each segment of the task is then summed to obtain a predicted energy use for the entire task. Energy required for many tasks could be predicted by developing multiple regression equations for a few standard segments.

The model will be examined using a second data set, collected after developing the prediction equations, to predict energy use for a few tasks. The actual energy use will be compared to the predicted energy use. This model will enable designers to size components by predicting the energy required for an electric tractor to

perform required tasks. Valuable information on chore task requirements will be provided by this model, because although power and energy requirements for field tasks have been documented (ASAE Yearbook, 1985 and Hunt, 1977), requirements for chore tasks are not well defined.

Agriculture Electric Vehicle Management

Three parameters that influence battery capacity are: (1) the rate of discharge, (2) the battery temperature and (3) previous DOD. A common method of representing the effect of rate of discharge on capacity, or the tradeoff between power and energy, is the Ragone plot of specific power versus specific energy. Data supplied by the battery manufacturer (Miller, 1984) were used to develop a Ragone plot for the battery in EC-I, which shows that when the usable energy capacity decreases by 25 percent the rate of discharge doubles (Figure 1). Giese and Walsh (1983) and Unnewehr and Nasar (1982) documented this relationship for other lead-acid batteries. The industrial storage battery used in EC-I has lower specific power and specific energy compared to traction lead-acid batteries because of its heavier construction. The Ragone plot illustrates how the energy available in a battery decreases as the power output of a battery increases.

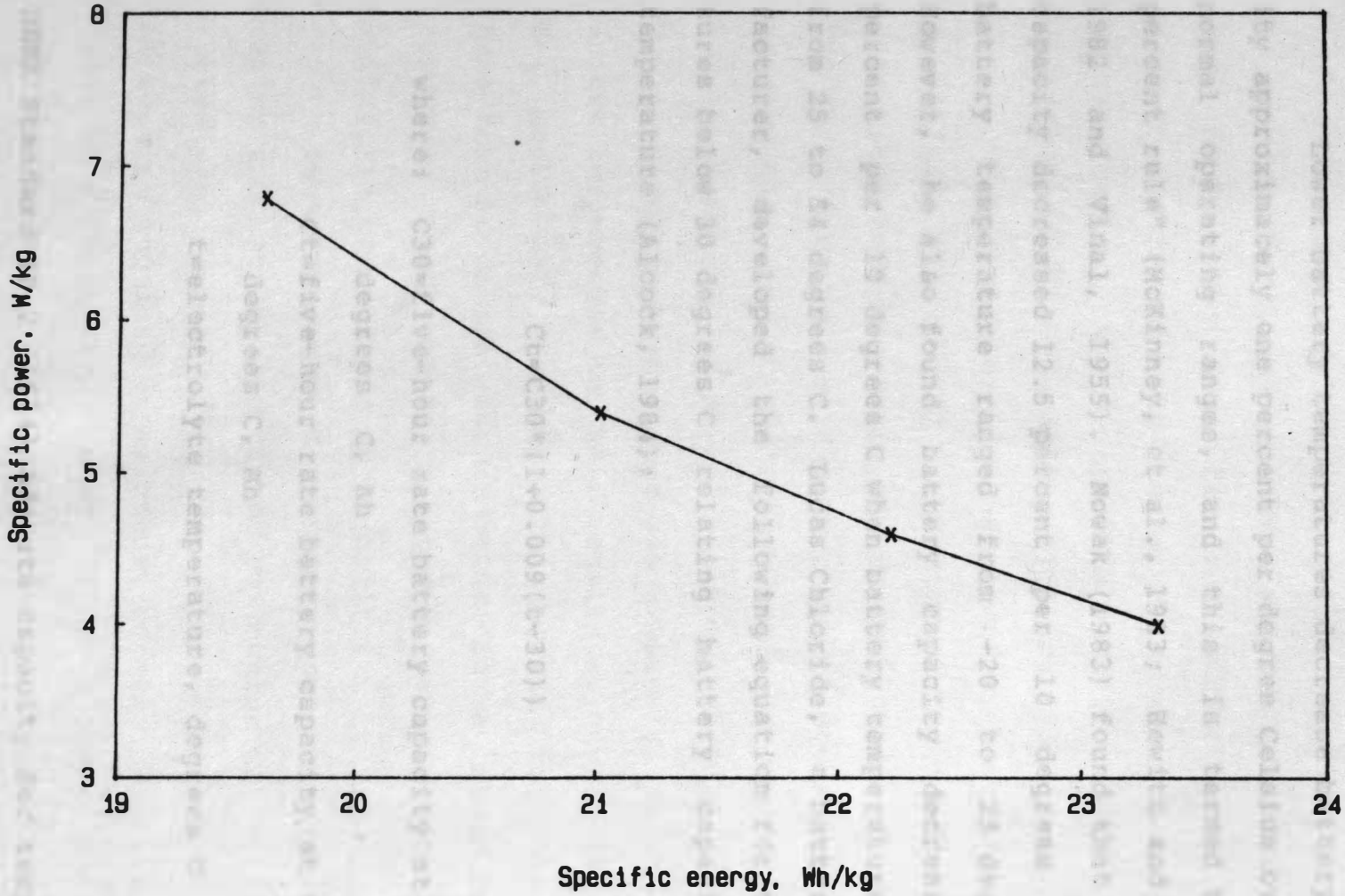

Figure 1. Ragone plot of EC-I battery.

Lower battery temperatures decrease battery capacity approximately one percent per degree Celsius over the normal operating ranges, and this is termed the "one percent rule" (McKinney, et al., 1983; Hewitt and Bryant, 1982 and Vinal, 1955). Nowak (1983) found that battery capacity decreased 12.5 percent per 10 degrees C when battery temperature ranged from -20 to 25 degrees C. However, he also found battery capacity decreased 4.1 percent per 10 degrees C when battery temperature ranged from 25 to 54 degrees C. Lucas Chloride, a battery manufacturer, developed the following equation for temperatures below 30 degrees C relating battery capacity and temperature (Alcock, 1984):

$$Ct=C30*(1+0.009(t-30))$$

where: C30=five-hour rate battery capacity at 30 degrees C, Ah

Ct=five-hour rate battery capacity at t degrees C, Ah

t=electrolyte temperature, degrees C

NEMA Standard IB-2 (1974) adjusts capacity for temperature changes (degrees Fahrenheit) with an equation of the same

form as the Lucas Chloride equation. Similar information was provided by the manufacturer about the EC-I battery (GBC, 1980). The data from the manufacturer, the "one percent rule" and the Lucas Chloride equation yield similar curves, while the NEMA equation shows a smaller capacity loss with temperature (Figure 2).

These relationships were used to estimate that on an extreme winter day (-30 degrees C) the EC-I battery would have about one-half of normal capacity available (170 Ah). Even on a mild winter day in South Dakota (zero degrees C), the EC-I battery would be expected to have only three-fourths of normal capacity available (225 Ah). The electrolyte temperature was assumed to be the same as ambient temperature in this analysis. This means that EC-I would only be able to operate for one-half to three-fourths of its normal time in a chore routine, indicating the need for management practices to keep the electrolyte temperature above ambient.

These management practices include insulating and heating the battery and timing the charge to utilize the electrolyte temperature rise during charging as part of the heating required to maintain normal capacity. Nowak (1983) concluded that most of the capacity loss at low temperatures was due to poor charge acceptance of the

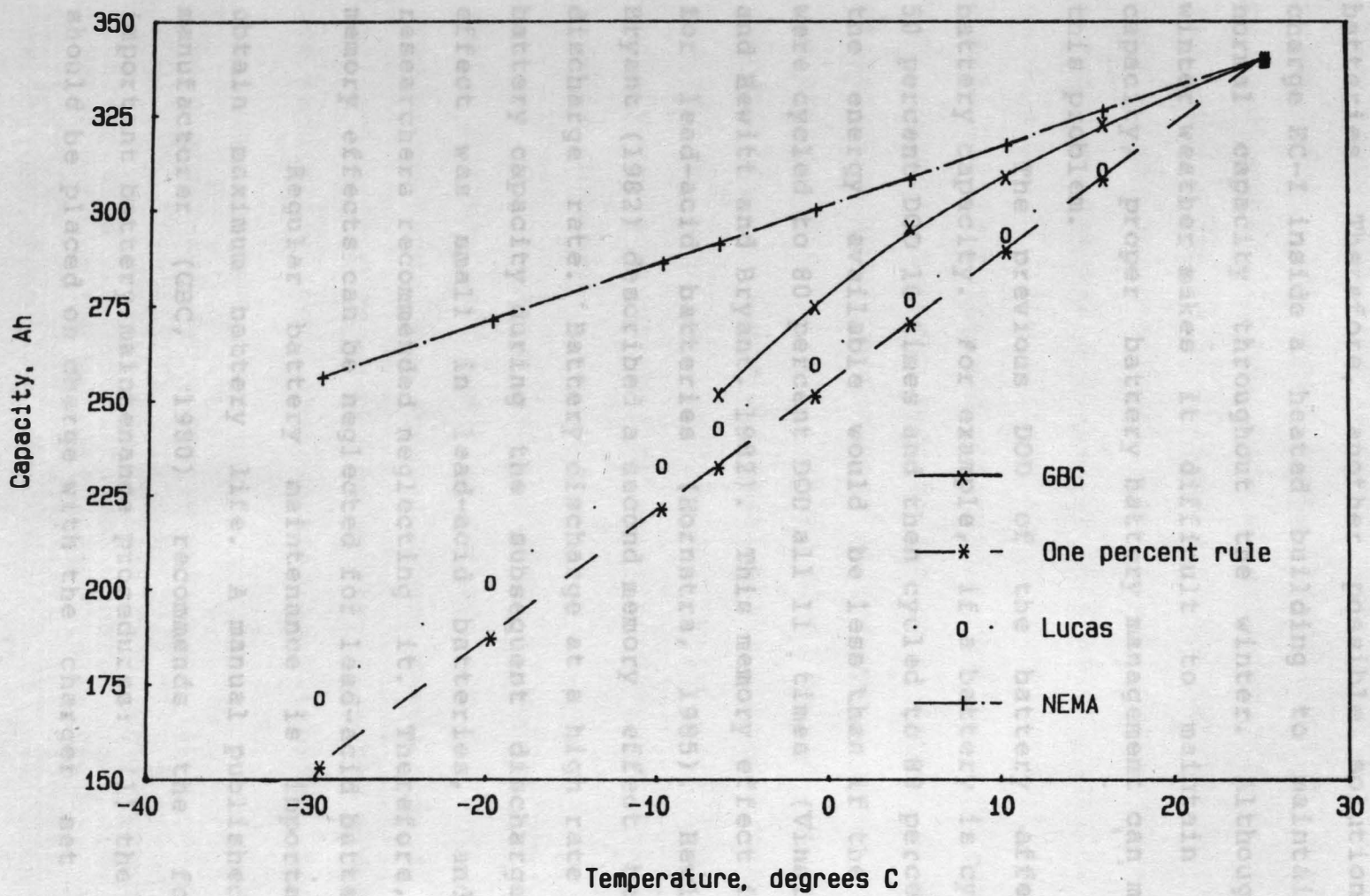

Figure 2. Comparison of capacity versus temperature relations.

batteries. Therefore, another possible solution is to charge EC-I inside a heated building to maintain near normal capacity throughout the winter. Although cold winter weather makes it difficult to maintain battery capacity, proper battery battery management can minimize this problem.

The previous DOD of the battery affects the battery capacity. For example, if a battery is cycled to 50 percent DOD 10 times and then cycled to 80 percent DOD, the energy available would be less than if the battery were cycled to 80 percent DOD all 11 times (Vinal, 1955 and Hewitt and Bryant, 1982). This memory effect is small for lead-acid batteries (Hornstra, 1985). Hewitt and Bryant (1982) described a second memory effect based on discharge rate. Battery discharge at a high rate impairs battery capacity during the subsequent discharge. This effect was small in lead-acid batteries, and these researchers recommended neglecting it. Therefore, these memory effects can be neglected for lead-acid batteries.

Regular battery maintenance is important to obtain maximum battery life. A manual published by the manufacturer (GBC, 1980) recommends the following important battery maintenance procedures: (1) the battery should be placed on charge with the charger set to the

daily charge position[1] whenever the specific gravity falls below 1.230, (2) once a week, the cell water level should be checked and, if low, pure water added, (3) once a week, the battery should be charged with the charger set to the weekly charge position, (4) once a month, the specific gravity of all cells should be read after charging , (5) once a month, the battery should be cleaned, (6) once a month, cable leads and connectors should be checked and (7) accurate battery records should be kept. Electrolyte temperature should not exceed 46 degrees C during normal operation (GBC, 1980). For EC-I to be economically competitive on an annual cost basis, these maintenance procedures must be performed. This will reduce the battery replacement cost by ensuring that maximum battery life is obtained.

Safety is another important aspect of EC-I management. Battery acid and high voltage are the main hazards. Some precautions to observe when servicing a battery include: (1) disconnect the battery from the tractor, (2) use insulating tools when working on batteries, (3) wear a

---

[1]The charger had two charging options: (1) a daily charge position which provided the battery with a normal charge and (2) a weekly charge position which provided the battery with an equalization charge. An equalization charge extends three hours longer to insure the complete restoration of active materials in all plates of all cells (GBC, 1980).

face shield or goggles and acid resistant aprons and gloves when taking specific gravity readings, (4) do not wear metallic jewelry when servicing a battery, (5) have water available nearby to wash any electrolyte spills off clothing or skin, (6) do not smoke, (7) protect the battery from flames and sparks and (8) charge the battery in a well-ventilated area to prevent buildup of hydrogen gas (GBC, 1980 and NEMA, 1984). Precautionary labels for batteries used for motive power are described in NEMA Standard IB-1 (1982). Although EC-I presents some different safety problems, EVs are not inherently more dangerous than conventional tractors, and proper operator education can minimize the safety risks.

TEST PROCEDURE

Component Tests

Component tests were performed on the battery and charger because these two components have the largest effect on vehicle performance. The objectives for battery and charger tests were to: (1) determine present battery capacity, which establishes a base for monitoring capacity changes during battery life, (2) measure battery and charger efficiency, (3) determine electrolyte temperature changes during discharge and charge, (4) monitor specific gravity changes during discharge and charge and (5) establish the charging profile of dc voltage and current the charger supplies to the battery. Similar parameters were measured, often using the same transducers for battery and charger tests, so they are discussed together. Lead-acid battery memory effects are measurable, though small, however, they are easily erased by the first constant-current discharge at the six-hour rate (Vinal, 1955 and Hewitt and Packard, 1982). Therefore, one constant-current discharge was used to eliminate the memory effects. The next two discharges were used to measure battery capacity. A battery capacity test, every 50 cycles, was recommended (Carter and Todd, 1983 and

Fenton and Olsen, 1983) to monitor capacity changes so that the effect of battery capacity on vehicle performance could be determined.

Instrumentation

Battery terminal voltage, dc current from the battery, electrolyte temperature in 18 selected cells (Figure 3), voltage of 16 groups of four cells each, dc current to the battery and ac voltage, current and power to the charger were measured in battery and charger tests. From these measurements, the following parameters were calculated: (1) charge, battery energy and battery ampere-hour efficiencies; (2) ampere-hours and energy discharged from the battery; (3) dc ampere-hours and energy delivered to the battery and (4) ac energy provided to the charger. Ten specific gravity measurements were taken during each discharge and charge.

An instrumentation circuit (Figure 4) was designed using electrical sensors and thermocouples to measure these quantities. Resistive voltage dividers reduced the dc voltage and ac voltage by factors of 11.75 and 5.07, respectively. A current transformer reduced the ac current by a factor of 10 to a level measurable by the ac current transducer. The current transducer produced a dc

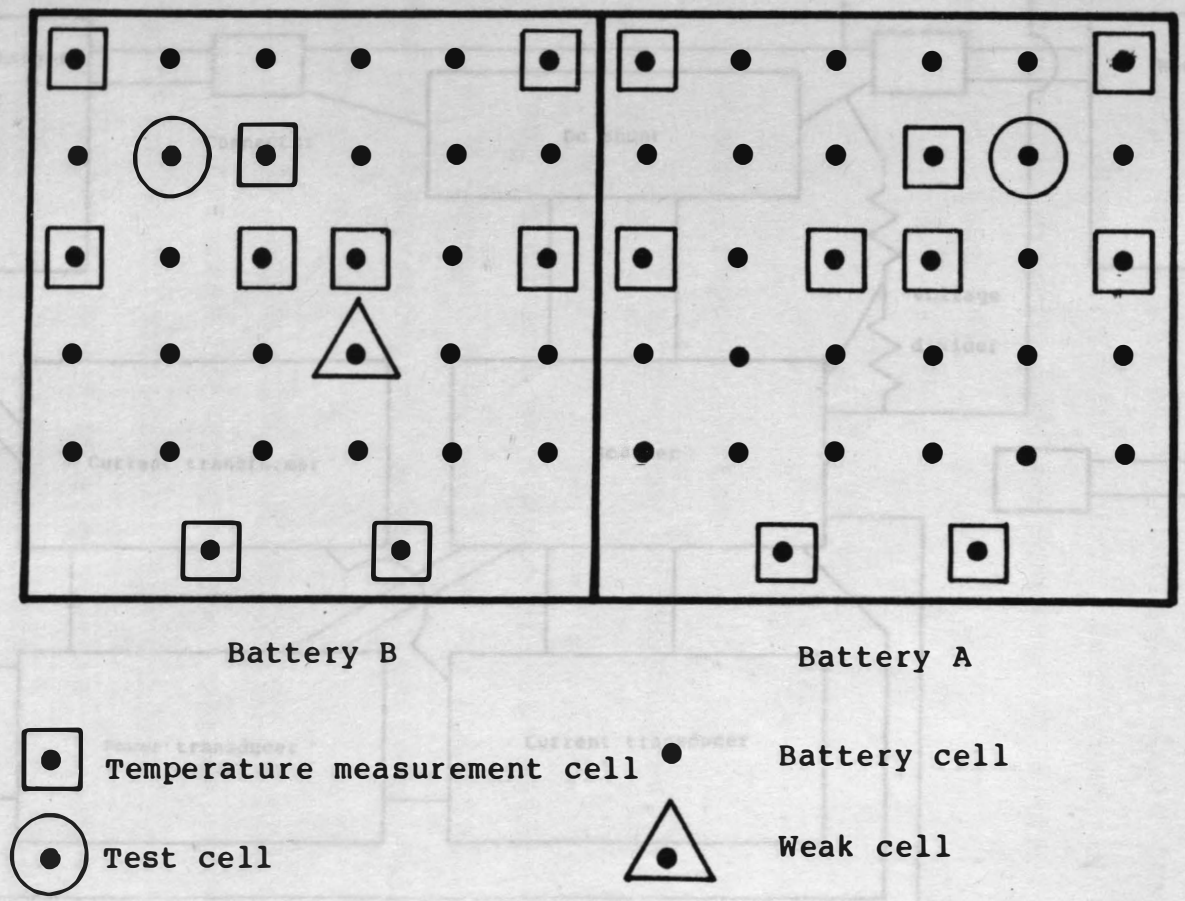

Figure 3. Cells for temperature and specific gravity measurements.

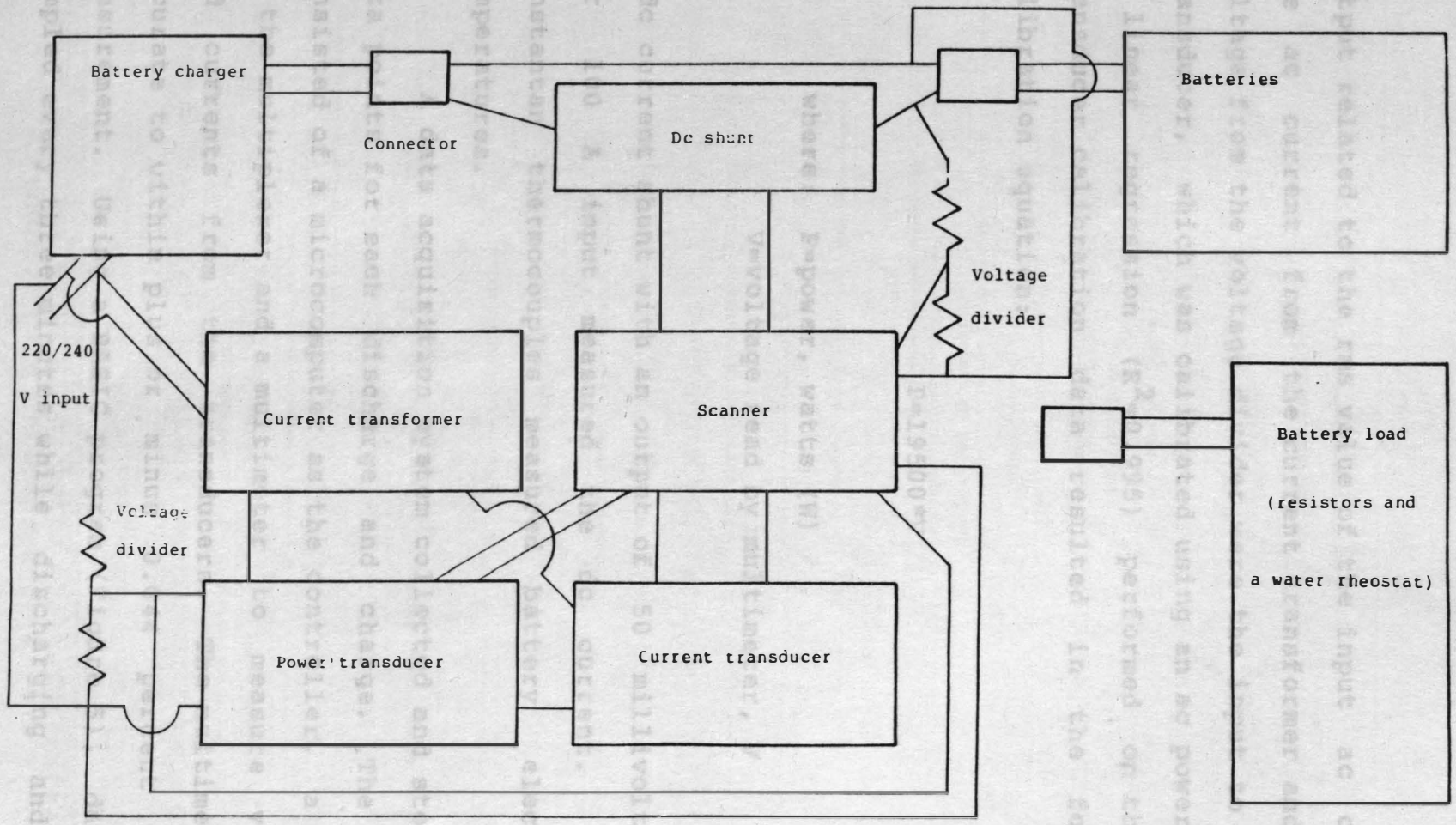

Figure 4. Instrumentation circuit for battery and charger tests.

output related to the rms value of the input ac current. The ac current from the current transformer and the ac voltage from the voltage divider were the input to a power transducer, which was calibrated using an ac power meter. A linear regression (R^2=0.995) performed on the power transducer calibration data resulted in the following calibration equation:

$$P=19500*V$$

where: P=power, watts (W)

V=voltage read by multimeter, V

A dc current shunt with an output of 50 millivolts (mV) per 100 A input measured the dc current. Copper-constantan thermocouples measured battery electrolyte temperatures.

A data acquisition system collected and stored 100 data points for each discharge and charge. The system consisted of a microcomputer as the controller, a scanner as the multiplexer and a multimeter to measure voltages and currents from the transducers. The multimeter was accurate to within plus or minus 0.044 percent of the measurement. Using a BASIC program (Figure 5), data were sampled every three minutes while discharging and every

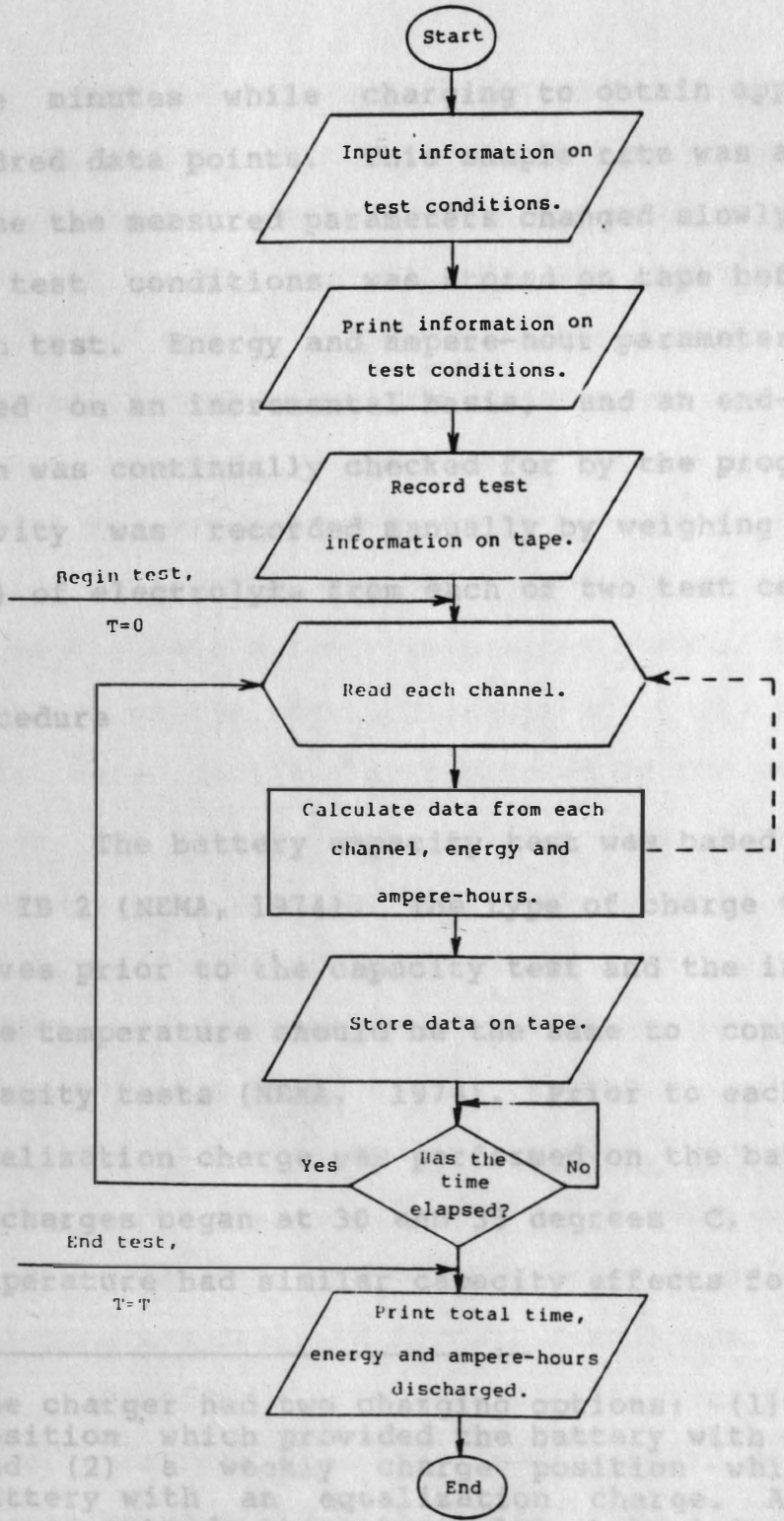

Figure 5. Data acquisition logic chart for battery and charger data collection program.

nine minutes while charging to obtain approximately one hundred data points. This sample rate was acceptable because the measured parameters changed slowly. Information on test conditions was stored on tape before initiating each test. Energy and ampere-hour parameters were calculated on an incremental basis, and an end-of-test condition was continually checked for by the program. Specific gravity was recorded manually by weighing 10 milliliters (ml) of electrolyte from each of two test cells.

Procedure

The battery capacity test was based on NEMA Standard IB 2 (NEMA, 1974). The type of charge the battery receives prior to the capacity test and the initial electrolyte temperature should be the same to compare different capacity tests (NEMA, 1974). Prior to each discharge, an equalization charge was performed on the battery.[1] The two discharges began at 30 and 33 degrees C, so electrolyte temperature had similar capacity effects for each test.

---

[1]The charger had two charging options: (1) a daily charge position which provided the battery with a normal charge and (2) a weekly charge position which provided the battery with an equalization charge. An equalization charge extends three hours longer to insure the complete restoration of active materials in all plates of all cells (GBC, 1980).

The battery was discharged at a constant-current, six-hour rate into a parallel circuit of four temperature-compensated resistors and one water rheostat. To obtain the six-hour rate for the battery, a constant current of 56.7 A was maintained by using the water rheostat to fine tune the resistance as the terminal voltage dropped. The discharge current was initially set at 56.8 A, and was reset every time it fell below 56.6 A. Closing a switch initiated the discharge about one second before the data collection program began. During the last two hours of the test, voltages of each group of four cells were continually monitored by the data acquisition system to detect weak cells. When a weak cell was detected, it was manually monitored to ensure that its polarity did not become reversed. The battery terminal voltage was continually monitored by the data acquisition system the last two hours of the test, and the test was terminated when the terminal voltage dropped below 108.8 V (1.70 V per cell). After a final datum point was taken, the discharge was stopped by opening a switch. The same procedure was followed for all discharges.

Specific gravity in the two test cells was manually checked every 30 minutes (min) during discharge and every 90 min during charge. The specific gravity was measured by withdrawing a 10 ml volume from the cell in a

syringe and weighing the volume on a scale that was accurate to plus or minus 0.05 grams (g). The following equation was used to calculate specific gravity:

$$SP=(SF-SE)/(SW-SE)$$

where: SP=specific gravity, dimensionless
SF=weight of the syringe and 10 ml of electrolyte, g
SE=weight of the syringe empty, g
SW=weight of the syringe and 10 ml of water at 25 degrees C, g

Temperature in each test cell was manually recorded at this time, and the specific gravity was corrected for temperature by adding or subtracting 0.001 for every 1.67 degree above or below 25 degrees C (NEMA IB-2, 1974).

Specific gravity and temperature were measured (as described for the capacity test) every 90 min during charge. The charger was started about one second before the data collection program. During the last half of the charging test, the dc current to the battery was

continually checked for an end-of-test condition (zero amperes). When the end-of-test condition occurred, the time of the charge was recorded and the program ended.

Vehicle Tests

Vehicle tests performed included loader, pto, draft, field and model development tests (tests to develop and check the energy use model of EC-I). These tests used the same instrumentation system and measured the same core of parameters. Additional parameters were measured, dependent on the test. The objectives of vehicle tests were to: (1) determine maximum pto and drawbar power and related operating characteristics and (2) develop a model that predicts energy use by summing predicted energy use for standard segments of a task.

Instrumentation

Battery voltage and current were measured and recorded during every test. A resistive voltage divider reduced the battery voltage by a factor of 11.75 to a value measurable by the digital voltmeter in the data acquisition system. A dc shunt measured the battery

current. The manufacturer specified a 100 mV output when 500 A flows through the shunt, so the shunt output in volts was multiplied by 5000 to determine the current. The measured battery voltage and current values were used to calculate the battery power required during tests.

A torque sensor with a capacity of 2300 newton-meters (Nm) and 0 to 6500 r/min measured pto torque and speed. Voltages to a four-arm strain gage bridge that measured shaft deflection were supplied via slip rings and brushes. The bridge output was directly related to torque. A magnetic pickup, outputting 60 pulses per revolution, sensed pto speed. A frequency conditioner converted the digital pto speed signal to an analog 0 to 5 V dc signal for measurement by the data acquisition system. A previous calibration (Stange, et al., 1982) was verified by using a portable engine dynamometer to load a tractor engine through the torque transducer mounted on the pto shaft. The recalibrated linear regression equations for torque and speed differed from the previous calibration by less than five percent. Therefore, the previous calibration with the following regression equations (R^2=0.999 and R^2=0.999, respectively) was used to calculate pto torque and speed:

$$PT=1074.4*(EO/EI)+2.1$$

where: PT=pto torque, Nm

EO=torque sensor strain gage bridge output, V

EI=torque sensor strain gage bridge power supply, V

and:

$$PS=200*V$$

where: PS=pto rotational speed, r/min

Pto power output was calculated from the measured pto torque and speed values.

Draft force was measured with a three-point hitch dynamometer designed and built by Johnson and Voorhees (1979). Draft was measured by a four-arm strain gage bridge attached to an aluminum torque tube and arranged to be sensitive only to draft forces. The dynamometer was set on the high range, capable of measuring draft forces of up to 67 kilonewtons (kN). The original calibration (Johnson and Voorhees, 1979) was verified by suspending known weights from the dynamometer. The data acquisition system recorded the data, and the resulting linear regression equation for draft differed from the original calibration by less than five percent. Therefore, the original

calibration with the following regression equation (R^2=0.992) was used to calculate draft force:

$$D=23.70*(EO/EI)$$

where: D=draft, kN

EO=drawbar dynamometer strain gage bridge output, V

EI=drawbar dynamometer strain gage bridge power supply, V

The measured values of draft and speed were used to calculate drawbar power.

A radar velocity sensor measured tractor speed. This sensor determined speed by reflecting microwaves from a moving surface and measuring the doppler shift of the microwave frequency. The sensor emitted a pulsed output over its usable range of 0.45 to 22.3 meters per second (m/s). A frequency conditioner changed the digital output signal to an analog 0 to 5 V dc signal for measurement by the data acquisition system. The sensor was calibrated by directing the microwaves at the moving belt of a constant-speed treadmill. Over a calibration range of 0.43 to 4.3 m/s, a linear regression (R^2=0.996) resulted in the following calibration equation:

GS=2.02*V-0.01

where: GS=speed, m/s

Other instruments used throughout the testing included power supplies, tachometers, stopwatches, thermocouples, a cone pentrometer and a dc kWh meter. A 0 to 20 V dc power supply provided five volts to the strain gages, and amplified the returning signal. A 0 to 60 volt dc power supply provided 12.0 V dc to the radar velocity sensor. The dial tachometer in EC-I monitored motor speed with the result recorded manually. A handheld digital tachometer was used to measure motor speed which was recorded manually when the tachometer in EC-I was not operative. A stopwatch was used to measure the time required to traverse the test course during draft testing. The same thermocouples used for component tests measured electrolyte temperature during pto tests. A cone penetrometer was used to determine cone index estimates of the soil for draft tests. A dc kWh meter measured the dc energy discharged during operation.

The data acquisition system used was the same as the one used for the component tests except that the multimeter was replaced by a digital voltmeter. The

voltmeter was accurate to 0.015 percent of the voltage measurement. Data were collected at approximately five to six readings per second for the loader, draft, field and model development tests using a BASIC program (Figure 6). Information on test conditions and the selected test length from 0 to 120 seconds (s) was stored on tape. After the test ended, the program performed calculations and stored the data on tape. A second BASIC program was designed to sample data once every minute for the pto tests (Figure 7), where the measured parameters changed more slowly. This program performed calculations and stored data on tape between data samples and allowed the operator to determine the end-of-test condition.

Power was supplied from the 110/120 V ac building system for the loader and pto tests since the vehicle was at rest. For the draft and model development tests, power was obtained from a deep-cycle 12 V battery through an inverter. This inverter converted the 12 V dc power supplied by the battery to the 110/120 V ac power required to operate the instrumentation system. The primary transducers were mounted on the tractor frame; the data acquisition system, power supplies and signal conditioning instruments were contained in a box mounted on the battery and the microcomputer was mounted in the tractor cab (Figure 8).

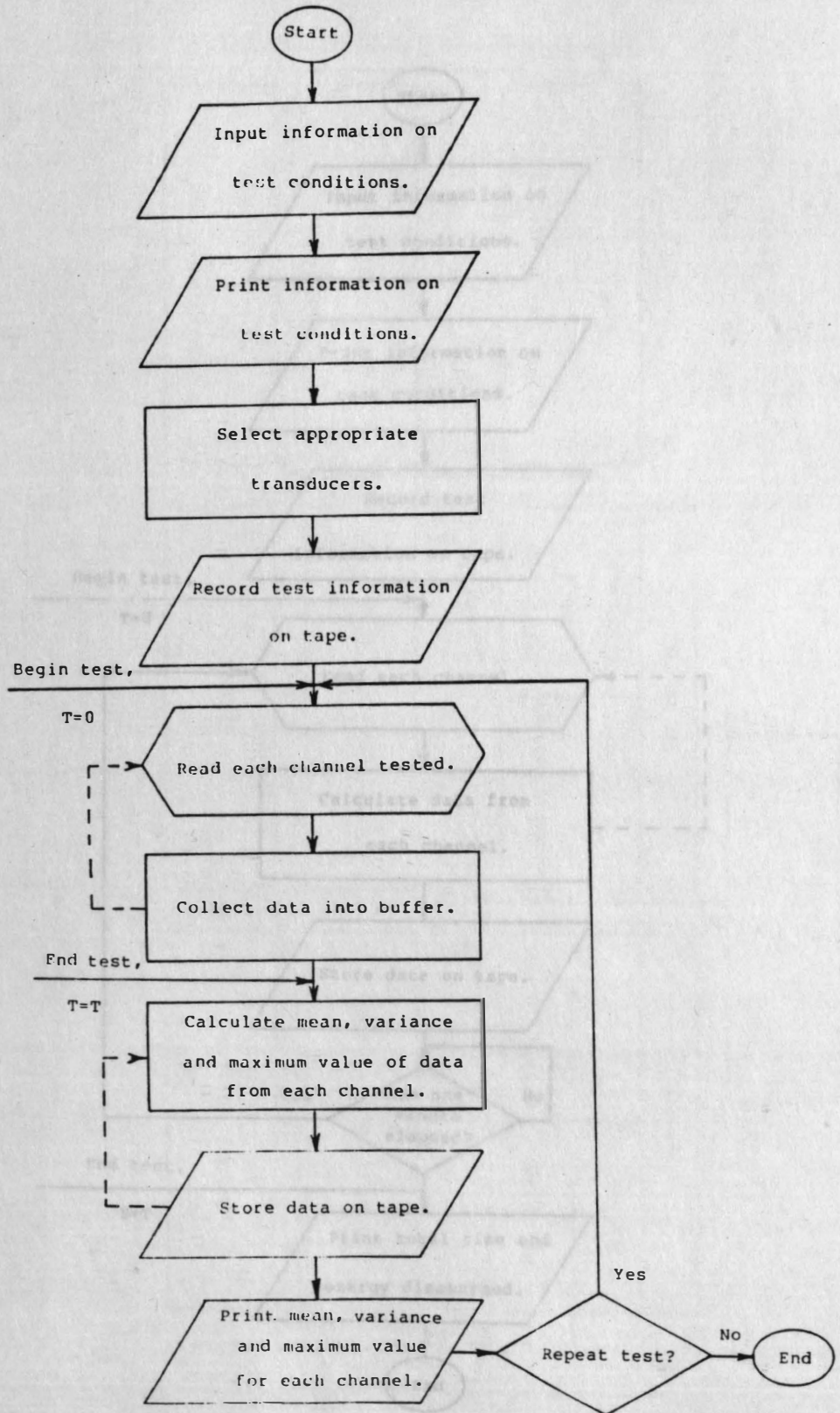

Figure 6. Data acquisition logic chart for loader, draft, field and model data collection program.

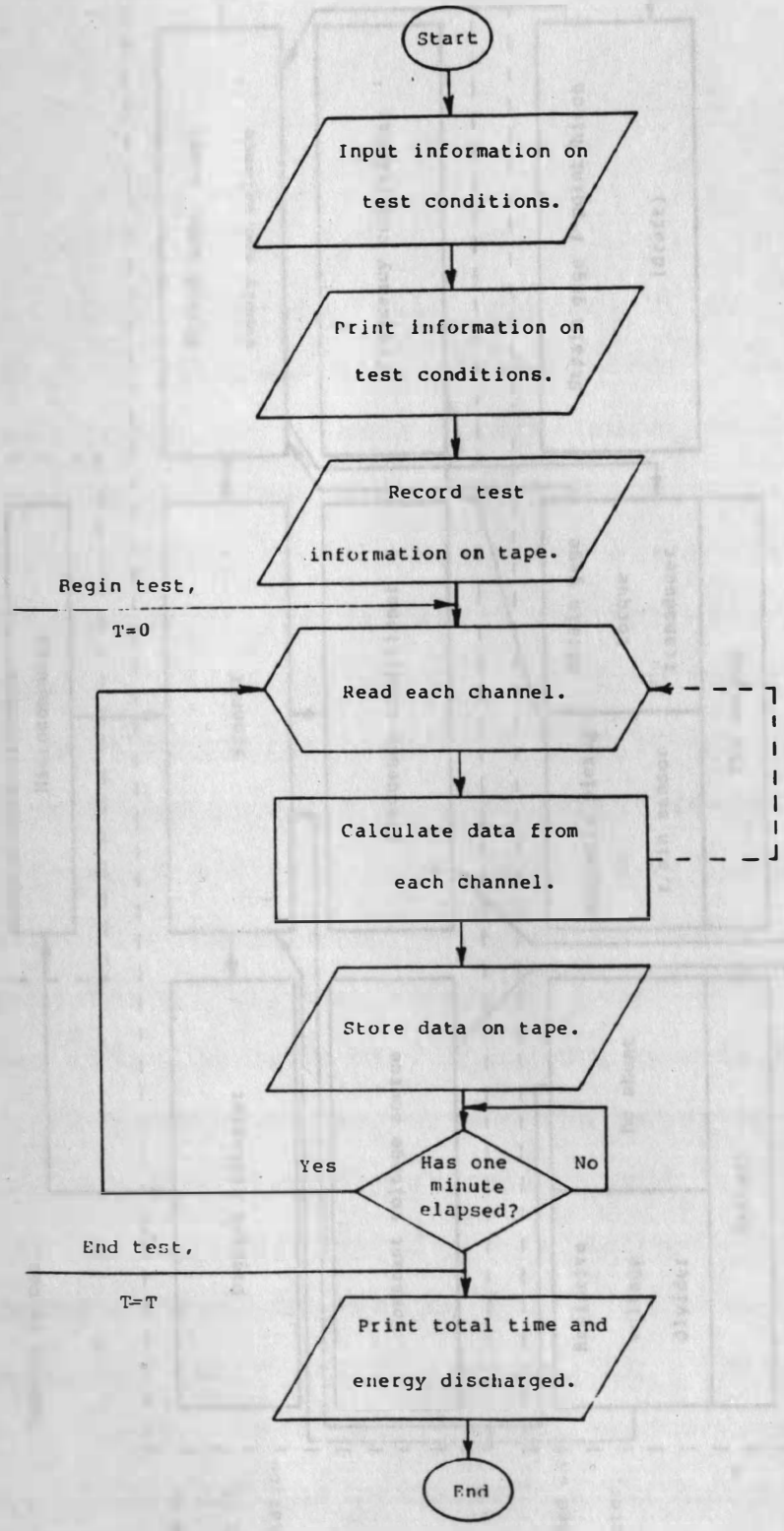

Figure 7. Data acquisition logic chart for pto data collection program.

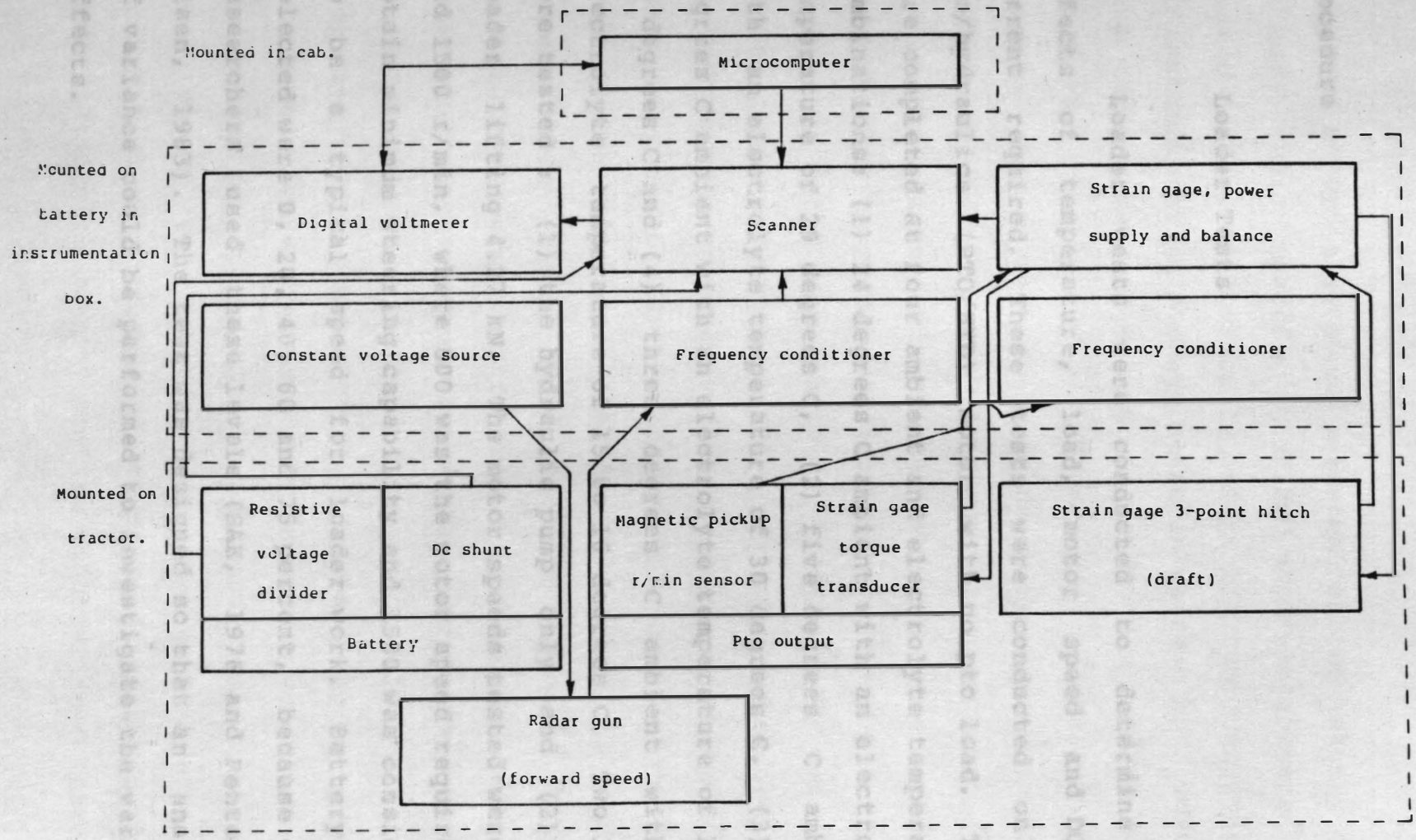

Figure 8. EC-I instrumentation block diagram.

Procedure

Loader Tests

Loader tests were conducted to determine the effects of temperature, load, motor speed and DOD on current required. These tests were conducted on the pto/hydraulics (PTO/HYD) motor with no pto load. Tests were completed at four ambient and electrolyte temperature combinations: (1) 24 degrees C ambient with an electrolyte temperature of 29 degrees C, (2) five degrees C ambient with an electrolyte temperature of 30 degrees C, (3) 9.5 degrees C ambient with an electrolyte temperature of 17 to 19 degrees C and (4) three degrees C ambient with an electrolyte temperature of 15 to 16 degrees C. Two loads were tested : (1) the hydraulic pump only and (2) the loader lifting 4.27 kN. The motor speeds tested were 800 and 1500 r/min, where 800 was the motor speed required to obtain minimum steering capability and 1500 was considered to be a typical speed for loader work. Battery DODs selected were 0, 20, 40, 60 and 75 percent, because other researchers used these levels (SAE, 1976 and Fenton and Olsen, 1983). The test was designed so that an analysis of variance could be performed to investigate the variable effects.

A normal charge was performed on the battery prior to each test. Specific gravity and temperature were checked in the two test cells before the test was started. The instrumentation package measured current and voltage, about three times per second each, for six seconds during the loader tests. The tractor was manuevered into position before the first test at zero percent DOD was started.

The first test was at 1500 r/min motor speed with the hydraulic pump as the load. The next test was at 1500 r/min motor speed with the loader lifting 4.27 kN. Next, a test was conducted at 800 r/min motor speed operating the hydraulic pump, and the last test was conducted at 800 r/min motor speed with the loader lifting 4.27 kN. The test order was the same at all DODs and for all temperatures. Motor speed was set using a handheld digital tachometer to record the pto speed, since the tachometer in the cab was inoperative during this testing. The pto speed was multiplied by the 4.17 to 1 gear reduction from the motor to pto to obtain the motor speed. Pto speeds were recorded within plus or minus five revolutions per minute of the desired speed, therefore motor speeds were within plus or minus 20 r/min. When raising 4.27 kN, the test was commenced after the loader began lifting the weight, and the loader lifted the weight

throughout data collection. The energy discharged during each test was recorded on the dc kWh meter in the cab.

The percent DOD was determined by using the energy discharged as a percent of the 100 percent DOD capacity (45.4 kWh), which was determined from the capacity test. Between tests, the battery was discharged into a bank of resistors at approximately the six-hour rate. Battery voltage and current during discharge were measured at the start of the discharge, and the power was calculated. One hour later, the voltage and current were measured again and power was recalculated. The average value of these two power measurements was multiplied by one hour and was considered to be the energy discharged during that hour. The energy discharged during the testing was added to this value to determine the total energy discharged. A one hour discharge reached 20 percent DOD. The energy discharged and approximate DOD were as follows: 0, 9.0, 18.0, 26.5 and 34.0 kWh, corresponding to 0, 20, 40, 60 and 75 percent, respectively.

Pto Tests

Pto tests were conducted to determine: (1) the maximum pto power available under different operating conditions and (2) the pto operating characteristics as a

function of time. These tests analyzed the effect of the motor speed feedback control (Helder, 1985) and the hydraulic pump on pto operating characteristics. The power versus time characteristics of the PTO/HYD motor were also determined. Tests were conducted, with and without feedback, with the motor operating the hydraulic pump; and, with and without feedback, with the motor not operating the hydraulic pump. Another test at different pto power levels, without feedback and without the hydraulic pump operating, determined the time that power could be output before thermal overload shutdown the motor (Vik, 1985).

The battery was given a normal charge and the dynamometer adjusted so that torque could be read directly from the dial prior to the test. Pto speed and torque, battery current and voltage and electrolyte and ambient temperature were measured and recorded once every minute. Because the pto torque and speed values were found to vary continually over a small range, forty measurements were averaged and the averages were recorded as the pto torque and speed datum points for each sixty-second interval. With the torque and speed averaging technique, pto and battery parameters changed slowly. Pto and battery power, efficiency and dc energy and ampere-hours discharged were calculated and stored with the measured parameters. As a

check, pto torque and speed from the dynamometer; and motor speed from the tachometer, battery current from the ammeter, voltage from the voltmeter, dc energy from the kWh meter and SoC from the SoC meter in EC-I were manually recorded every five minutes. The initial and final specific gravity and temperature of the two test cells were measured and manually recorded.

The pto speed and load were adjusted to obtain the maximum power output possible at 540 r/min to initiate the test to determine power versus time characteristics. This power was limited by the controller, which limits the PTO/HYD motor to a maximum current of 200 A (Helder, 1985). Data collection was initiated when this power level was set and continued until the motor shutdown. A fan cooled the motor for 90 min by blowing air at ambient temperature, with an average velocity of 5.2 m/s, over the motor. After 90 min of cooling, the power was reduced five percent and the test repeated. This procedure was repeated until the motor ran continuously or the battery reached 80 percent DOD.

The other pto tests were begun by setting the pto speed and load at the maximum continuous power level obtainable at 540 r/min. This level was found by experimentation. The data acquisition system was started as soon as the initial power level was set and stabilized

(usually two to five minutes after the pto was started). The test was terminated when the dc energy discharged reached 70 to 80 percent battery DOD, as confirmed by the ampere-hours discharged. The data acquisition system and EC-I were shutdown by the operator.

Draft Tests

The draft test objectives were to: (1) determine the maximum drawbar power available under repeatable, standardized conditions and (2) examine the effects of operating conditions on the power available. Maximum drawbar power was developed in all three gear ratios on a bituminous surface (asphalt). Surface condition and tire tread direction effects on drawbar power were analyzed. Maximum drawbar draft was developed in all gear ratios for a wet soil surface, and several tests in second gear were conducted on dry soil at various drawbar pulls. Tests in third gear were conducted on dry soil with the tire tread direction the only variable changed. Although these tests did not examine all possible combinations of operating conditions, they were used to estimate the effect of single variables on the operating power required.

A 91 m course with a 46 m approach on a level, bituminous surface was used for testing. Prior to the

test, the battery was given a normal charge, and specific gravity and temperature measurements from the two test cells were recorded manually. A diesel tractor supplied the load by throttling back, thereby, using the engine as a brake. The load was increased or decreased by changing the tractor throttle setting. A 12 m, 150 kN-test cable was connected to the hitch point of the load tractor so that it was pulled forward. The approach served to stabilize the load and speed. The operator pressed a key which started the data acquisition system reading draft, speed and battery current and voltage about once per second during the 91 m test. In all three gears, the load was least the first time over the course, and slowly increased each subsequent traverse. The same throttle setting of the load tractor was used as a load at a battery DOD of about 0 and 75 to 80 percent. Tests repeated on different soil surfaces and with different tire tread direction were conducted with the load tractor at the same throttle settings as for the tests on asphalt. All these tests were conducted at maximum speed.

Rolling resistance on asphalt and dry soil was measured by pulling EC-I in neutral using the drawbar dynamometer to measure the draft required. This test was conducted at two different speeds. EC-I was driven over the bituminous test course with no load to evaluate the

power required to overcome rolling resistance in second gear. The effect of speed on the power required to overcome rolling resistance was analyzed by conducting the test at several different speeds in second gear.

Field Tests

The field test objectives were to: (1) determine power requirements for certain chore tasks and (2) subjectively evaluate EC-I performance while completing chores in a farm environment. One set of tests was performed on a farm near Brandon, SD from January 26-30, 1985. Throughout the test period temperatures ranged from -30 to 0 degrees C, and the tractor remained outside during charging and use. The vehicle was recharged overnight three times. EC-I was used to load a feed wagon with silage and hay in the chore routine on this farm. On January 28, the vehicle was driven to a neighboring farm where it was used to load a feed wagon with corn and silage.

A second set of tests was performed March 6-8, 1985 on the SDSU campus. EC-I was used to move snow each day until the battery reached 80 percent DOD.

Battery current and voltage were measured while using the loader to load silage and hay, to move snow and

while driving between tasks. The current and voltage values were used to determine the battery power required for these tasks, and to note whether power requirements differed from those under more ideal temperature and soil surface conditions.

Model Development Tests

The model development test objectives were to: (1) establish the energy required to complete standard segments of farm chore tasks and (2) use a second data set to compare predictions with measured energy use for five cycles composed of standard segments. Operating the pto, accelerating a load, pulling a load at constant speed, decelerating a load and setting at rest were defined as standard segments. Prediction equations were developed for the first set of test data using multiple regression techniques for each segment. After the prediction equations were developed, the standard cycles to examine the model were chosen. The cycles increased in complexity to allow a preliminary evaluation of model utility in simple and complex types of motion.

Establishment of Model Equations

The battery was given a normal charge prior to, and battery current and voltage were measured during, each test. Test cell specific gravity and electrolyte temperature were measured before and after each test. The battery DOD was monitored during these tests, but was disregarded as a factor in energy use since these tests were conducted at part-load (low power levels). The pto energy use data were obtained by varying the pto power output during one discharge. Six pto power levels were obtained by varying the pto torque and speed. Each level was held for 10 min, and the first four levels were repeated twice. The data were collected in the same manner as the pto tests discussed previously.

Three loads and four speeds were used to predict energy use at constant speed. The three loads were provided by pulling one, two and three tractors in neutral. Each of the four speeds was repeated three times at each load, and different speeds were obtained by setting the traction motor speed control at different levels. The PTO/HYD motor was operated at 800 r/min, and the data were collected in the same manner and over the same course as the draft tests discussed previously.

The acceleration tests were conducted with the same three loads accelerated to four different final speeds. Each final speed obtained was repeated three times at each load. Acceleration tests were completed on the bituminous surface used for the draft tests. For 15 s, the data collection program sampled the same variables as in the draft test. The program was started with the tractor at rest and the PTO/HYD motor running at 800 r/min. After the program had collected data for one to two seconds, the traction motor speed control was steadily increased to a certain point, and the tractor allowed to accelerate to a final speed. While at rest, decelerating (coasting) and plugging,[1] the speed control was either in neutral or reversed, therefore, it was assumed that energy use by the traction motor was zero (Unnewehr and Nasar, 1982). The energy to power the PTO/HYD motor at 800 r/min was obtained from the loader tests. Data from these standard segment tests were used to develop multiple regression prediction equations for the model.

---

[1] A method of braking the tractor by reversing the motor field while the tractor is in motion (Helder, 1985).

Evaluation of Model Performance

The energy use model was examined using five cycles of increasing complexity to determine predictive value over a range of conditions. The first three cycles were performed on asphalt pulling one and two tractors (both in neutral) as the load. These tractors provided different loads than were used to develop the prediction equations. Each cycle was repeated twice with each load, and data were collected on the same course with the same variables sampled as for the draft tests. The draft and speed data collected during these tests were used to predict energy use for each cycle and compared to actual energy use calculated from the battery current and voltage measurements. Cycle I was on asphalt with no turns (Table 3). Cycle II and III were on asphalt with turns and had the segment order rearranged (Tables 4 and 5). In cycle IV, EC-I pulled a partially loaded feed wagon on a gravel surface, around a turn, to a feed bunk (Table 6). EC-I unloaded the feed wagon into the feed bunk with the pto, while driving along the bunk in cycle V (Table 7). During this last cycle, pto torque and speed were measured along with the variables measured for the other cycles. These cycles were designed to predict model utility by examining prediction error as cycle complexity increased.

Table 3. Model evaluation data for energy use cycle I, on asphalt with no turns.

	Segment	Abbreviation	Time, s
1.	Motionless with PTO/HYD motor operating.	SITWPTO	2
2.	Accelerate to a speed.	ACCEL	15
3.	Operate at a constant speed.	CSPEED	10
4.	Coast to a stop.	COAST	5
5.	Motionless with PTO/HYD motor operating.	SITWPTO	2
6.	Motionless without PTO/ HYD motor operating.	SIT	10
7.	Motionless with PTO/HYD motor operating.	SITWPTO	5
8.	Creep forward to tighten load cable.	CREEP	5
9.	Accelerate to a speed.	ACCEL	15
10.	Operate at a constant speed.	CSPEED	5
		Total time	74

Table 4. Model evaluation data for energy use cycle II, on asphalt with turns using plugging to stop.

	Segment	Abbreviation	Time, s
1.	Motionless with PTO/HYD motor operating.	SITWPTO	2
2.	Accelerate to a speed.	ACCEL	15
3.	Operate at a constant speed.	CSPEED	20
4.	Coast to a speed.	COAST	3
5.	Operate at a constant speed.	CSPEED	20
6.	Use plugging to stop.	COAST	2
7.	Motionless with PTO/HYD motor operating.	SITWPTO	2
8.	Motionless without PTO/ HYD motor operating.	SIT	10
9.	Motionless with PTO/HYD motor operating.	SITWPTO	2
10.	Creep forward to tighten load cable.	CREEP	3
11.	Accelerate to a speed.	ACCEL	15
12.	Operate at a constant speed.	CSPEED	20
		Total time	114

Table 5. Model evaluation data for energy use cycle III, on asphalt with turns, coasting to a stop.

	Segment	Abbreviation	Time, s
1.	Motionless with PTO/HYD motor operating.	SITWPTO	2
2.	Accelerate to a speed.	ACCEL	15
3.	Operate at a constant speed.	CSPEED	20
4.	Accelerate to maximum speed.	ACCEL	10
5.	Operate at a constant speed.	CSPEED	20
6.	Coast to a stop.	COAST	10
7.	Motionless with PTO/HYD motor operating.	SITWPTO	2
8.	Motionless without PTO/ HYD motor operating.	SIT	10
9.	Motionless with PTO/HYD motor operating.	SITWPTO	3
10.	Creep forward to tighten load cable.	CREEP	10
11.	Accelerate to a speed.	ACCEL	15
12.	Operate at a constant speed.	CSPEED	15
		Total time	132

Table 6. Model evaulation data for energy use cycle IV, pulling a feed wagon on gravel with turns.

Segment	Abbreviation	Time, s
1. Motionless with PTO/HYD motor operating.	SITWPTO	5
2. Accelerate to a speed.	ACCEL	15
3. Operate at a constant speed.	CSPEED	25
4. Coast to a speed.	COAST	3
5. Operate at a constant speed.	CSPEED	10
	Total time	58

Table 7. Model evaluation data for energy use cycle V, unloading a feed wagon with the pto on gravel.

Segment	Abbreviation	Time, s
1. Operate pto at 1500 r/min to unload feed wagon during the entire cycle.	PTO	60
2. Accelerate to a speed.	ACCEL	15
3. Operate at a constant speed.	CSPEED	45
	Total time	60

RESULTS AND DISCUSSION

Component Tests

Capacity Tests

Average battery ampere-hour capacity and energy capacity at the six-hour discharge rate for an initial battery electrolyte temperature of 30 degrees C were 365.5 Ah and 45.4 kWh, respectively. These were above the capacity of 340 Ah and 42.2 kWh specified by the manufacturer at 25 degrees C. The electrolyte temperature remained nearly the same during discharge, and specific gravity decreased at a constant rate. These results were similar to results obtained by other researchers (GBC, 1980; Marsh, 1981; Unnewehr and Nasar, 1982 and Vincent, et al., 1984). Due to instrumentation problems, battery efficiency was not determined.

The dc discharge current through the load resistors averaged 56.62 A with a variance of 0.026 and 56.60 A with a variance of 0.030 for the first and second capacity tests, respectively. This differed from the six-hour rate of 56.7 A by 0.18 percent. The minimum current was 55.8 A, and the maximum was 57.2 A. Although 55.8 A was outside the one percent tolerance for current

variation during discharge set by NEMA (IB-2, 1974), it was the only point outside the tolerance and occurred at the end of the second discharge. These values indicated that the discharges met NEMA requirements (IB-2, 1974) for a capacity test.

The battery terminal voltage decreased slowly for the first three hours of the discharge, then decreased more rapidly approaching a vertical line at the end of the discharge (Figure 9). The voltage of each cell group followed a similar curve. In one of the "weaker" cell groups, the curve rapidly approached a vertical line at the end of the discharge (Figure 10). One cell in this group (the weakest found, Figure 3) was as low as 0.5 V by the end of the discharge.

Electrolyte temperature remained constant during discharge. Capacity tests were initiated before the electrolyte temperature returned to ambient following charging, and the results were adjusted to a standard temperature. The copper-constantan thermocouple used to measure temperature was accurate to one degree C, and the electrolyte temperature rarely varied by more than one degree C averaging 30 degrees C with a variance of 0.80 (Figure 11). Cells on the outside edge of the battery tended to have an electolyte temperature one to two degrees C below those cells in the center of the battery

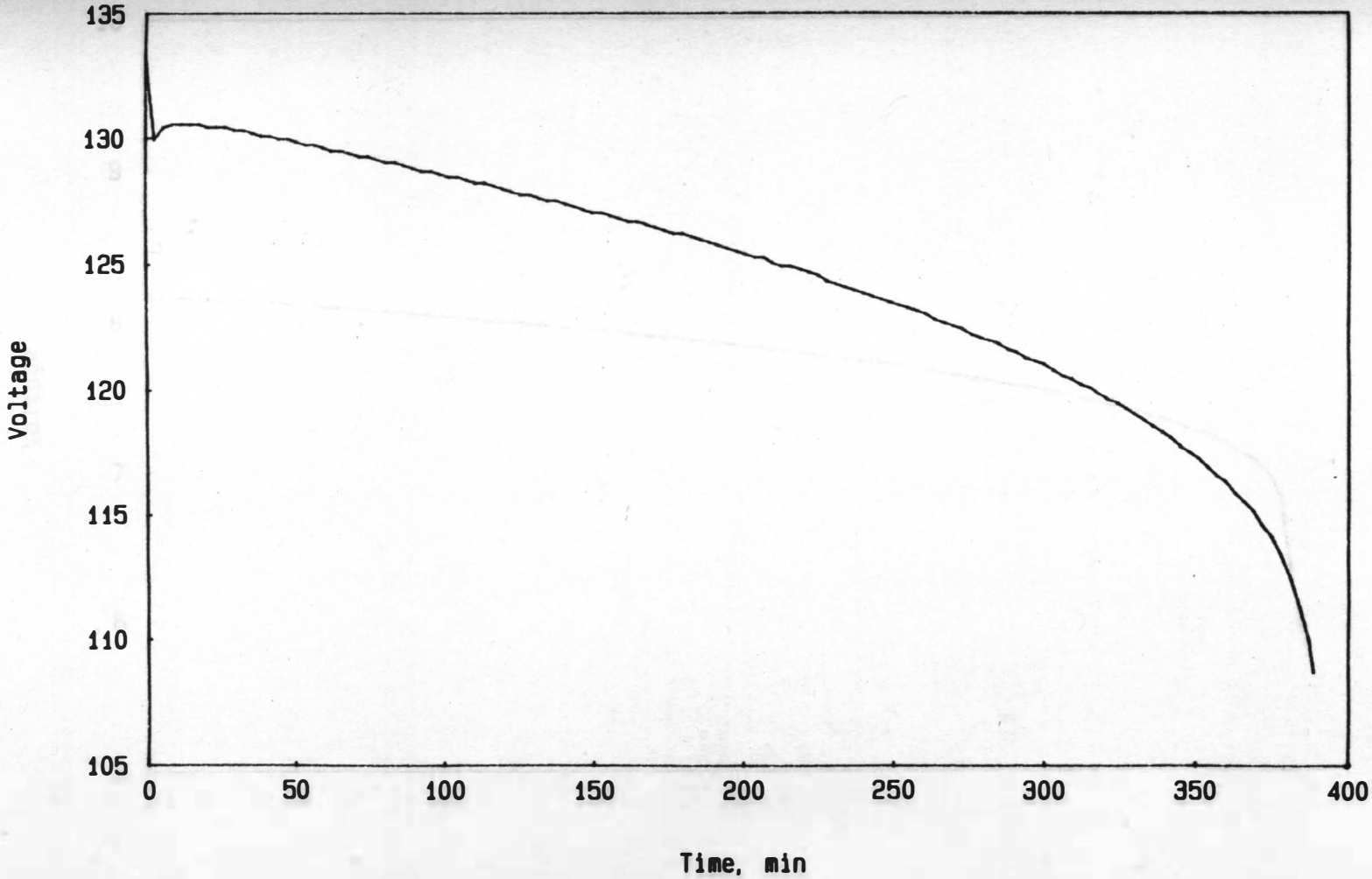

Figure 9. Battery terminal voltage during discharge at the constant-current, six-hour rate.

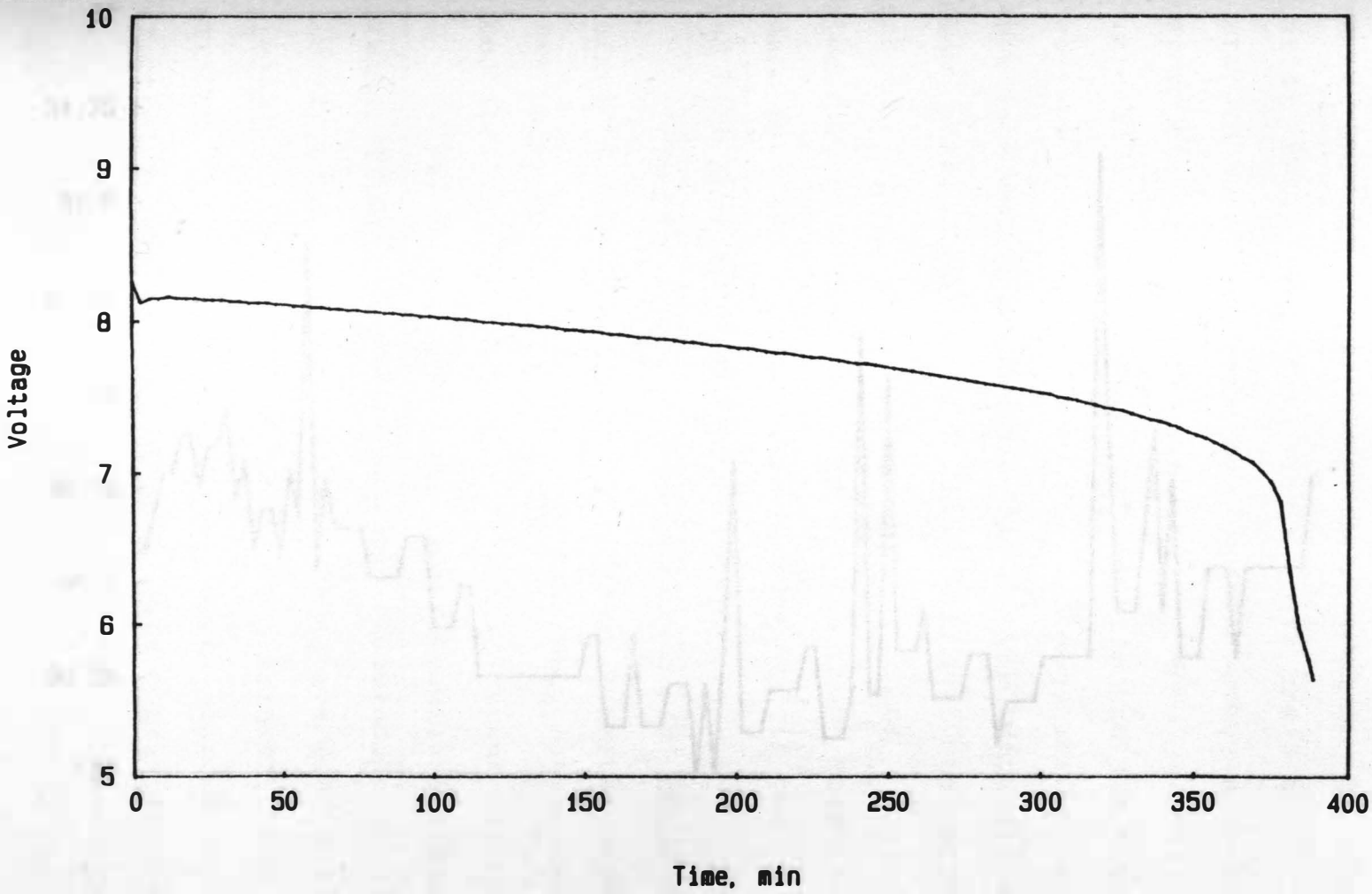

Figure 10. Battery cell group voltage during discharge at the constant-current, six-hour rate.

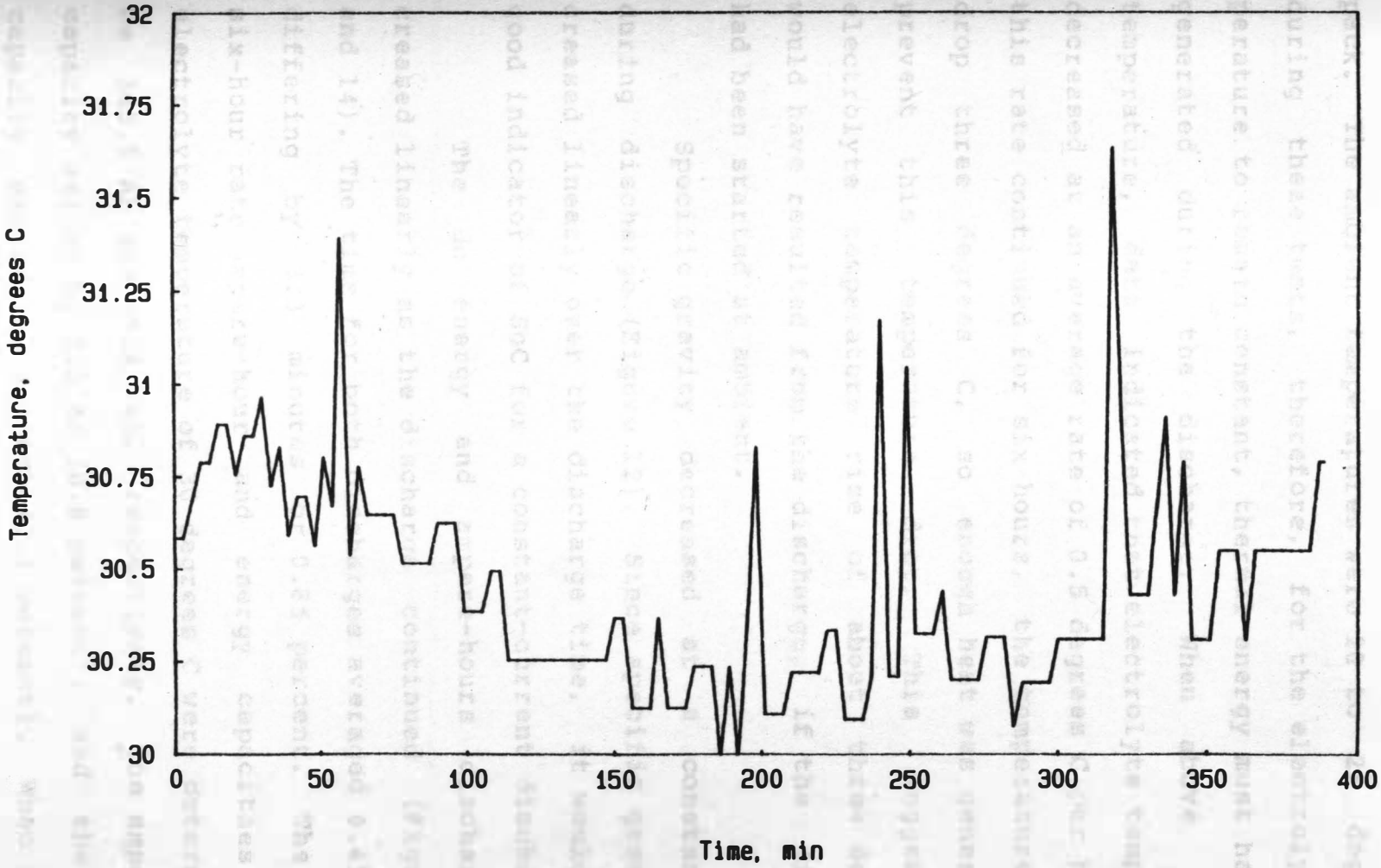

Figure 11. Battery electrolyte temperature during discharge at the constant-current, six-hour rate.

pack. The ambient temperatures were 20 to 23 degrees C during these tests, therefore, for the electrolyte temperature to remain constant, thermal energy must have been generated during the discharge. When above ambient temperature, data indicated that electrolyte temperature decreased at an average rate of 0.5 degrees C per hour. If this rate continued for six hours, the temperature would drop three degrees C, so enough heat was generated to prevent this temperature drop. This suggests an electrolyte temperature rise of about three degrees C would have resulted from the discharge, if the discharge had been started at ambient.

Specific gravity decreased at a constant rate during discharge (Figure 12). Since specific gravity decreased linearly over the discharge time, it would be a good indicator of SoC for a constant-current discharge.

The dc energy and ampere-hours discharged increased linearly as the discharge continued (Figures 13 and 14). The time for both discharges averaged 6.45 hours, differing by 3.3 minutes or 0.85 percent. The average six-hour rate ampere-hour and energy capacities at an electrolyte temperature of 30 degrees C were determined to be 365.5 Ah and 45.4 kWh, respectively. The ampere-hour capacity varied by 3.0 Ah (0.8 percent), and the energy capacity varied by 0.5 kWh (1.1 percent). When adjusted

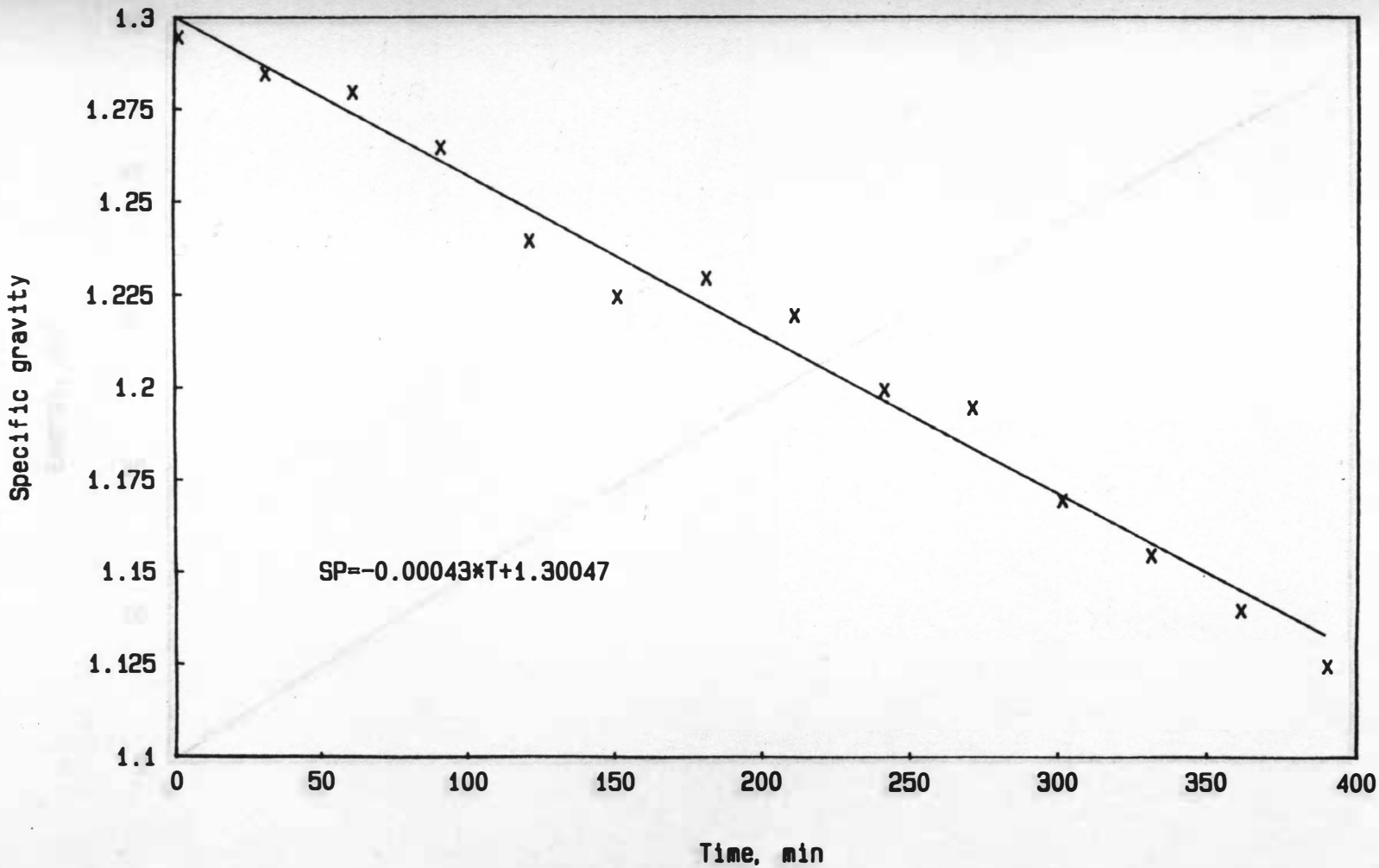

Figure 12. Battery specific gravity during discharge at the constant-current, six-hour rate.

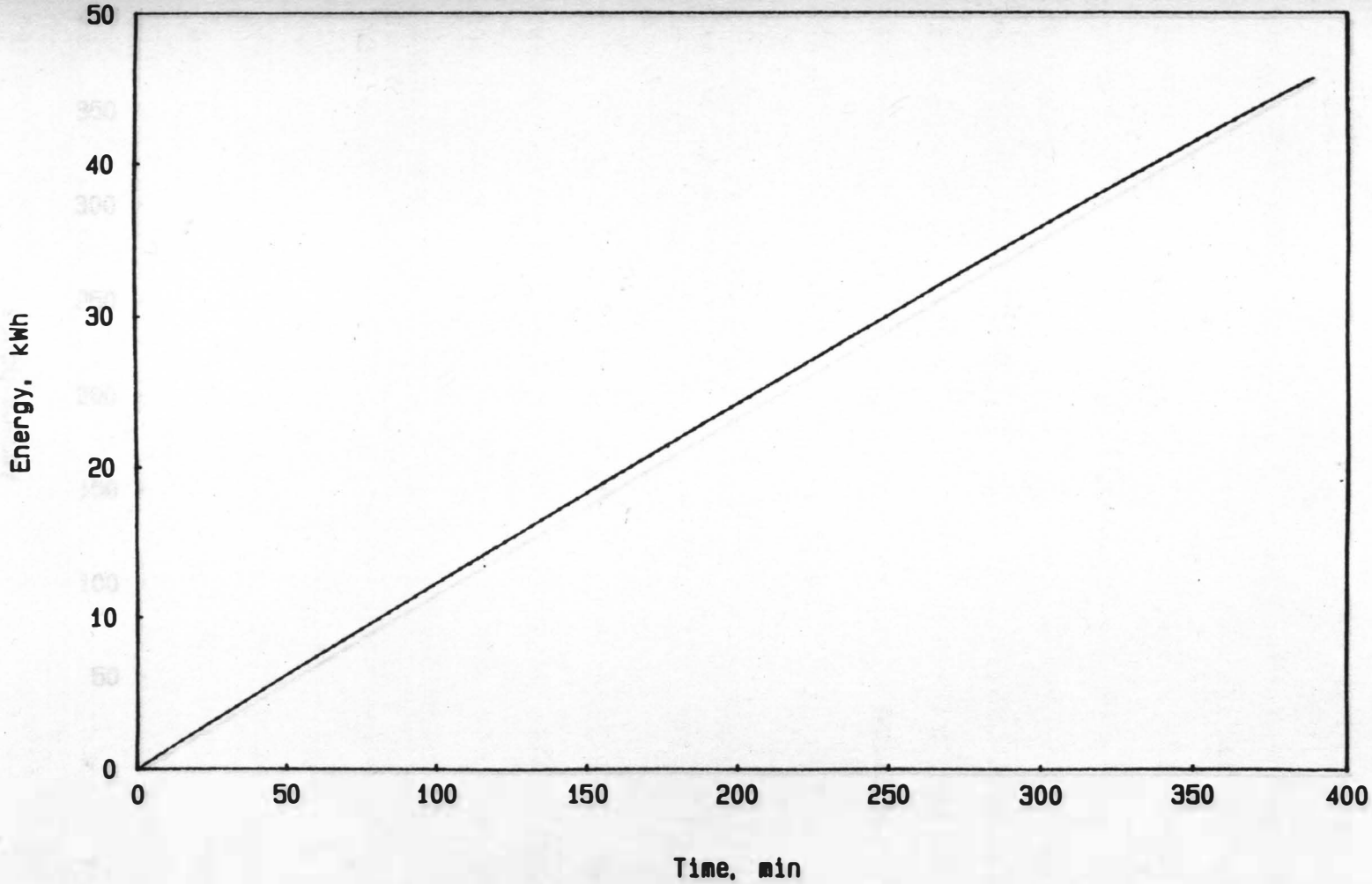

Figure 13. Battery energy during discharge at the constant-current, six-hour rate.

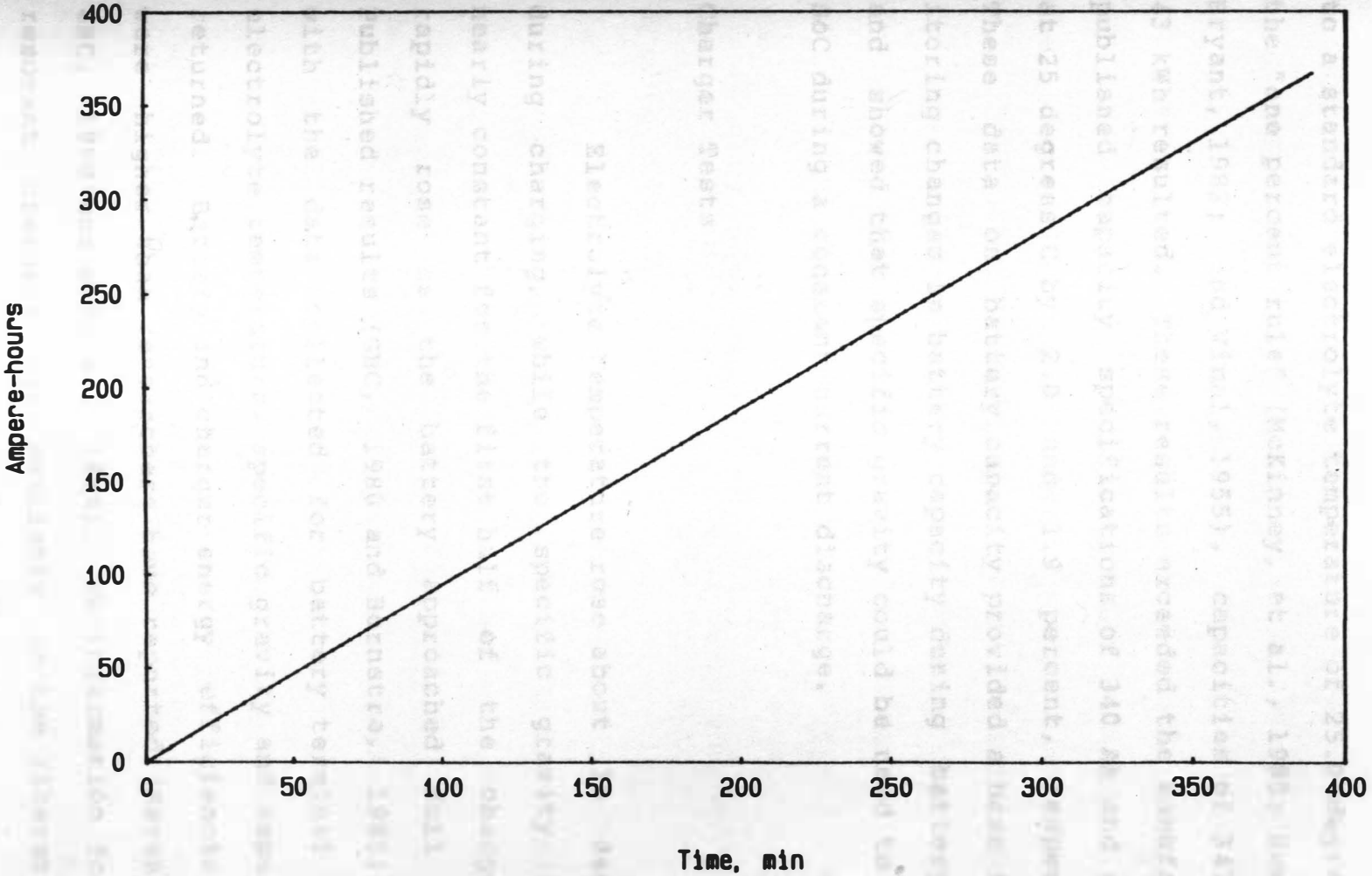

Figure 14. Battery ampere-hours during discharge at the constant-current, six-hour rate.

to a standard electrolyte temperature of 25.0 degrees C by the "one percent rule" (McKinney, et al., 1983; Hewitt and Bryant, 1982; and Vinal, 1955), capacities of 347 Ah and 43 kWh resulted. These results exceeded the manufacturers published capacity specifications of 340 Ah and 42.2 kWh at 25 degrees C by 2.0 and 1.9 percent, respectively. These data on battery capacity provided a base for monitoring changes in battery capacity during battery life, and showed that specific gravity could be used to monitor SoC during a constant-current discharge.

Charger Tests

Electrolyte temperature rose about 10 degrees C during charging, while the specific gravity remained nearly constant for the first half of the charge, then rapidly rose as the battery approached full charge. Published results (GBC, 1980 and Hornstra, 1985) agreed with the data collected for battery terminal voltage, electrolyte temperature, specific gravity and ampere-hours returned. Battery and charger energy efficiencies found were higher than researchers have reported (Marsh, 1981; GBC, 1980 and Schober, 1984). No information for ferroresonant chargers was available in the literature concerning the remaining parameters measured.

The ac 240 voltage supplied to the charger for the two charges averaged 237.6 V and 238.7 V with a variance of 3.45 and 2.38, respectively. The maximum values were 241.3 V in both cases, and minimum values were 234.2 V and 235.2 V, which means that the constant voltage output from the 240 ac outlet actually varied within a small range.

The ac current decreased slowly during the first 10 hours (h) of charging, then decreased rapidly for the next 3.5 h, and decreased slowly again for the last 3.5 h of charging (Figure 15). The initial ac current draw was about 33.5 A, and decreased to about 6.4 A. During the period of rapid decrease, the current reduced from about 20 A to about 7.5 A.

The dc voltage increased at a nearly constant rate for the first 10 h of charging, then increased rapidly for the next 1.5 h, and finally increased very slowly for the last five hours (Figure 16). The voltage jumped from 130 V to about 133 V while stabilizing during the first nine minutes of the charge. The voltage of the individual cell groups followed a similar pattern.

The dc current curve followed the same pattern as the ac current (Figure 17). It began at about 35.3 A, decreased to about 7.8 A, and dropped about 18 A during the period of rapid decline. Four times during testing a

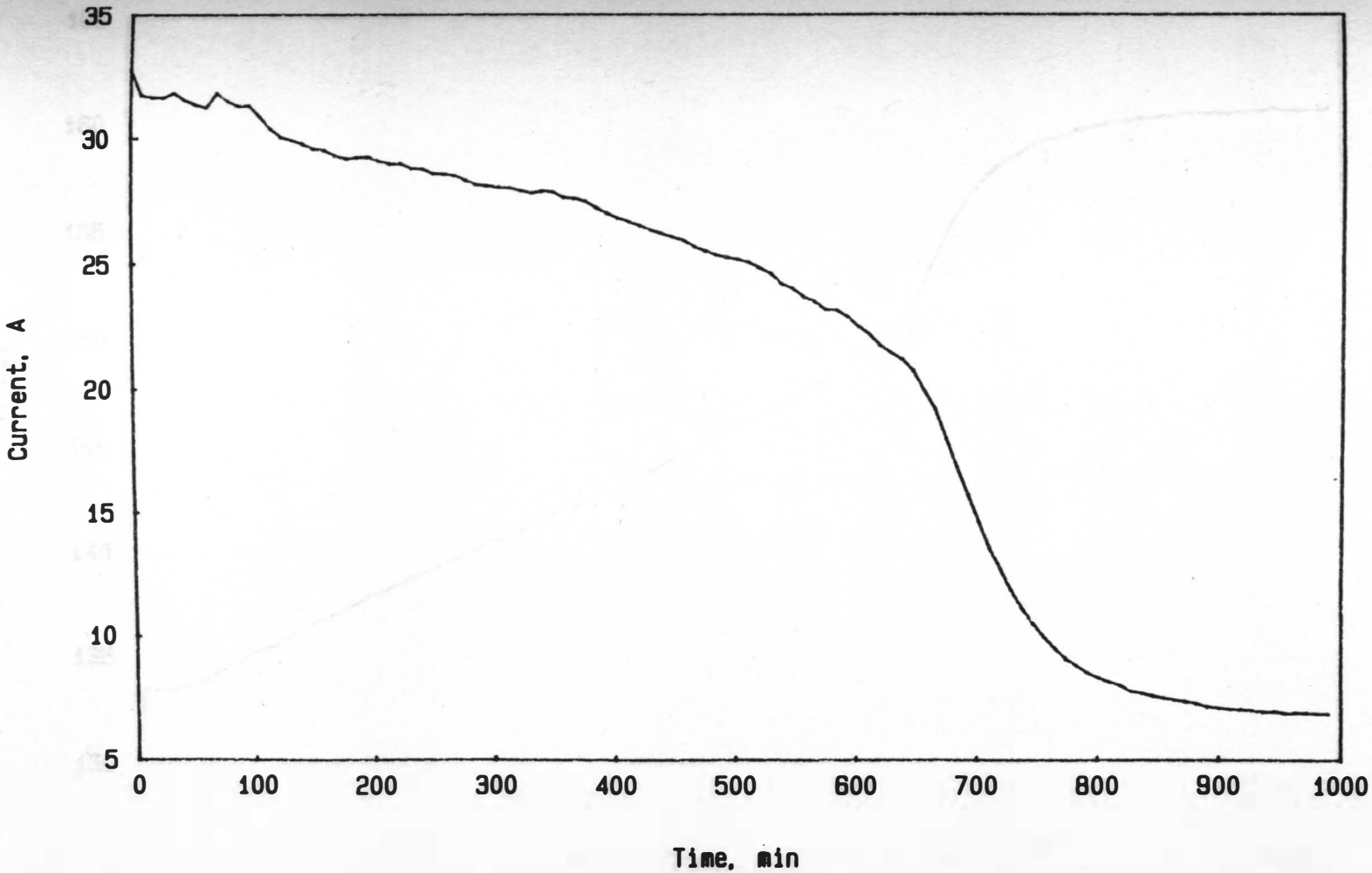

Figure 15. Ac current required for charger operation.

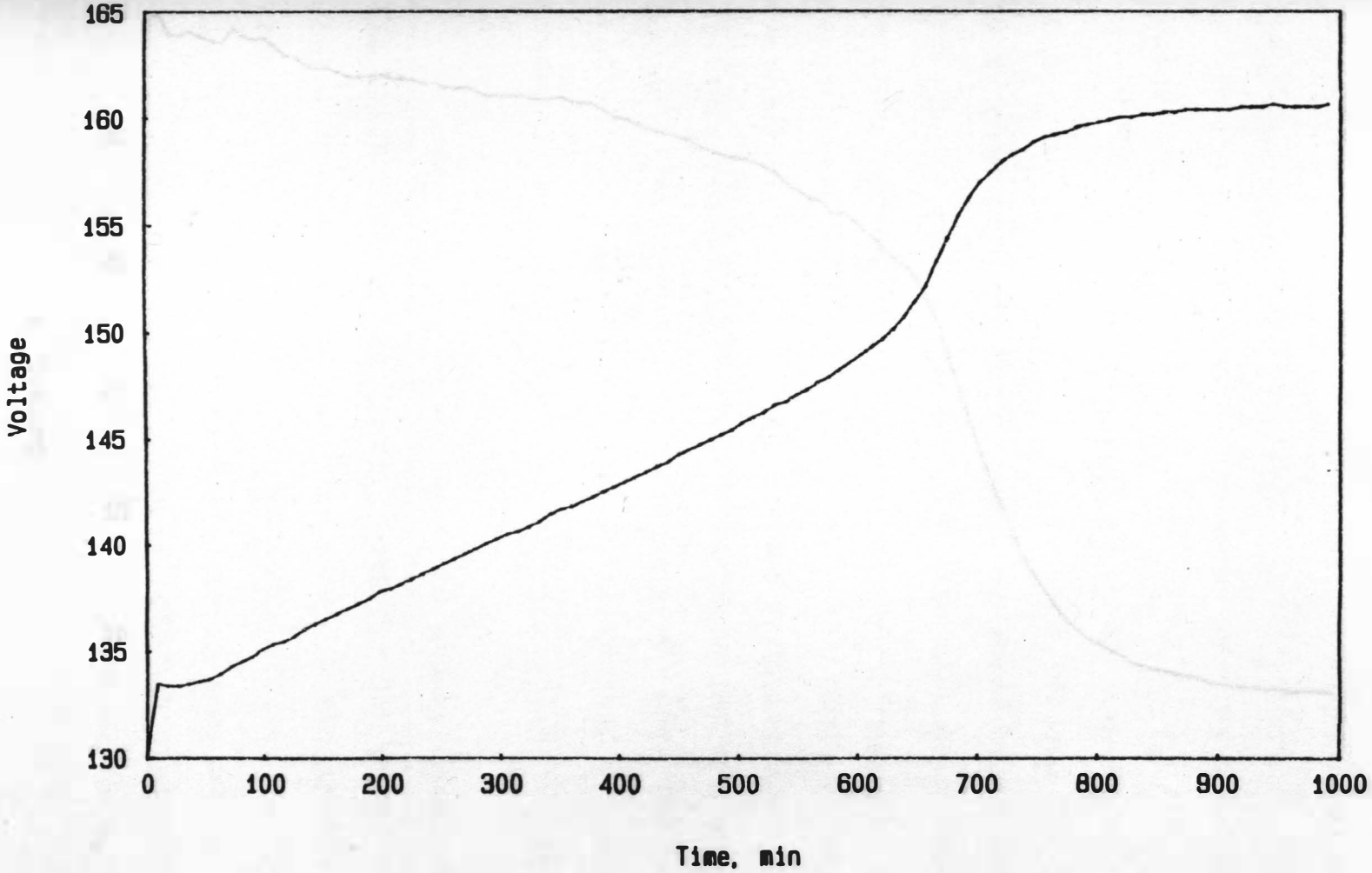

Figure 16. Battery terminal voltage during charging.

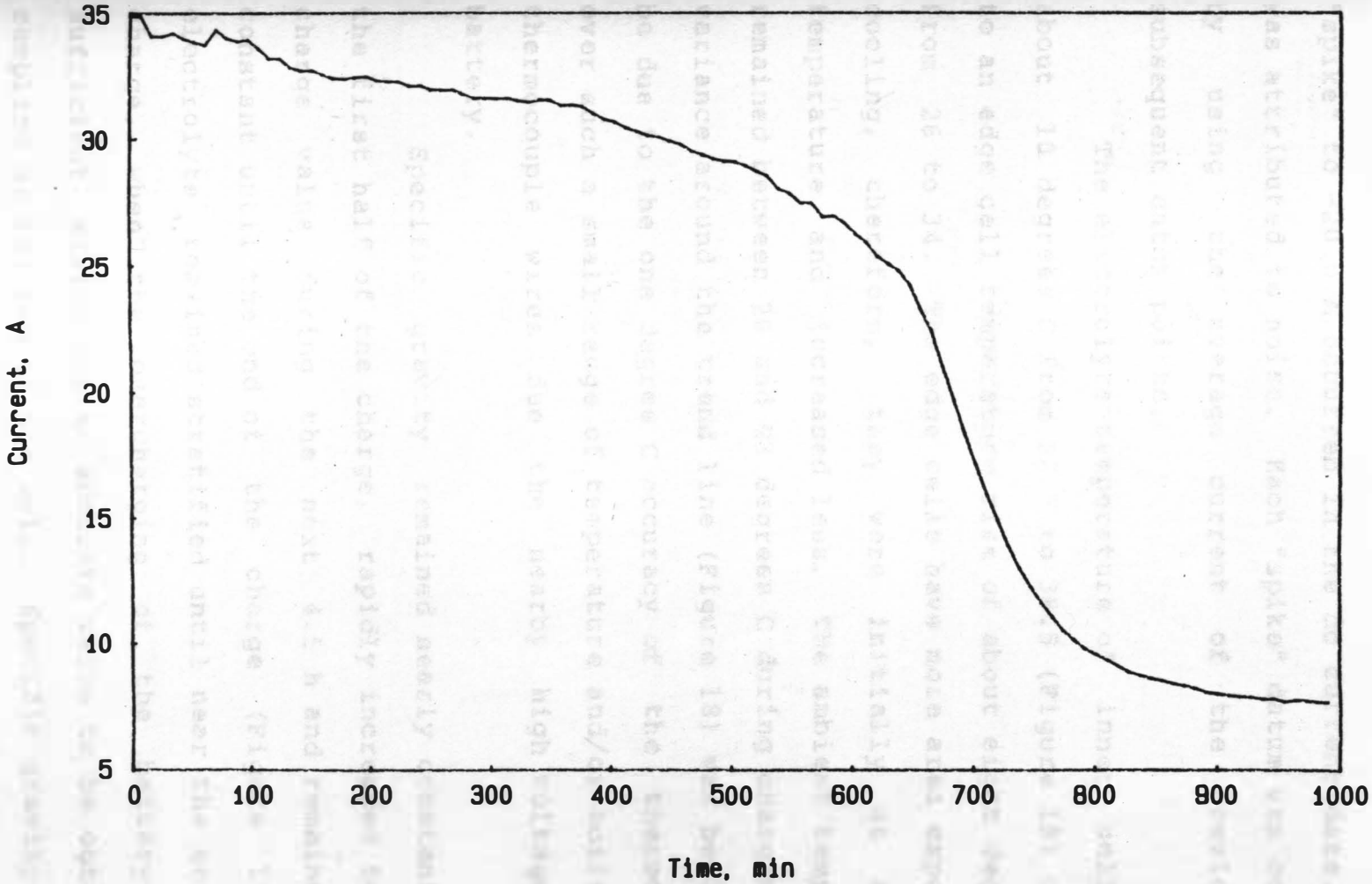

Figure 17. Dc current to the battery during charging.

"spike" to -20.0 A occurred in the dc current data, which was attributed to noise. Each "spike" datum was corrected by using the average current of the previous and subsequent datum points.

The electrolyte temperature of inner cells rose about 10 degrees C from 28.5 to 38.5 (Figure 18) compared to an edge cell temperature rise of about eight degrees C from 26 to 34. The edge cells have more area exposed for cooling, therefore, they were initially at a lower temperature and increased less. The ambient temperature remained between 20 and 23 degrees C during charging. The variance around the trend line (Figure 18) was believed to be due to the one degree C accuracy of the thermocouples over such a small range of temperature and/or noise in the thermocouple wires due the nearby high voltage of the battery.

Specific gravity remained nearly constant during the first half of the charge, rapidly increased to a full charge value during the next 4.5 h and remained about constant until the end of the charge (Figure 19). All electrolyte remained stratified until near the end of the charge, when the overcharging of the battery caused sufficient mixing for an accurate value to be obtained by sampling at the top of the cell. Specific gravity in one test cell was consistently 0.010 to 0.020 higher than the

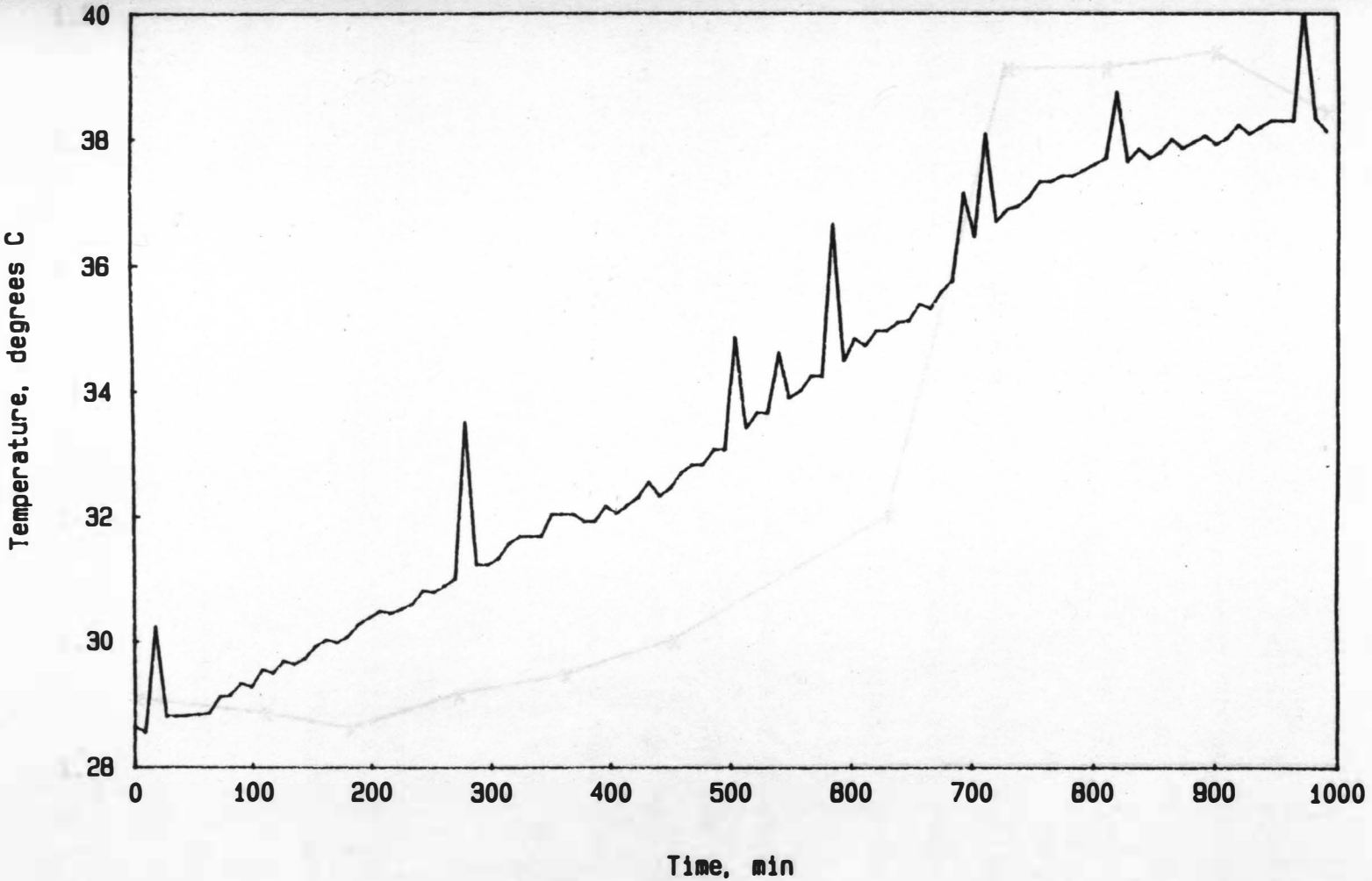

Figure 18. Battery electrolyte temperature during charging.

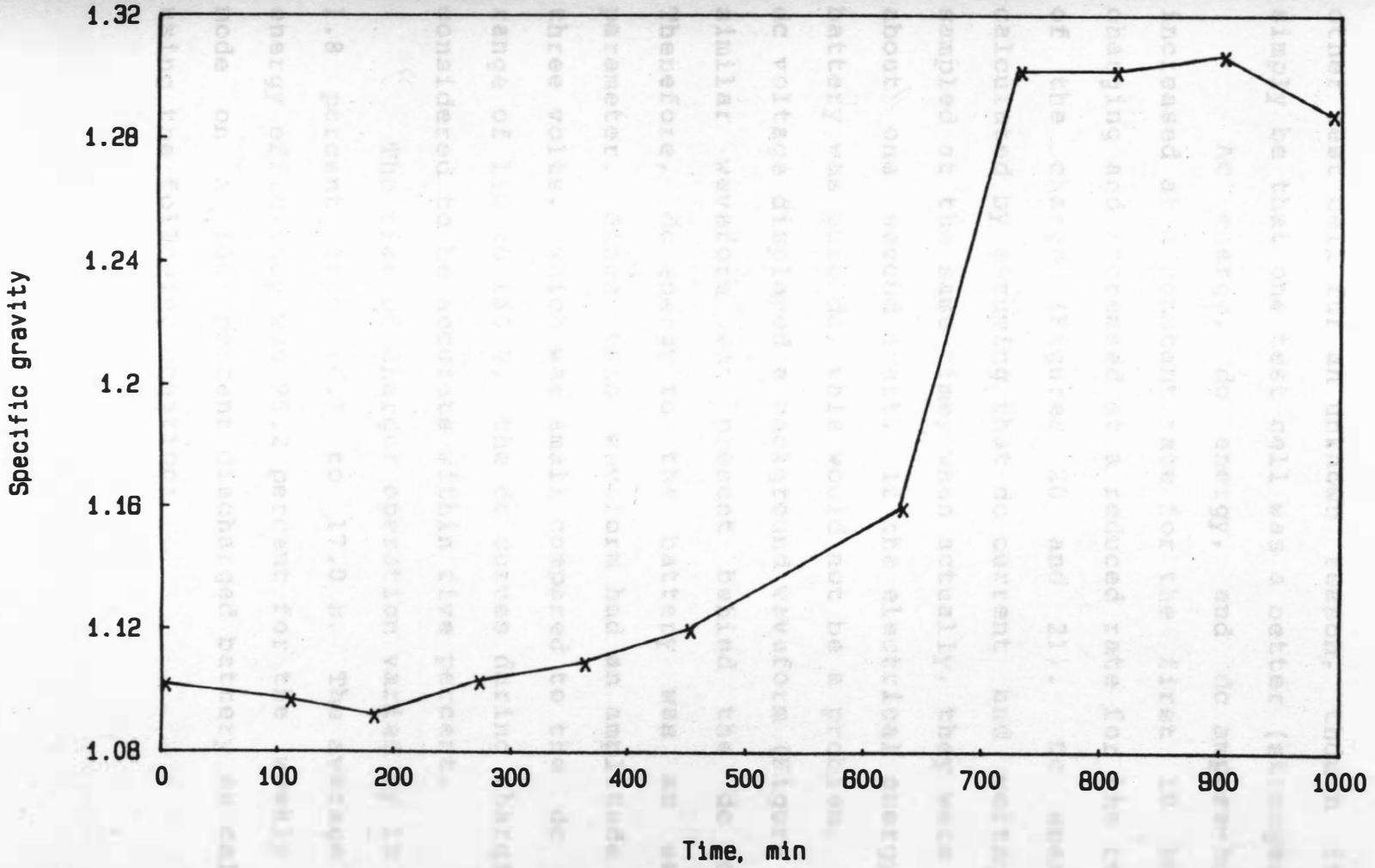

Figure 19. Battery specific gravity during charging.

other test cell for an unknown reason, though it could simply be that one test cell was a better (stronger) cell.

Ac energy, dc energy, and dc ampere-hours all increased at a constant rate for the first 10 hours of charging and increased at a reduced rate for the remainder of the charge (Figures 20 and 21). Dc energy was calculated by assuming that dc current and voltage were sampled at the same time, when actually, they were sampled about one second apart. If the electrical energy to the battery was pure dc, this would not be a problem, but the dc voltage displayed a background waveform (Figure 22). A similar waveform was present behind the dc current. Therefore, dc energy to the battery was an estimated parameter. Since this waveform had an amplitude of only three volts, which was small compared to the dc voltage range of 130 to 160 V, the dc curves during charging were considered to be accurate within five percent.

The time of charger operation varied by 18 min or 1.8 percent from 16.7 to 17.0 h. The average charger energy efficiency was 95.2 percent for the weekly charge mode on a 100 percent discharged battery as calculated using the following equation:

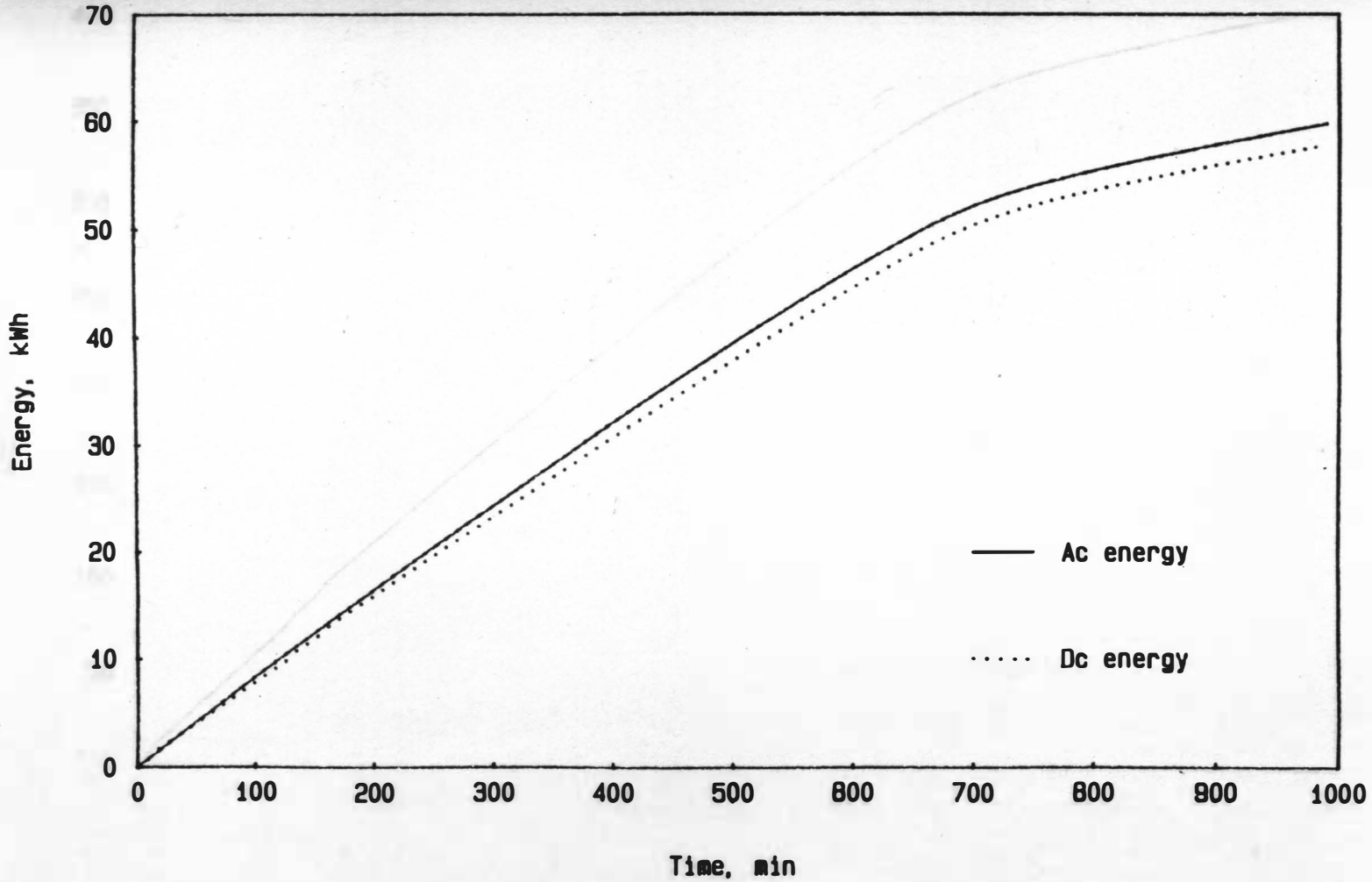

Figure 20. Ac energy required for charger operation and dc energy returned to the battery during charging.

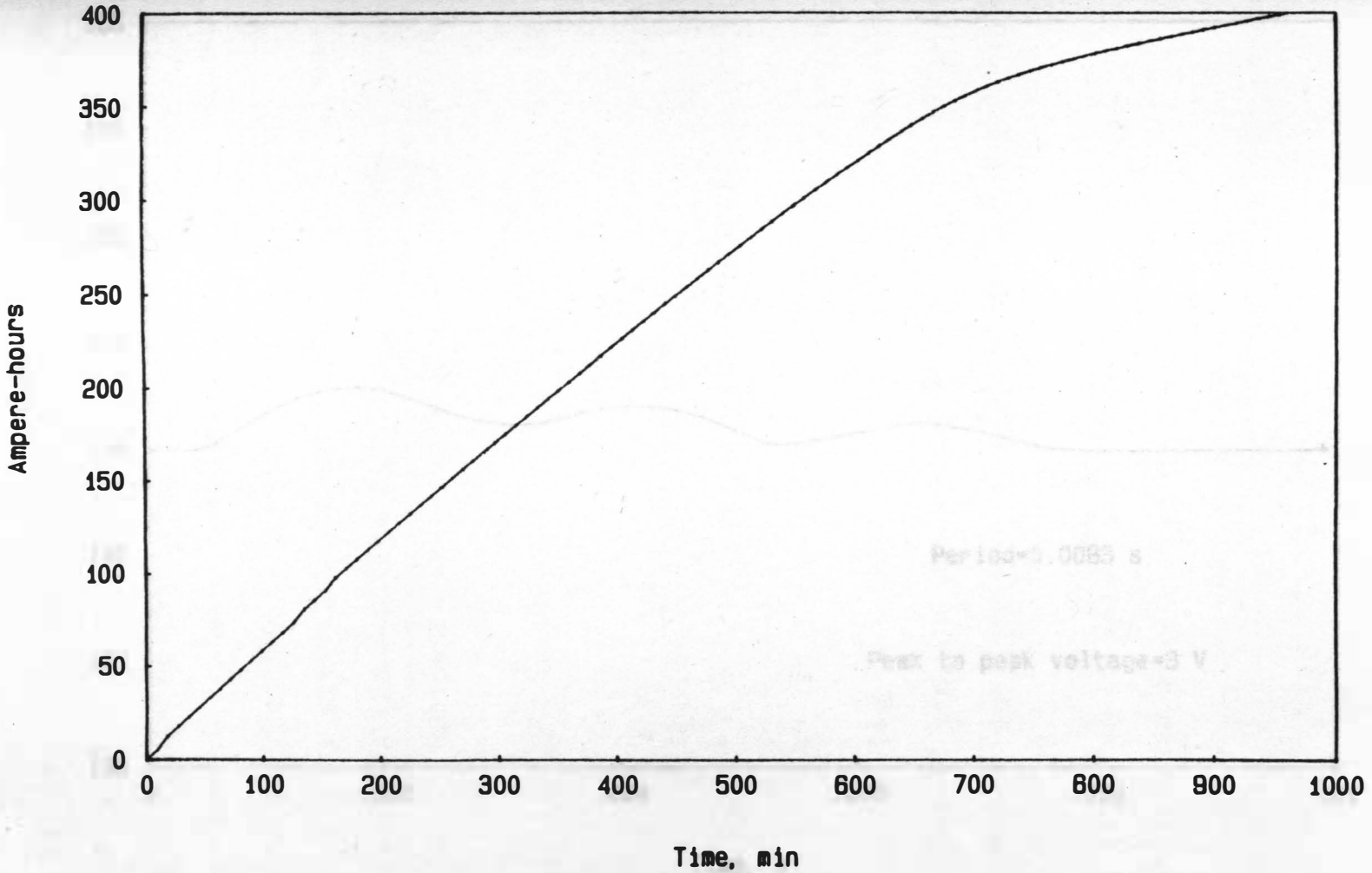

Figure 21. Dc ampere-hours returned to the battery during charging.

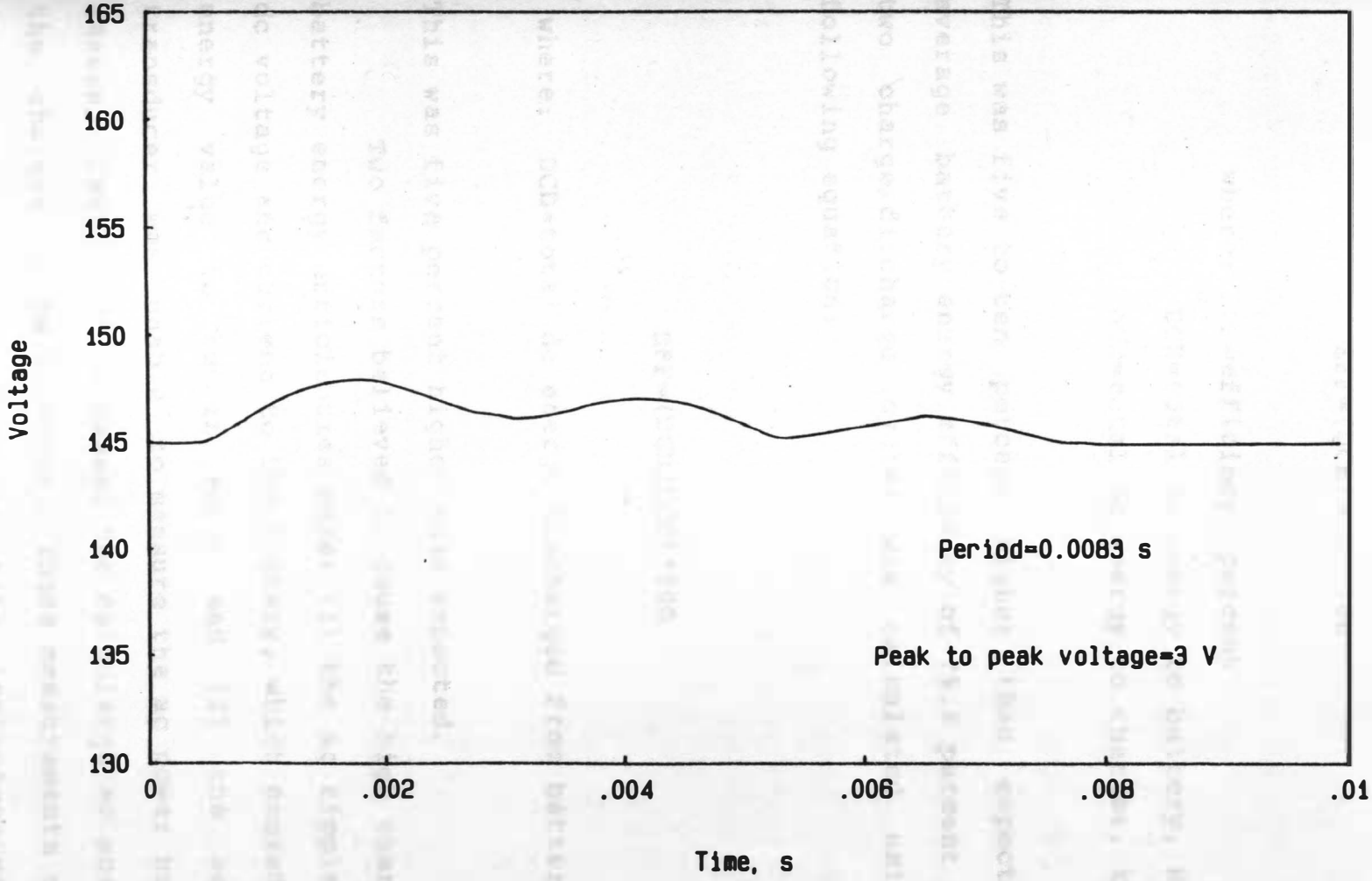

Figure 22. Ac ripple in dc voltage from charger.

$$EFF=(DCE/ACE)*100$$

where: EFF=efficincy, percent

DCE=total dc energy to battery, kWh

ACE=total ac energy to charger, kWh

This was five to ten percent higher than expected. An average battery energy efficiency of 79.6 percent for the two charge/discharge cycles was calculated using the following equation:

$$EFF=(DCD/DCE)*100$$

where: DCD=total dc energy discharged from battery, kWh

This was five percent higher than expected.

Two factors believed to cause the high charger and battery energy efficiencies were: (1) the ac ripple in the dc voltage and current to the battery, which caused the dc energy value to be in error and (2) the ac power transducer was unable to measure the ac power harmonics (Reese, 1983), which caused the calculated ac energy to the charger to be in error. These measurements could be checked using power meters to take instantaneous power

readings, and by calculating the efficiency from the instantaneous power. Due to time constraints this was not attempted.

The charger tests determined the charging profile of the ferroresonant charger and indicated that a 10 degrees C temperature rise could be expected during charge. They also demonstrated that, due to slow response time, specific gravity measurements could not be used to indicate the amount of charge returned to the battery. This information was helpful during field tests when trying to determine, if the battery was fully charged after a period on-charge.

Vehicle Tests

Loader Tests

The loader tests evaluated the effect of temperature, load, motor speed and DOD on the current required by the PTO/HYD motor. Current, rather than power, was used as the dependent variable because current was easier to measure and is directly related to power. To obtain more degrees of freedom for statistical analyses, each six-second test was divided into three subsets. Each subset contained six values of current and voltage. Five

of these values were randomly selected and used to calculate mean current and voltage. The data contained scattered spurious readings of 10,000 billion A and 0 V, which were rejected as physically impossible because they were out of the following plausible ranges: (1) 0 to 1000 A and (2) 50 to 200 V.

The analysis of variance was conducted three times with different temperature groupings each time. All four temperatures were considered separately, similar battery temperatures (plus or minus four degrees C) were considered together and similar environment temperatures (plus or minus 6.5 degrees C) were considered together.

Increasing the load from operating the hydraulic pump to lifting 4.27 kN in the loader increased current required by 80 to 100 percent. Increasing motor speed from 800 to 1500 r/min increased current required by 100 to 120 percent. Ambient temperatures increasing from 3 to 24 degrees C decreased current required 20 to 30 percent. These effects were significant at the 0.05 level when similar environmental temperatures were considered together. DOD displayed no discernible trends while interacting with all other variables. All possible variable interactions had a significant effect (0.05 level) on the current required.

Results from a comparison of the analysis of variance outcome for each different temperature grouping suggested that temperatures below 10 degrees C affect tractor components rather than the battery. During the test conducted with an ambient temperature of five degrees C and an electrolyte temperature of 30 degrees C, the electrolyte temperature remained near 30 degrees C due to the discharge energy inefficiency. However, the hydraulic system temperature, originally at 30 degrees C, rapidly dropped toward ambient during the test. If the temperature effect was due to the change in electrolyte temperature, the analysis of variance with the same battery temperatures together should have shown a significant effect due to temperature, but this did not happen. Instead, the analysis with similar environment temperatures grouped together demonstrated a significant effect for temperature. This result suggested that the cold weather affected the hydraulics rather than the battery. Subjective assessment of the vehicle during tests showed a somewhat noiser and stiffer hydraulic system during cold weather. Earlier test results (Vik, 1985) suggested that cold weather affected the gear train more than the battery.

Two important results were obtained from this testing: (1) DOD alone did not significantly affect the current required and (2) a decrease in ambient temperature significantly increased the current required. The first result indicated that at low power and SoC levels, the battery was able to provide the power needed without increasing the current flow a significant amount. This suggested that the effect of DOD on performance at low power levels can be neglected as long as DOD is between 0 and 80 percent. The second result indicated that, not only was capacity lowered at decreased temperatures, but the power required was increased. This power increase appeared to be caused by temperature effects on the vehicle components, rather than by temperature effects on the battery.

Pto Tests

The most pto power available on a continuous basis was 17.5 kW and occurred when the hydraulic pump was not connected and the feedback system was switched on (Table 8). This combination was the most efficient at 80 percent instantaneous efficiency calculated as follows:

$$EFF=(PP/BP)*100$$

where: EFF=efficiency, percent
PP=instantaneous pto power, kW
BP=instantaneous battery power, kW

Operating the PTO/HYD motor without the hydraulic pump connected increased power from 12.2 to 17.5 kW and 11.4 to 15.6 kW with and without feedback, respectively. Apparently four to five kW were wasted pumping hydraulic oil past the pressure relief valve. If the pto and hydraulic pump were operated by separate motors, a power increase of 30 to 40 percent with an efficiency increase of four to ten percent would be available at the pto power shaft using the same size motor. Torque variance was less when the hydraulic pump was not connected, which indicated that a steadier output power was then available. The steadier, increased power available without the hydraulic pump suggested that the option of separate motors for the pto and hydraulic systems would result in a more energy efficient vehicle.

Table 8. Pto motor, dynamometer test maximums with hydraulics connected and disconnected.[1]

Parameters	Test 1	Test 2	Test 3	Test 4
Pto power, kW	11.4	12.2	15.6	17.5
Battery power, kW	17.2	19.6	20.0	21.8
Efficiency, %	68.2	77.2	78.6	80.6
Torque, Nm	211.1	197.1	276.3	291.3
Pto speed, r/min	538.5	600.9	541.1	573.2
Current, A	137.1	155.6	161.6	177.5
Operation time, min	150.0	104.0	114.0	87.0

[1]Test 1 was with hydraulic pump and without feedback.
Test 2 was with hydraulic pump and with feedback.
Test 3 was without hydraulic pump and without feedback.
Test 4 was without hydraulic pump and with feedback.

The motor speed control lever had to be set higher to obtain the same power setting during those tests with feedback control. Pto speed was set higher than 540 r/min during these tests because the pto speed would either be stable at 500 r/min or at 600 r/min and points between were unattainable. A possible explanation for this phenomena was provided by the controller design (Helder, 1985). The silicon-controlled-rectifier (SCR) that controls current flow becomes saturated at 95 percent of maximum current flow, beyond which by-pass connectors engage allowing full current flow. There are no

intermediate settings between 95 to 100 percent current flow with this design. Speed control was noted to be in by-pass mode during one of the two tests with feedback.

The pto speed and motor current suddenly decreased about five minutes into the test without hydraulics and with feedback, and just as suddenly increased back to their former levels about 20 min later even though the speed control remained in the same position. The only satisfactory explanation was that the feedback control, which had not been tested at high pto speeds and loads, was malfunctioning. Due to these problems, the tests with and without feedback were not comparable.

Current suddenly decreased 60 minutes into the test before stabilizing at 70 A in both tests without feedback control (Figure 23). A postulated explanation was that the SCR reduced the current flow to prevent controller overheating, which was supported by the amount of heat emanating from the SCR. To check this explanation, the test without hydraulics and without feedback was repeated with a fan cooling the SCR. The current continued a steady, slow decline with no rapid decline, providing evidence supporting this explanation. Therefore, the SCR must be kept cool if continuous pto operation at a power level near by-pass mode is desired.

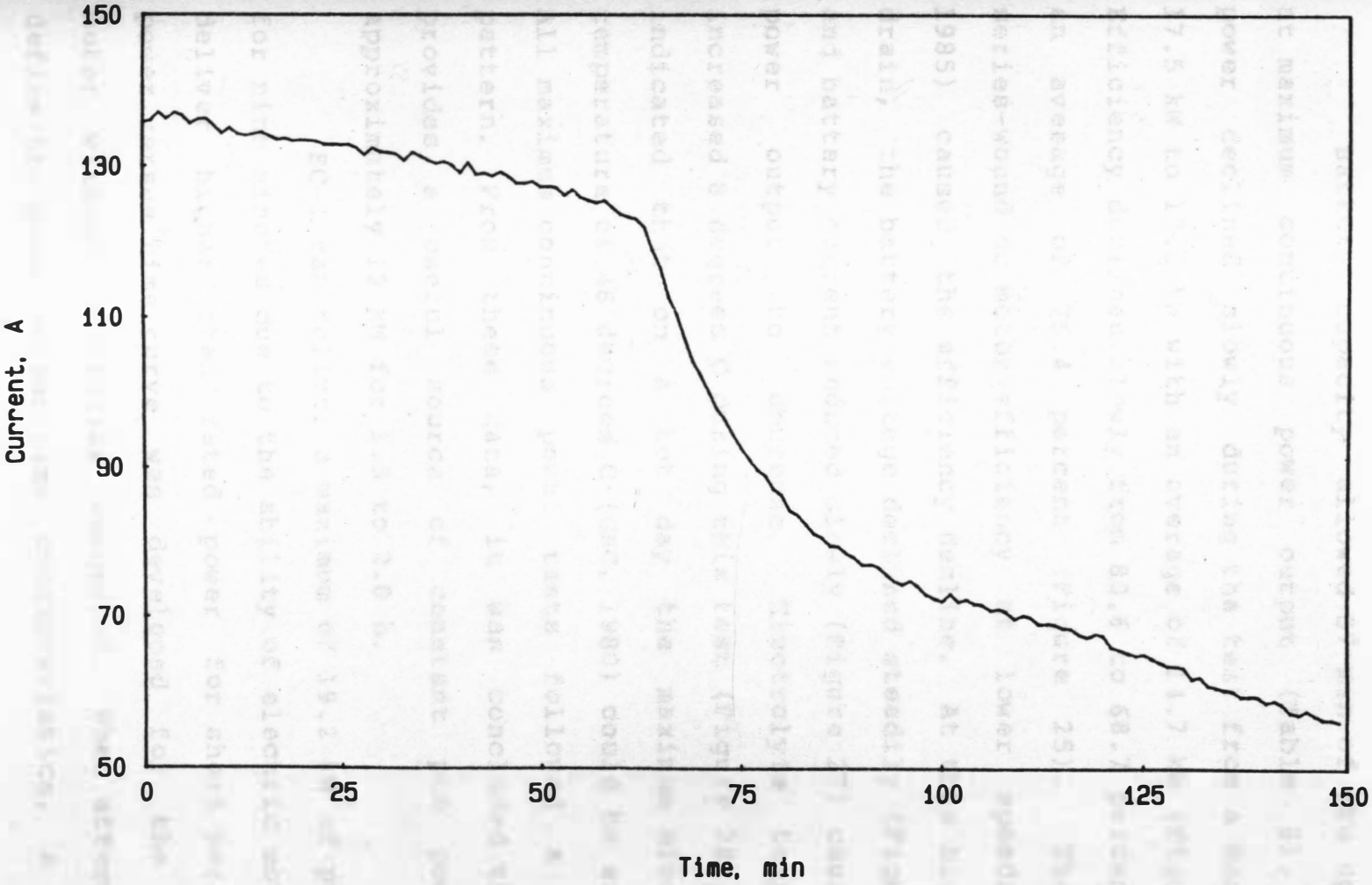

Figure 23. Battery current required to operate pto without feedback.

Battery capacity allowed 87 min of pto operation at maximum continuous power output (Table 8). Output power declined slowly during the test from a maximum of 17.5 kW to 12.0 kW with an average of 14.7 kW (Figure 24). Efficiency declined slowly from 80.6 to 68.7 percent with an average of 76.4 percent (Figure 25). The lower series-wound dc motor efficiency at lower speeds (Vik, 1985) caused the efficiency decline. At this high power drain, the battery voltage declined steadily (Figure 26), and battery current reduced slowly (Figure 27) causing the power output to decrease. Electrolyte temperature increased 8 degrees C during this test (Figure 28), which indicated that on a hot day the maximum electrolyte temperature of 46 degrees C (GBC, 1980) could be exceeded. All maximum continuous power tests followed a similar pattern. From these data, it was concluded that EC-I provides a useful source of constant pto power of approximately 12 kW for 1.5 to 2.0 h.

EC-I can deliver a maximum of 19.2 kW of pto power for nine minutes due to the ability of electric motors to deliver higher than rated power for short periods. A power versus time curve was developed for the PTO/HYD motor without hydraulics connected. When attempting to define the power versus time characteristics, a 90 min

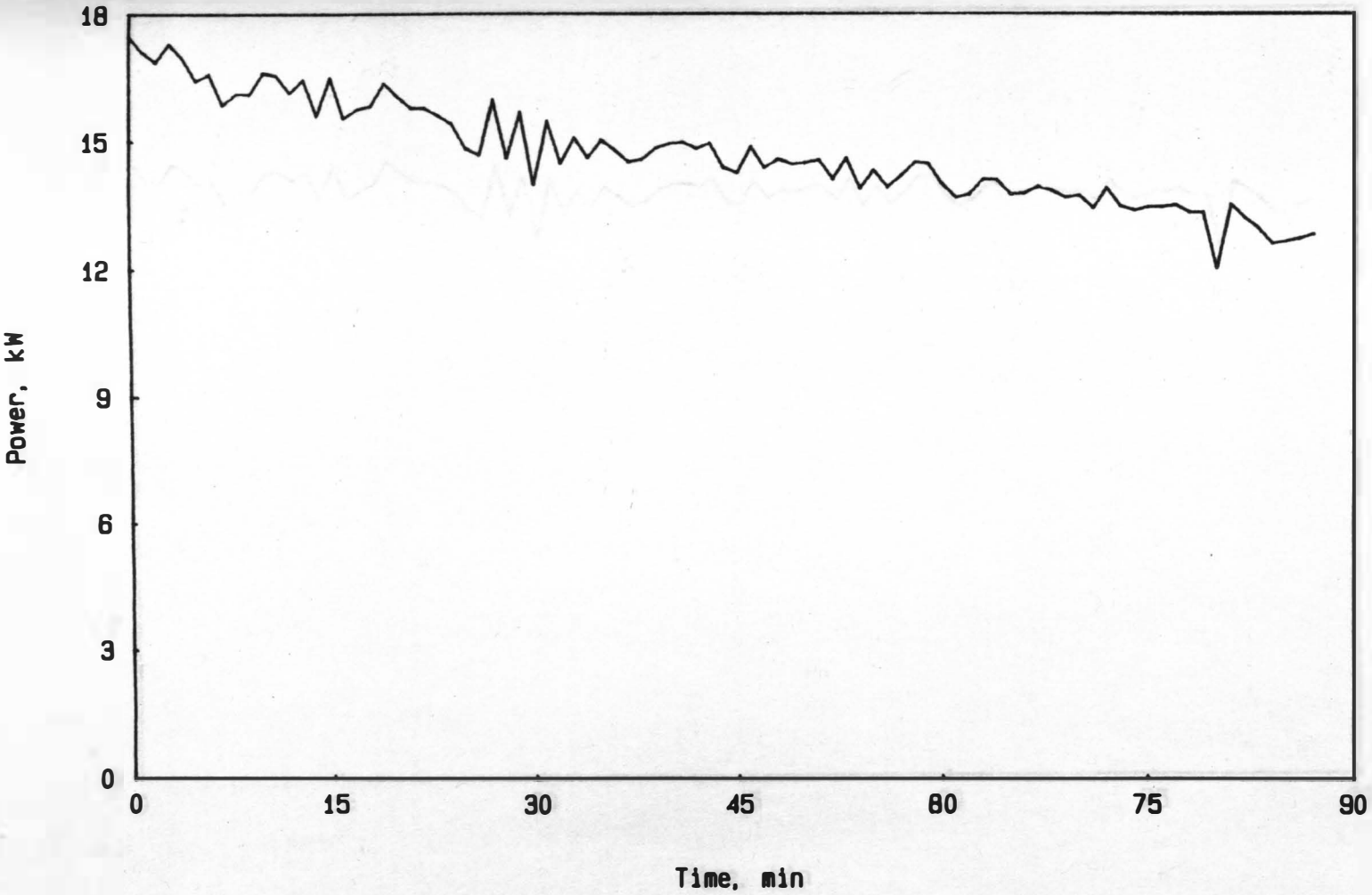

Figure 24. Maximum continuous pto power with feedback and without hydraulic pump.

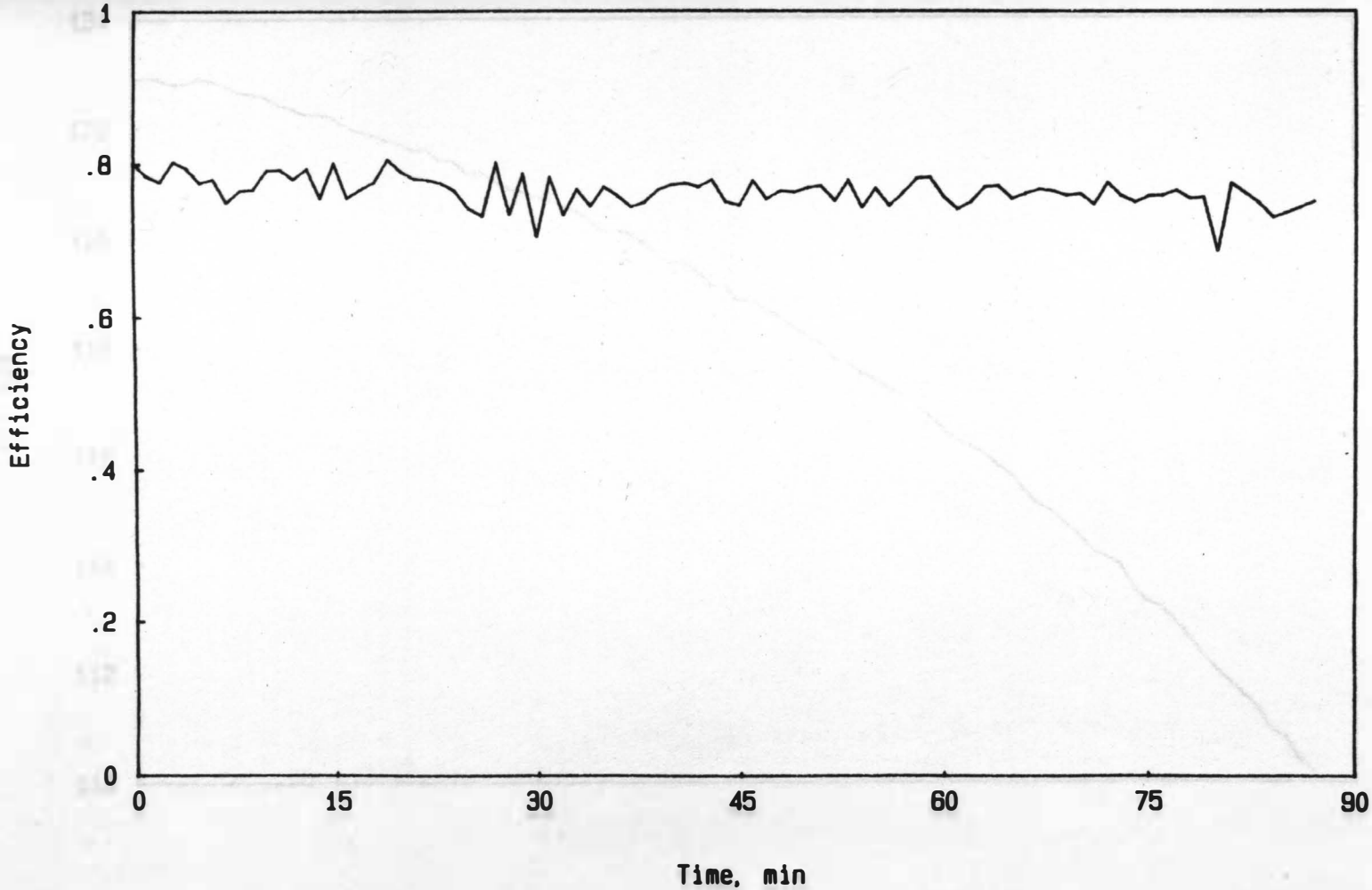

Figure 25. Pto efficiency at maximum continuous power with feedback and without hydraulic pump.

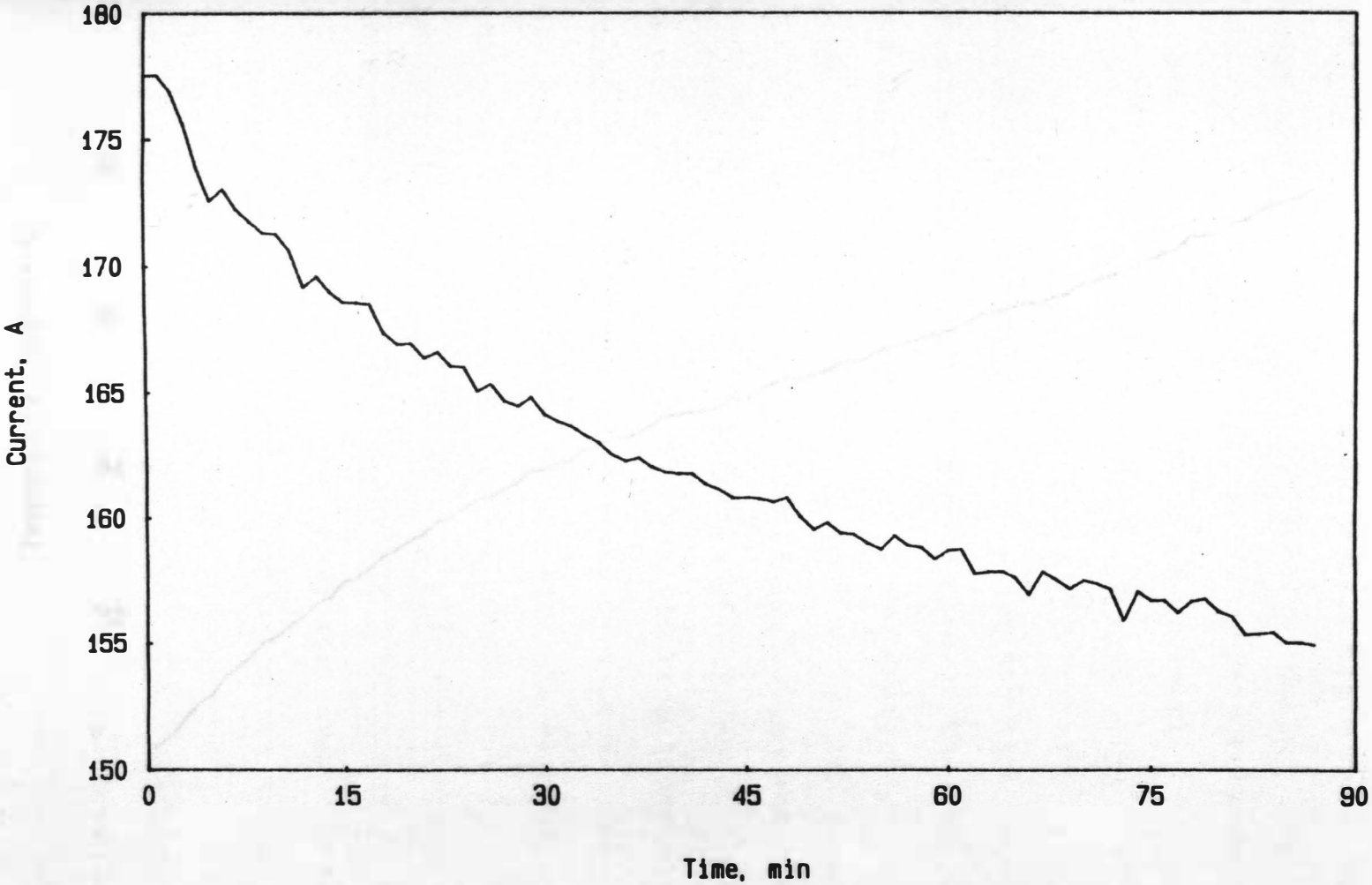

Figure 27. Battery current during continuous pto operation at maximum power with feedback and without hydraulic pump.

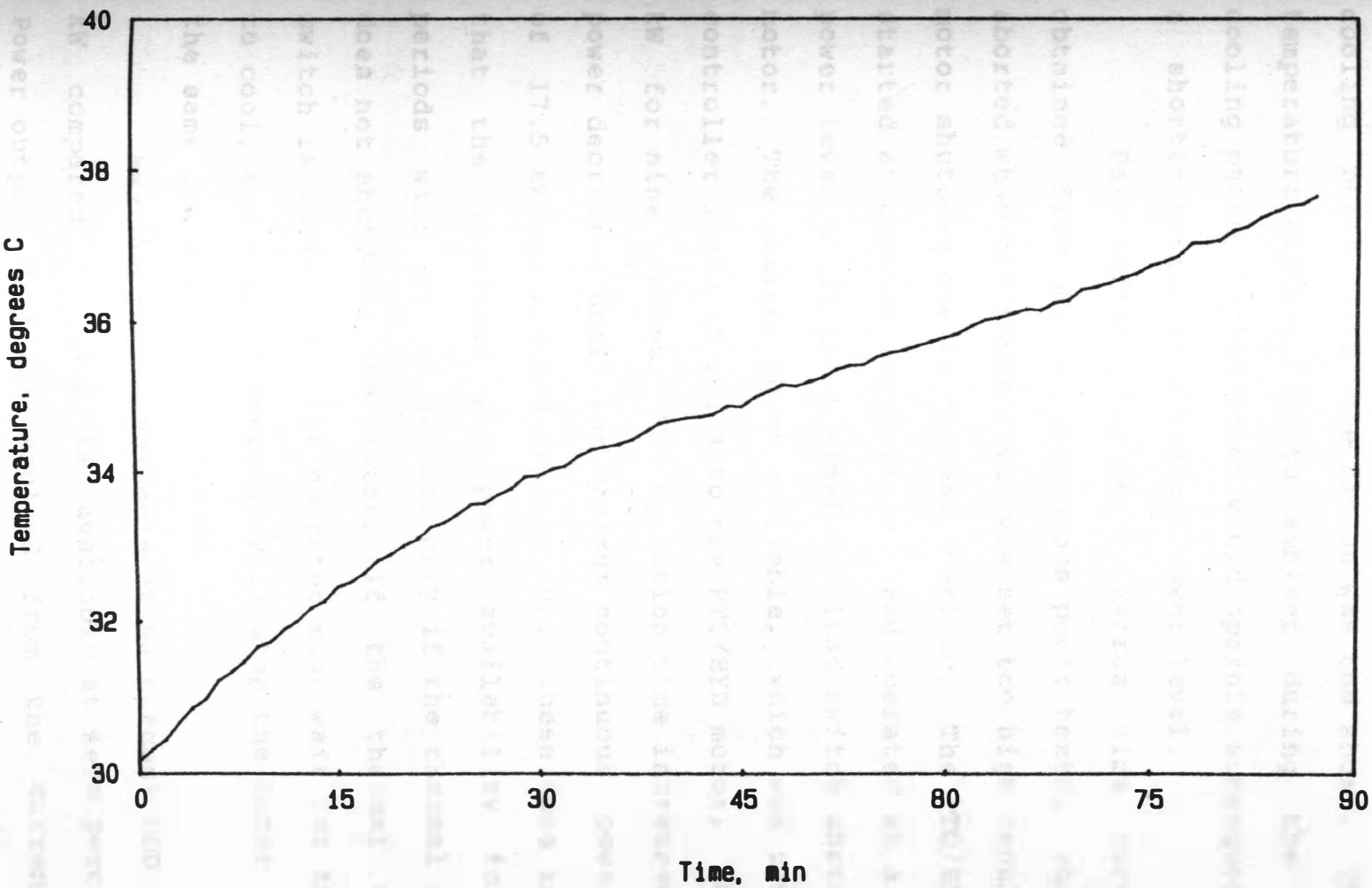

Figure 28. Battery electrolyte temperature during continuous pto operation at maximum power with feedback and without hydraulic pump.

cooling phase with the fan on was too short. The motor temperature did not cool to ambient during the 90 min cooling phase, so the motor would operate subsequently for a shorter period at a reduced power level.

Data defining the power versus time curve were obtained from maximum continuous power tests, which were aborted when the power level was set too high resulting in motor shutdown due to thermal overload. The PTO/HYD motor started at ambient temperature, and operated at a certain power level until the thermal overload switch shutdown the motor. The maximum power available, which was set by the controller limit of 200 A to the PTO/HYD motor, was 19.2 kW for nine minutes. The operation time increased as the power decreased until the maximum continuous power level of 17.5 kW was reached (Figure 29). These data indicated that the increased pto power availability for short periods will be of benefit only if the thermal overload does not shutdown the motor. If the thermal overload switch is activated, the operator must wait for the motor to cool, and thermal overload will stop the motor again if the same operation is continued.

Maximum power available at 80 percent DOD was 14 kW compared to 19.2 kW available at zero percent DOD. Power output decline resulted from the current limit imposed on the PTO/HYD motor by the controller and the

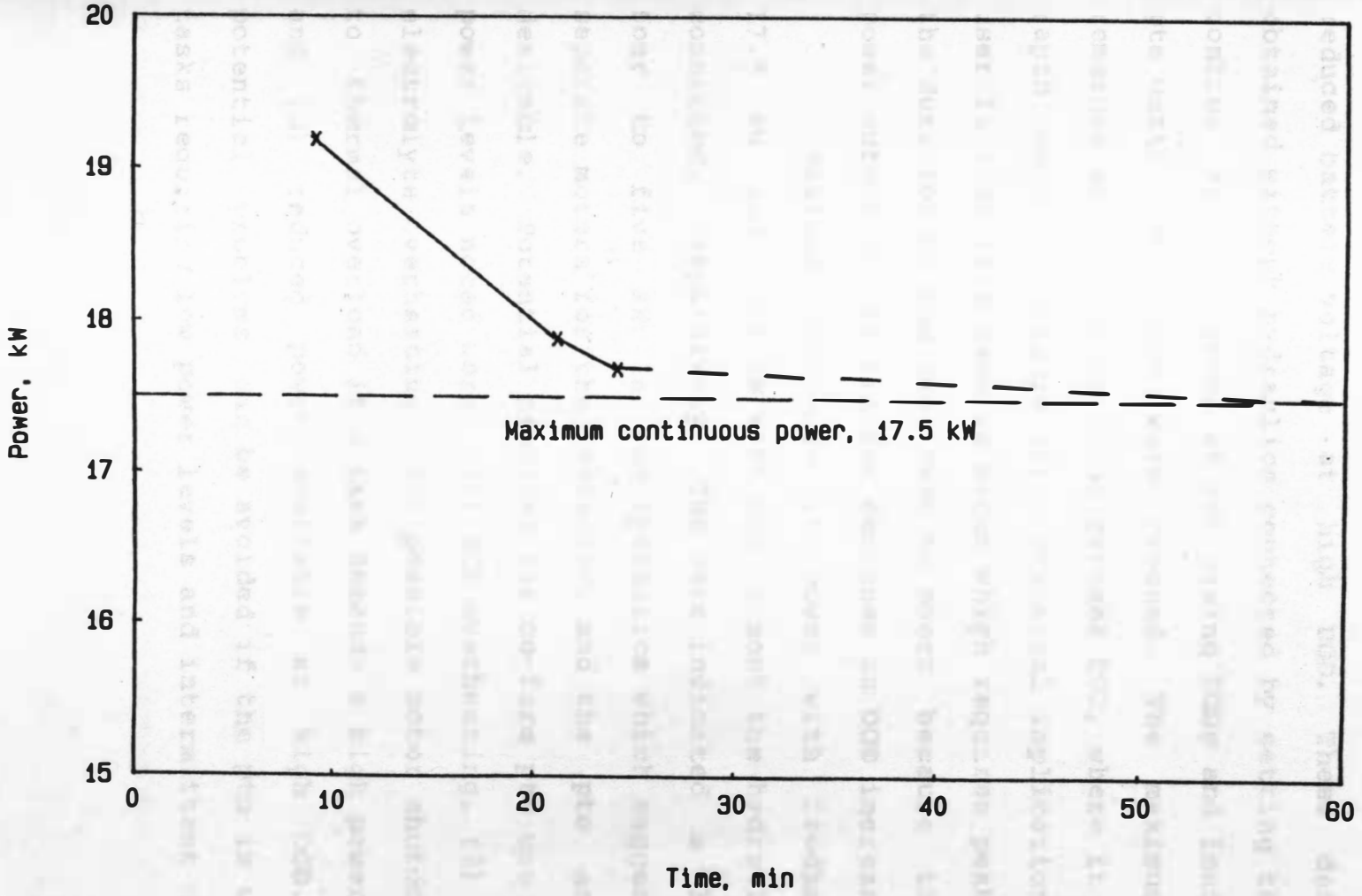

Figure 29. Maximum power versus time characteristics of PTO/HYD motor.

reduced battery voltage at high DOD. These data were obtained without hydraulics connected by setting the speed control at full speed at increasing DODs and loading the pto until 540 r/min were reached. The maximum power remained at 19.2 kW until 30 percent DOD, where it began a rapid decline (Figure 30). Practical implication to the user is that if a task is begun which requires peak power, the duration of the task must be short because the peak power output of the tractor declines as DOD increases.

Maximum continuous pto power with feedback was 17.5 kW and 12.2 kW with and without the hydraulic pump connected, respectively. The data indicated a loss of four to five kW in the hydraulics which suggests that separate motors for the hydraulics and the pto are more desirable. Potential problems for on-farm pto use at high power levels noted were: (1) SCR overheating, (2) battery electrolyte overheating, (3) possible motor shutdown due to thermal overload if a task demands a high power level, and (4) reduced power available at high DOD. These potential problems can be avoided if the pto is used for tasks requiring low power levels and intermittent duty.

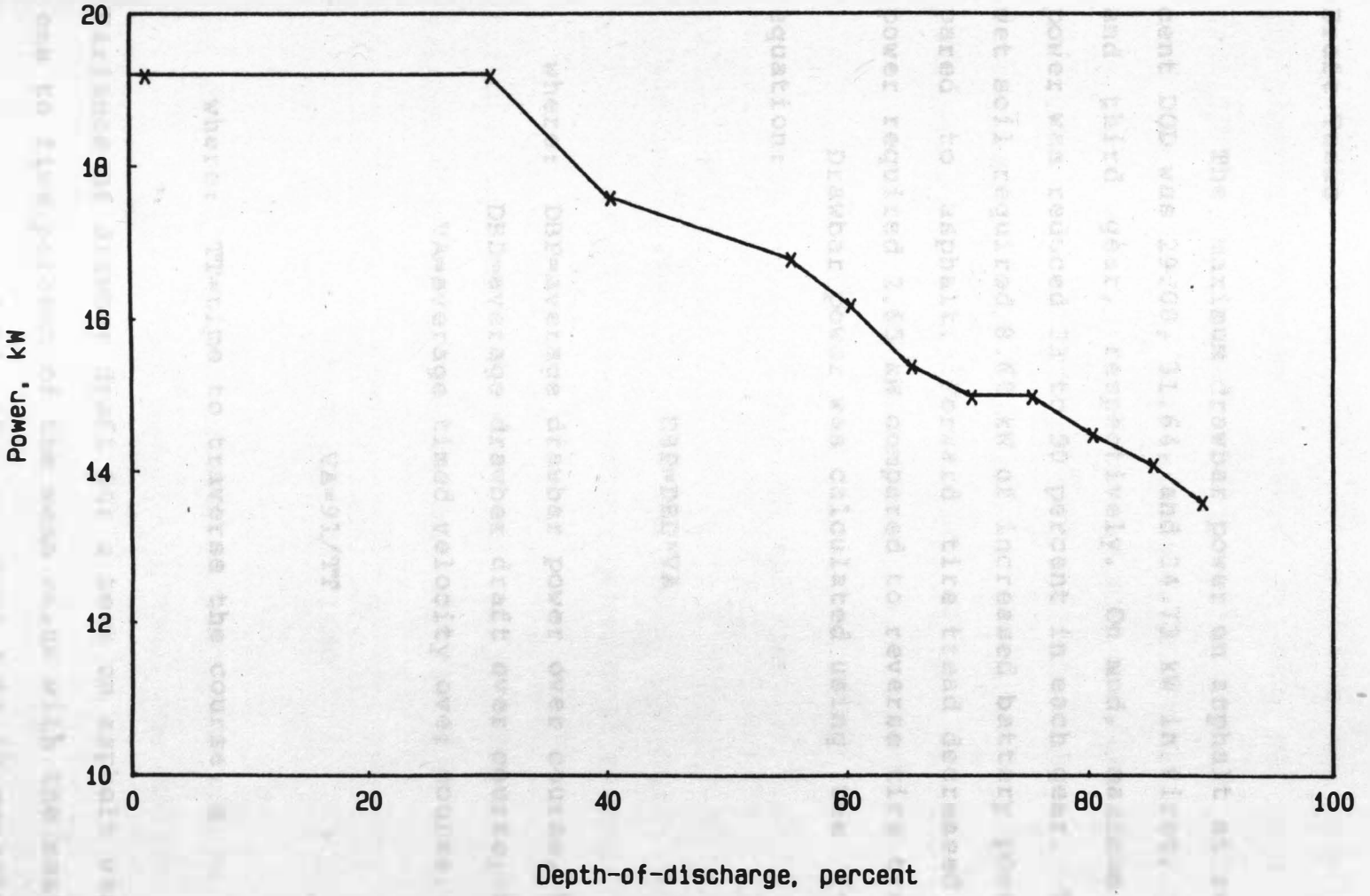

Figure 30. Power versus DOD level characteristics of PTO/HYD motor.

Draft Tests

The maximum drawbar power on asphalt at zero percent DOD was 29.00, 31.64, and 34.73 kW in first, second, and third gear, respectively. On mud, maximum drawbar power was reduced 33 to 50 percent in each gear. Tests on wet soil required 8.68 kW of increased battery power compared to asphalt. Forward tire tread decreased battery power required 2.65 kW compared to reverse tire tread.

Drawbar power was calculated using the following equation:

$$DBP=DBD*VA$$

where: DBP=average drawbar power over course, kW
DBD=average drawbar draft over course, kN
VA=average timed velocity over course, m/s

$$VA=91/TT$$

where: TT=time to traverse the course, s

Variance of drawbar draft for a test on asphalt was about one to five percent of the mean value with the maximum and minimum values within plus or minus 4 to 10 percent of the

mean. This was slightly greater than the plus or minus one percent typically achieved at the Nebraska tractor test course (Sampson, 1985). Variance of the drawbar draft for a test on soil was about 20 to 30 percent of the mean value with the maximum and minimum values within plus or minus 20 to 50 percent of the mean, which was consistent with values other researchers have obtained (Stange, et al., 1982 and Bandy, et al., 1985).

Efficiency was defined as:

$$EFF=(DBP/ABP)*100$$

where: EFF=efficiency, percent
ABP=average battery power over course, kW

Battery power was found by multipling battery current and voltage together, since the battery was a dc source:

$$ABP=(C1*V1)/1000$$

where: C1=average battery current over course, A
V1=average battery voltage over course, V

Slip was calculated using the following equation:

$$SL=1-(VA/VT)$$

where: SL=average slip over course, percent

VT=theoretical velocity over course, m/s

Theoretical velocity was calculated from the number of wheel revolutions, the average rolling radius of the four wheels and the time to cover the course:

$$VT=(NR*RR)/TT$$

where: NR=number of wheel revolutions, dimensionless

RR=average rolling radius of the four wheels, m

RR=3.46 m

The number of wheel revolutions was calculated from traction motor rotational speed measured by the tachometer in EC-I, gear reduction and time to traverse the course:

$$NR=(RPM*TT)/(GR*60)$$

where: RPM=rotational speed of traction motor, r/min

GR=gear reduction from traction motor to wheel, dimensionless

An accuracy problem was encountered with the slip measurements. At low loads, the slip was calculated to be negative which is physically impossible. Two possible problems were identified: (1) the time for traversing the course was low and/or (2) the EC-I tachometer rotational speed measurement was low. A second person timed a number of course traverses to check the first problem, and the two times were always within one percent so the times were considered accurate. The second problem was checked using a handheld tachometer accurate to plus or minus one revolution per minute. The tachometer in EC-I was found to read low, and a linear regression of handheld tachometer values versus EC-I tachometer values (R^2=0.999) was used to correct the EC-I tachometer readings:

$$ADJT=0.986*TACH+41.591$$

where: ADJT=adjusted tachometer reading, r/min
TACH=original tachometer reading, r/min

However, the adjusted tachometer readings still resulted in a negative slip at light loads. It was felt that the slip values could be compared with each other, but all tended to be four to five percent low based on the most negative slip value of -4.83 percent. A judgement was

made, therefore, that five percent should be added to each slip value to obtain a more accurate value.[1] Accurate slip values were considered less important than other testing aspects, so no further attempt was made to obtain more accurate values.

Maximum drawbar power on asphalt was 34.73 kW in third gear with 6.47 percent slip and an efficiency of 59.9 percent (Table 9). Although the drawbar pull increased, maximum power and efficiency decreased with gear reductions due to lower gear box efficiency at greater gear reductions. As torque increased in low gears, motor speed decreased causing efficiency to decline, which is typical of a series-wound dc motor (Vik, 1985). Slip increased as the drawbar pull increased.

---

[1]The slip values reported are the actual slip values obtained, and it is left to the readers to adjust the slip values as they see fit.

Table 9. Maximum drawbar power[1] at zero percent DOD for each gear on asphalt.

Gear	Power, kW	Pull, kN	Efficiency, %	Slip, %
1[2][3]	29.00	36.0	65.8	13.40
2[3]	31.64	33.2	54.3	10.05
3	34.73	16.1	59.9	6.47

[1]Average of two tests.
[2]Power was limited by transmission maximum design load (Walker, 1985).
[3]Average of three tests.

Maximum drawbar power on wet soil was 23.70 kW in third gear with 9.57 percent slip and an efficiency of 44.8 percent (Table 10). The greatest pull was 22.7 kN, since the excessive slip in first gear prevented a larger pull from being developed. The soil cone index in the 0 to 49 centimeter (cm) depth range averaged 17.8 and 28.3 kilopascals (kPa) for undisturbed soil and for soil in the wheel track, respectively. An error while weighing soil samples, prevented the determination of moisture content. The maximum drawbar power on a wet soil surface follows the same pattern as on asphalt, but at a lower level.

Table 10. Maximum drawbar power[1] at zero percent DOD for each gear on wet soil.

Gear	Power, kW	Pull, kN	Efficiency, %	Slip, %
1	13.63	20.0	41.4	68.06
2	21.03	22.7	40.1	32.76
3	23.70	11.4	44.8	9.57

[1]Average of two tests.

Maximum drawbar power of 31.3 kW was obtained at a speed of 1.7 m/s (Figure 31). It was not determined if the drawbar power curve declined after reaching a peak due to battery DOD (drawbar power and DOD increased together for the followed procedure) or as a natural interaction between increasing drawbar pull and decreasing speed. These tests were conducted with the speed control at maximum, so battery DOD could be expected to affect results. When two repeats were performed at maximum drawbar power beginning at zero percent DOD, the second repeat always developed less power, which indicated that battery DOD was having an effect. After reaching a peak of 76 percent at 2.5 m/s in second gear, efficiency decreased as speed decreased (Figure 31) because series-wound dc motors are less efficient at lower speeds (Vik, 1985). First and third gear drawbar power on asphalt peaked at 25.4 kW at 0.8 m/s and 32.0 kW at 2.6

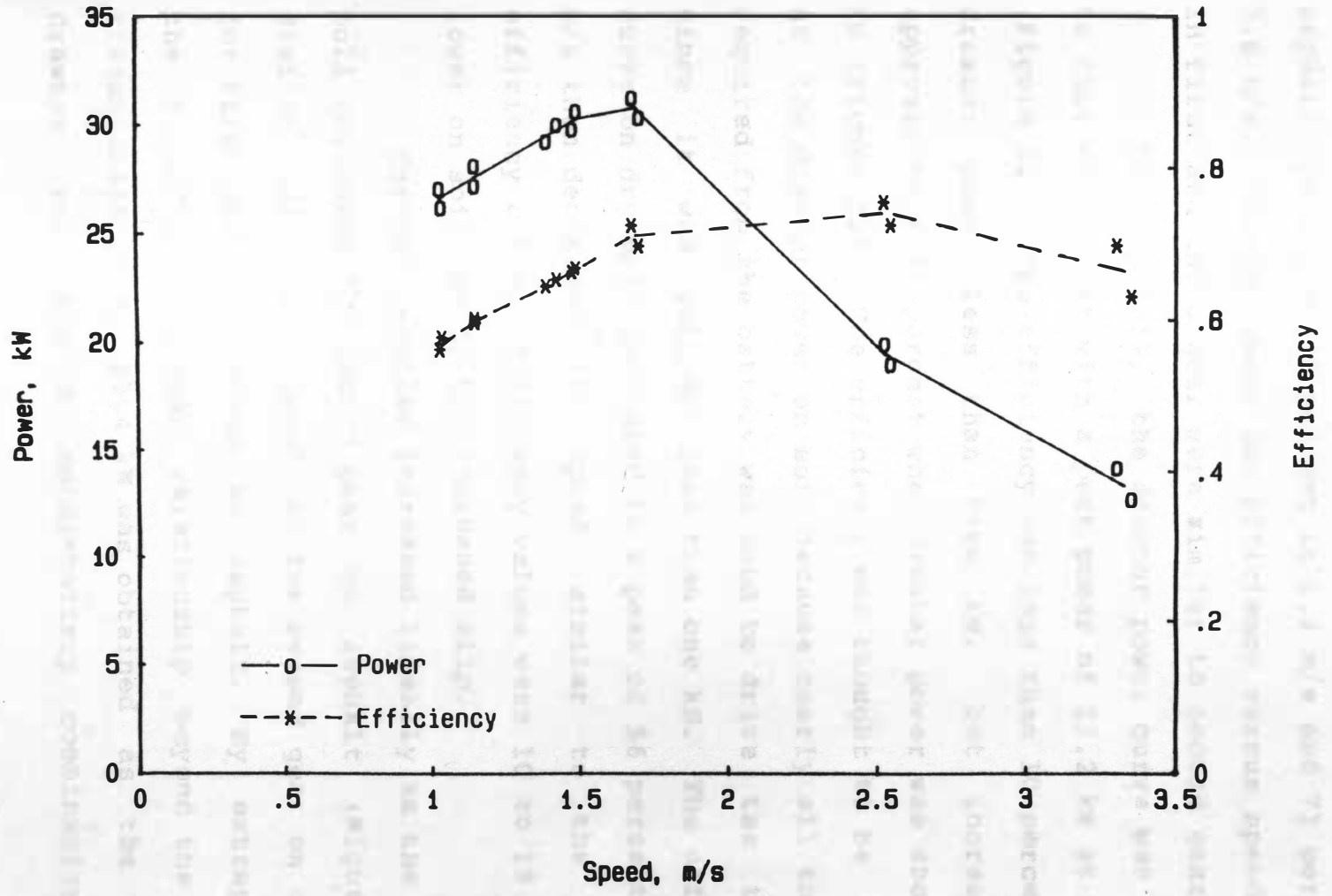

Figure 31. Power and efficiency at various speeds in second gear on asphalt.

m/s, respectively. First and third gear efficiency on asphalt peaked at 75 percent at 1.2 m/s and 73 percent at 3.6 m/s. Drawbar power and efficiency versus speed curves in first and third gear were similar to second gear.

On dry soil, the drawbar power curve was similar to that on asphalt with a peak power of 23.2 kW at 1.3 m/s (Figure 32). The efficiency was less than 10 percent for drawbar power less than five kW, but increased to approximately 50 percent when drawbar power was above five kW (Figure 32). The efficiency was thought to be so low at low drawbar power on soil because nearly all the power required from the battery was used to drive the tractor, since it was pulling less than one kN. The efficiency curve on dry soil increased to a peak of 56 percent at 1.6 m/s then decreased with speed, similar to the asphalt efficiency curve. Efficiency values were 10 to 15 percent lower on soil due to the increased slip.

Current required increased linearly as the drawbar pull increased for second gear on asphalt (Figure 33). Similar curves were developed for second gear on soil and for first and third gears on asphalt. By extrapolating the first gear linear relationship beyond the maximum transmission load, 53.4 kN was obtained as the maximum drawbar pull the dc motor-battery combination could

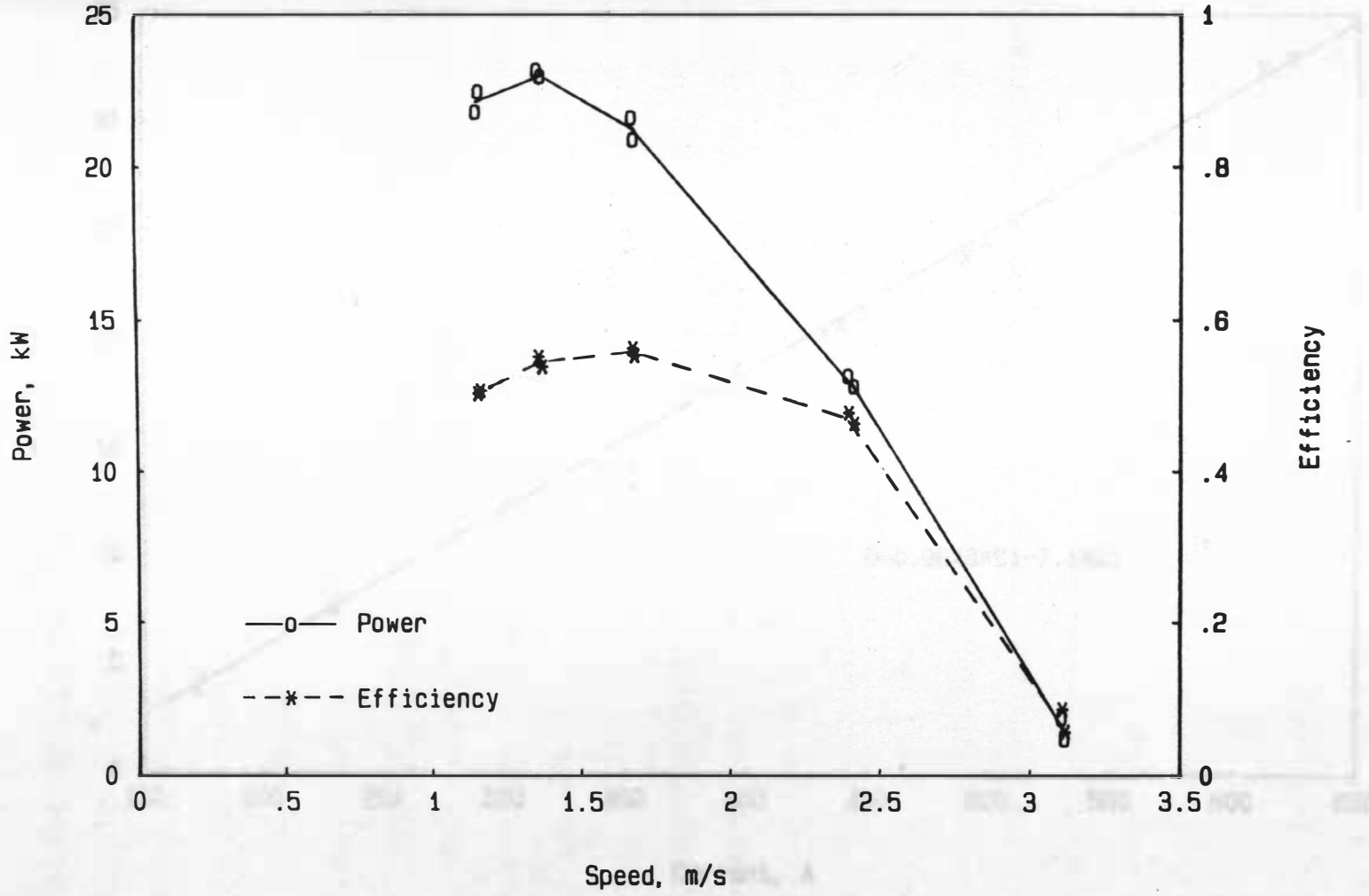

Figure 32. Power and efficiency at various speeds in second gear on dry soil.

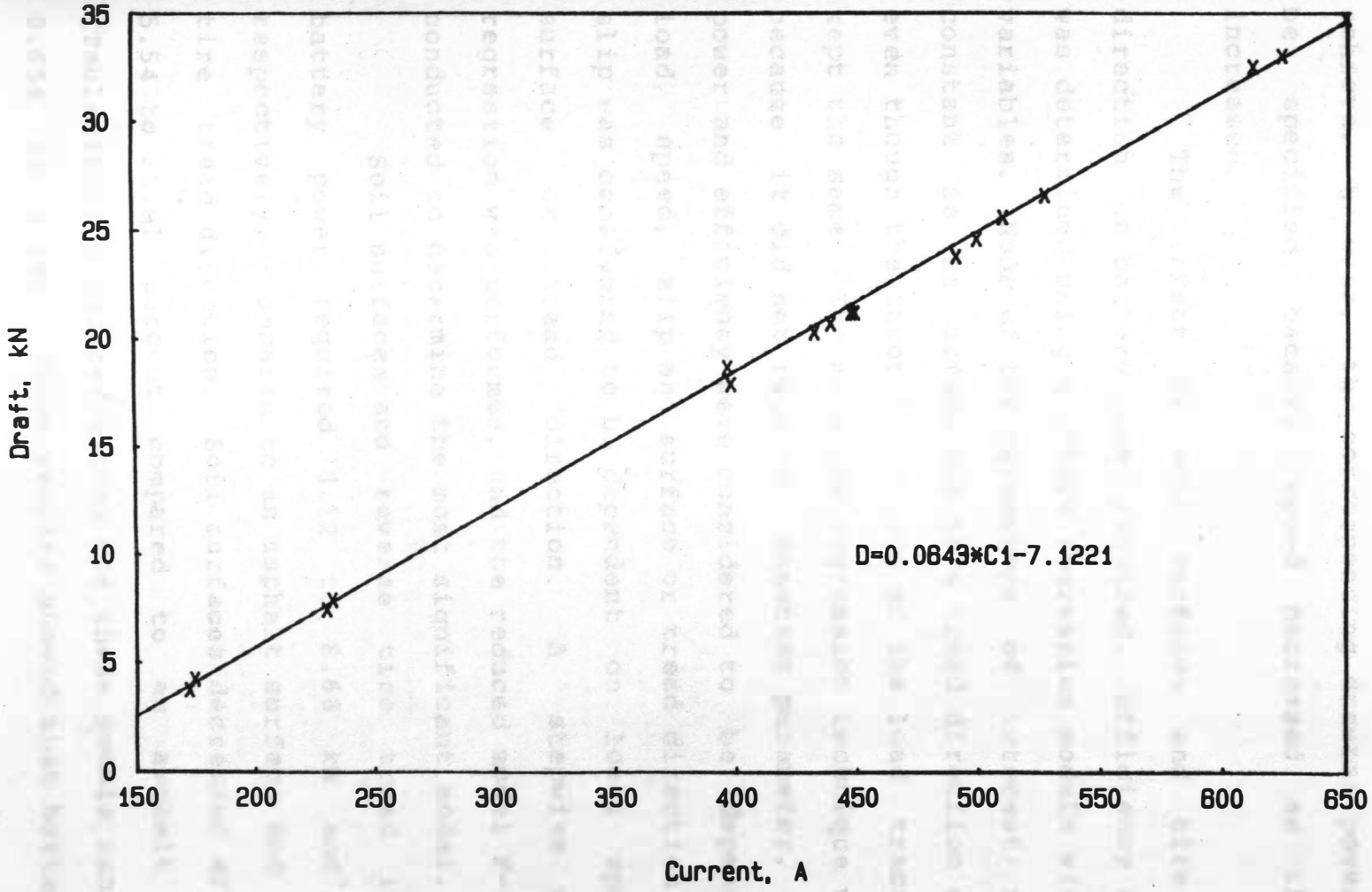

Figure 33. Battery current required for various drawbar pulls in second gear on asphalt.

achieve. However, the corresponding drawbar power cannot be specified because speed decreased as the load increased.

The effect of soil surfaces and tire tread direction on battery power required, efficiency and slip was determined using multiple regression models with dummy variables. None of the parameters of interest remained constant as the surface and tire tread direction changed, even though the throttle setting of the load tractor was kept the same. The multiple regression technique was used because it did not require a constant parameter. Battery power and efficiency were considered to be dependent on load, speed, slip and surface or tread direction, while slip was considered to be dependent on load, speed and surface or tread direction. A stepwise multiple regression was performed, and the reduced model F-test was conducted to determine the most significant model.

Soil surfaces and reverse tire tread increased battery power required 3.12 to 8.68 kW and 2.65 kW, respectively, compared to an asphalt surface and forward tire tread direction. Soil surfaces decreased efficiency 5.54 to 25.91 percent compared to an asphalt surface (Table 11). R-squared values for these models ranged from 0.654 to 0.999. These results showed that battery power

required increased and efficiency decreased as the standardized testing surface changed to a typical operating surface.

Table 11. Multiple regression equations demonstrating surface and tire tread direction effects on battery power required, efficiency and slip.

Dry soil versus asphalt in second gear			R^2
BP=0.72*L-5.97*GS+37.68			0.975
EFF=-1.79*L+3.09*SL-25.91*SU[1]+82.16			0.896
SL=-5.37*GS+15.13			0.932
Variable[2]		Minimum	Maximum
Battery power (BP), kW		19.98	47.78
Efficiency (EFF), percent		46.40	75.50
Load (L), kN		3.61	25.12
Slip (SL), percent		- 3.31	10.37
Speed, (GS), m/s		1.09	3.43

Moist soil versus asphalt in third gear			R^2
BP=1.04*L-12.42*GS-0.92*SL+3.12*SU[1]+74.78			0.988
EFF=0.51*L-2.43*SL-12.41*SU[1]+68.23			0.980
SL=-0.33*L-6.68*GS-1.55*SU[1]+26.45			0.935
Variable[2]		Minimum	Maximum
Battery power, kW		46.11	62.57
Efficiency, percent		46.90	68.00
Load, kN		7.84	16.71
Slip, percent		2.91	7.24
Speed, m/s		2.06	2.99

Table 11. (continued)

Forward versus reverse tire tread in third gear	R^2
$BP=1.06*L-8.15*GS-2.65*TD^3+62.90$	0.982
$EFF=1.04*L+10.66*GS+12.28$	0.654
$SL=-4.16*GS+15.07$	0.815

Variable[2]	Minimum	Maximum
Battery power, kW	44.73	62.57
Efficiency, percent	46.40	52.20
Load, kN	7.40	14.43
Slip, percent	1.99	6.81
Speed, m/s	2.06	2.91

[1]SU=1 when the surface is soil. SU=0 when the surface is asphalt.

[2]These were the ranges of the variables used to obtain the multiple regression model.

[3]TD=1 when forward tire tread direction was used. TD=0 when reverse tire tread direction was used.

Rolling resistance of EC-I averaged 2.06 kN for three trips over the asphalt test course at an average speed of 1.92 m/s compared to 1.99 kN for three trips at 1.47 m/s. Therefore, the mean rolling resistance on asphalt was 2.03 kN. Rolling resistance on dry soil was 5.86 kN at 1.87 m/s and 5.85 kN at 1.40 m/s for an average of 5.85 kN. The soil cone index in the 0 to 49 cm depth

range averaged 17.8 and 25.8 kPa for undisturbed soil and soil in the wheel track, respectively. Soil moisture content was not determined due to an error in weighing the wet soil samples.

Mean power required to drive EC-I at certain speeds in second gear with no load on asphalt was determined (Table 12). Reported speed was the average speed measured by the radar gun corrected to the timed speed, as discussed in the model development tests section. Battery power was calculated in the same manner as for the draft tests. Power required increased linearly with speed. A linear regression of power required versus speed produced the following equation (R^2=0.980):

$$BP=2.24*VA+2.74$$

where: BP=battery power, kW

VA=average velocity, m/s

This equation was developed for speeds from 0.69 to 3.03 m/s. These results indicated that driving EC-I at full speed in second gear (about 3 m/s) on a level surface with no load, consumed 9 to 10 kW resulting in an operating time per battery charge of three to four hours.

Table 12. Battery power requirements to operate EC-I in second gear with no load at different speeds.

Speed, m/s	Battery power, kW
0.69	4.27
1.49	5.50
1.57	6.85
2.61	8.84
3.02	9.73
3.03	9.11

Draft tests determined that the maximum drawbar power EC-I could develop was 34.73 kW on asphalt in third gear. However, the potential draft in first gear was 48 percent higher than the maximum draft the transmission and axles were designed to withstand (Walker, 1985). Therefore, the transmission and axles of electric tractors either need to be designed to withstand greater loads compared to conventional tractors or have an overload protection system. Soil surfaces were found to increase the battery power required 3.12 to 8.68 kW and decrease the efficiency 5.54 to 25.91 percent. Forward tire tread direction decreased battery power required 2.65 kW. In first, second and third gear on asphalt, peak drawbar powers were 25.4 kW at 0.8 m/s, 31.3 kW at 1.7 m/s and 32.0 kW at 2.6 m/s, respectively. Peak efficiencies on

asphalt in first, second and third gear were 75 percent at 1.2 m/s, 76 percent at 2.5 m/s and 73 percent at 3.6 m/s, respectively. The rolling resistance was 2.03 kN on asphalt contrasted with 5.85 kN on dry soil.

Field Tests

The power requirements for driving between tasks, moving snow, and loading silage and hay were determined. Power was calculated from instantaneous current and voltage. Power requirements changed suddenly and rapidly during operation (Figure 34). For these chore tasks, the average power required was low, varying from 9.29 to 12.73 kW, but the power requirement range was from 0 to 57.4 kW (Table 13). Tasks with these characteristics are ideal for an electric tractor that is highly efficient at low power levels and has the overload capacity of electric motors enabling it to meet peak power demands.

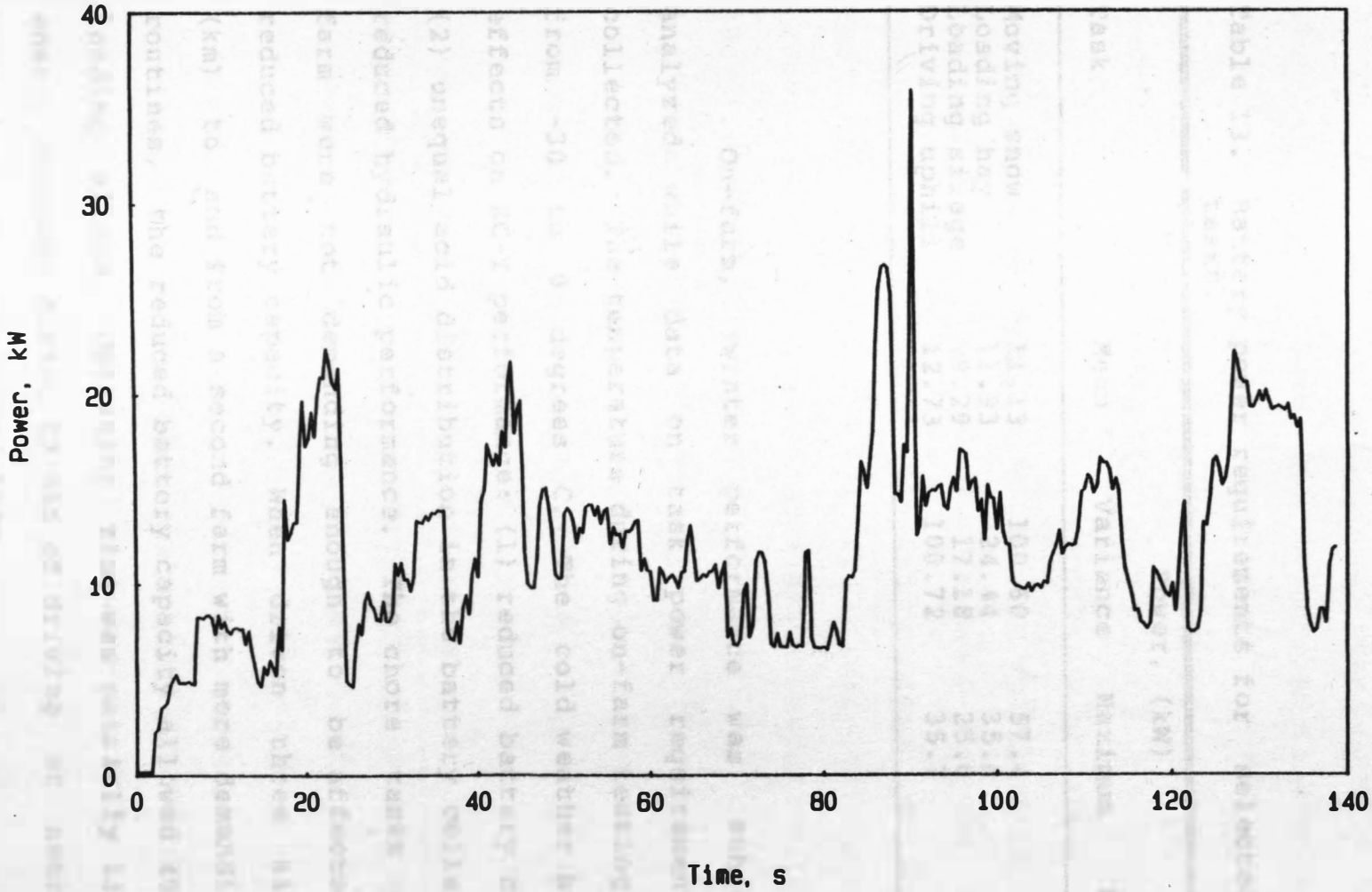

Figure 34. Battery power variations while loading hay.

Table 13. Battery power requirements for selected chore tasks.

Task	Power, (kW) Mean	Variance	Maximum	Minimum
Moving snow	11.13	100.60	57.4	3.2
Loading hay	11.93	24.44	35.8	0.2
Loading silage	9.29	17.18	25.0	1.6
Driving uphill	12.73	100.72	35.7	0.0

On-farm, winter performance was subjectively analyzed while data on task power requirements were collected. The temperature during on-farm testing ranged from -30 to 0 degrees C. The cold weather had three effects on EC-I performance: (1) reduced battery capacity, (2) unequal acid distribution in the battery cells and (3) reduced hydraulic performance. The chore tasks on this farm were not demanding enough to be affected by the reduced battery capacity. When driven three kilometers (km) to and from a second farm with more demanding chore routines, the reduced battery capacity allowed 45 min of loading silage. Operating time was partially limited by energy consumed during 10 min of driving at nearly full speed to reach the second farm.

When charging at -15 degrees C, the charging profile was the same and the no-load voltage indicated full charge, but the temperature corrected specific gravity indicated only one-half charge. In this state, EC-I was operated, and its performance indicated that it was fully charged, but more testing is needed to check this result. A possible explanation was that due to the low electrolyte temperature of zero degrees C during charge, the specific gravity did not equalize throughout the cell causing a low specific gravity value at the top of the cell. This unequal acid distribution would cause a reduction in battery life.

The hydraulics were stiff and did not perform well in the cold conditions. Although their performance improved with operation, at temperatures below -15 degrees C they never reached a satisfactory performance level. All these effects could be counteracted by storing and charging EC-I in a heated building. When snow was moved at temperatures from -15 to 0 degrees C with EC-I charged in a heated building maintained at 20 degrees C, none of these problems occurred. The tractor was able to move snow for three to four hours on a single charge.

Three safety problems were noted during on-farm tests: (1) coasting down hills, (2) pto always operating due to need for steering hydraulics, and (3) high voltage

at the motor controls accessible when the protective cover was removed. When driving downhill, the electric motor offered no retarding force so vehicle speed increased by coasting unless braked by shifting to reverse. In third gear, it was possible for the motor overspeed switch to shutdown both motors by overspeeding the traction motor while coasting downhill. This was a dangerous situation because with both motors off the vehicle had no steering and the only method of stopping the vehicle was the hand-operated parking brake. A control system that limits coasting would solve this problem.

The pto must be shielded better if it is to be operating whenever the tractor is operated. A farmer could get caught in the pto while hitching an implement to the tractor. Using one motor to operate the hydraulic pump and a second motor to power the pto, as discussed in the pto results section, would solve this problem.

The motor control covering can be removed easily, allowing unauthorized access. If the controls are connected to the battery, the battery terminal voltage of 128 volts is "live" at the controls. A possible solution to this problem is a pressure switch that opens when the control covering is removed so that the controls are not

"hot". These safety problems are unique, to the prototype EC-I and through design modification can be minimized or eliminated for farm EVs.

Model Development Tests

Establishment of Model Equations

The model development tests established multiple regression equations to predict energy use for standard segments of farm chore tasks. Battery power was predicted and energy use determined by multiplying power by time where battery power was expected to remain constant, that allowed more flexibility in the model. Data collected during five different cycles consisting of these standard segments were used to examine the model. A preliminary judgement was made on model utility based on goodness of model fit as cycle complexity increased.

Data from the loader tests were used to predict the energy required to operate the PTO/HYD motor at 800 r/min with no load. Loader tests at an electrolyte temperature of 29 degrees C and an ambient temperature of 24 degrees C were chosen because these temperatures were near the temperatures expected for the model examination cycles. Mean power required to operate the PTO/HYD motor

at 800 r/min with no load was 1732.4 W with a variance of 9264.2 (standard deviation of 96 W). Energy required for this segment was predicted by multiplying the mean power by time in the following equation:

$$E1=1732.4*T/1000$$

where: E1=energy for PTO/HYD motor operation at 800 r/min, kWh
T=time of operation, h

This equation was used to predict energy use when the PTO/HYD motor was operating during coasting, and traction motor enrgy use was zero.

Data from the six pto power levels used in the varying pto power cycle were used to predict the energy required for pto operation. Pto power and speed were determined to be the two main variables affecting the battery power required, so a multiple regression considered battery power as a function of pto power and speed. Using the reduced model F-test, pto power and speed were found to be the best predictors of battery power. The following regression equation (R^2=0.999), which was developed for pto power from 1.5 to 11.5 kW, was used to predict battery power required for pto operation:

$$BP1=1.221*PP+0.004*PS+1.445$$

where: BP1=battery power for pto operation segment, kW

PP=pto power, kW

PS=pto speed, r/min

The next step was to determine energy required by multiplying the battery power by the time of operation. Energy use by the pto was predicted with the following equation:

$$E2=BP1*T$$

where: E2=energy required for pto operation, kWh

Energy required to pull a constant load at a constant velocity was predicted using a multiple regression equation developed from tests conducted with three loads at four velocities. Load was measured by the drawbar dynamometer, and the speed was calculated from the time required to cover the draft course (91 m). The multiple regression routine considered the battery power required to be a function of the average load and average velocity during the test. Both load and velocity

significantly contributed to the following prediction equation (R^2=0.933):

$$BP2=2.248*L+4.671*VA-3.585$$

where: BP2=battery power for constant speed segment, kW
L=average load, kN
VA=average timed velocity, m/s

This equation was developed for loads from 2.62 to 9.84 kN and velocities from 0.84 to 3.66 m/s. Energy used was found by multiplying battery power by the operation time:

$$E3=BP2*T$$

where: E3=energy required for constant speed segment, kWh

Energy required to accelerate a load from rest to a final velocity was predicted by a multiple regression equation using data from acceleration tests. Because battery power was not constant during acceleration, energy was predicted directly from the multiple regression equation. Load, final speed reached and average acceleration were believed to be important factors for predicting energy required. The loads from constant speed

tests were used for the accelerations. Since the load varied during acceleration due to inertia (Figure 35), the mean load from constant velocity tests was used. Radar gun calibration indicated that readings at a constant velocity could vary as much as five percent, therefore, the acceleration was considered complete when three consecutive velocities were within five percent. The final velocity reached was the maximum velocity obtained during acceleration.

Acceleration varied considerably, as calculated by dividing the velocity difference by the time:

$$A=(VA2-VA1)/(T2-T1)$$

where: A=acceleration, m/s^2
VA2=velocity at second data point, m/s
VA1=velocity at first data point, m/s
T2=time of second data point, s
T1=time of first data point, s

Acceleration was found to increase to a peak at the beginning of an acceleration, and slowly decrease to zero as constant velocity was approached (Figure 36). The area under the acceleration versus time curve was expected to be an important factor affecting energy required, so this

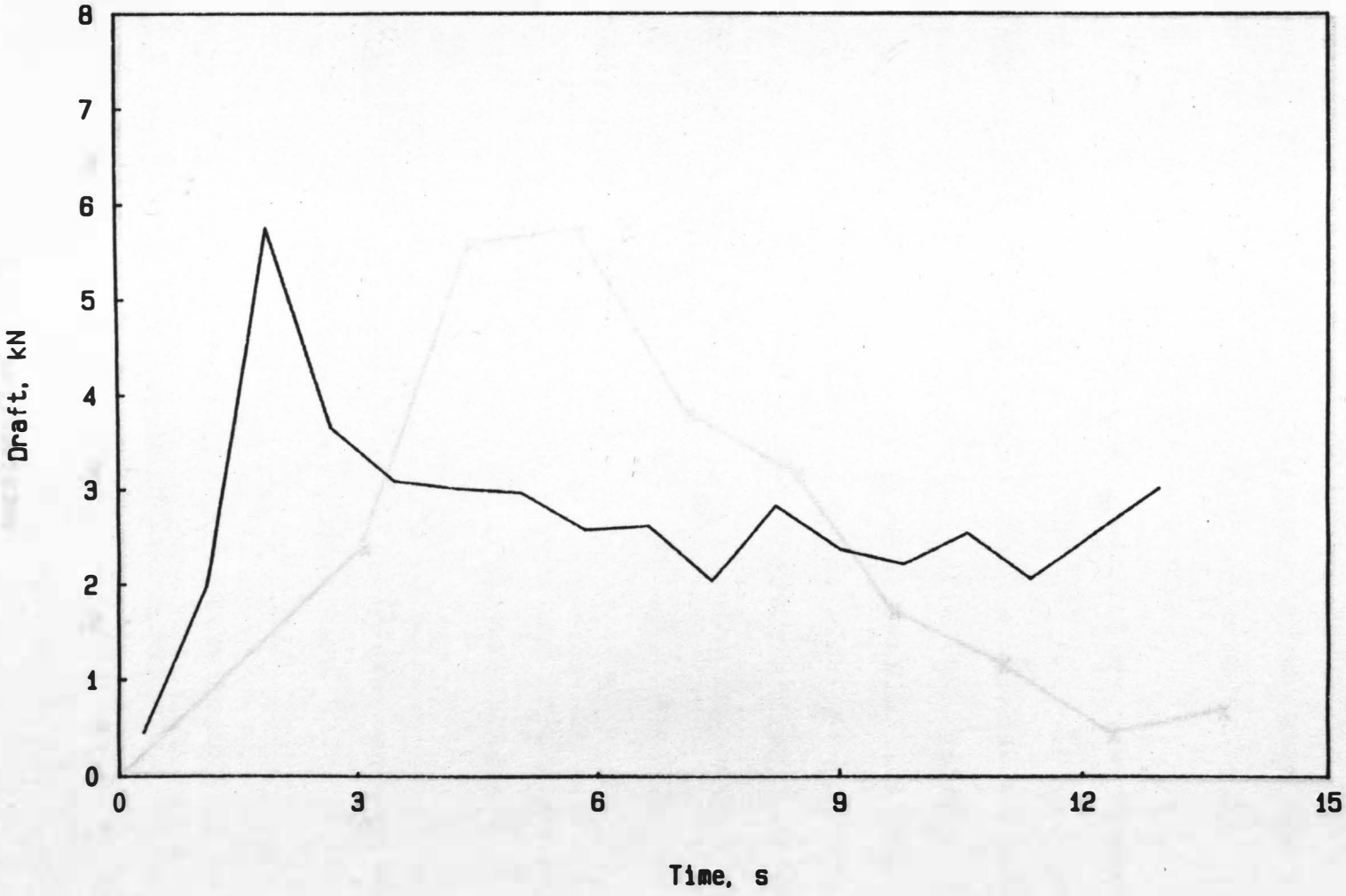

Figure 35. Drawbar draft changes during acceleration segment.

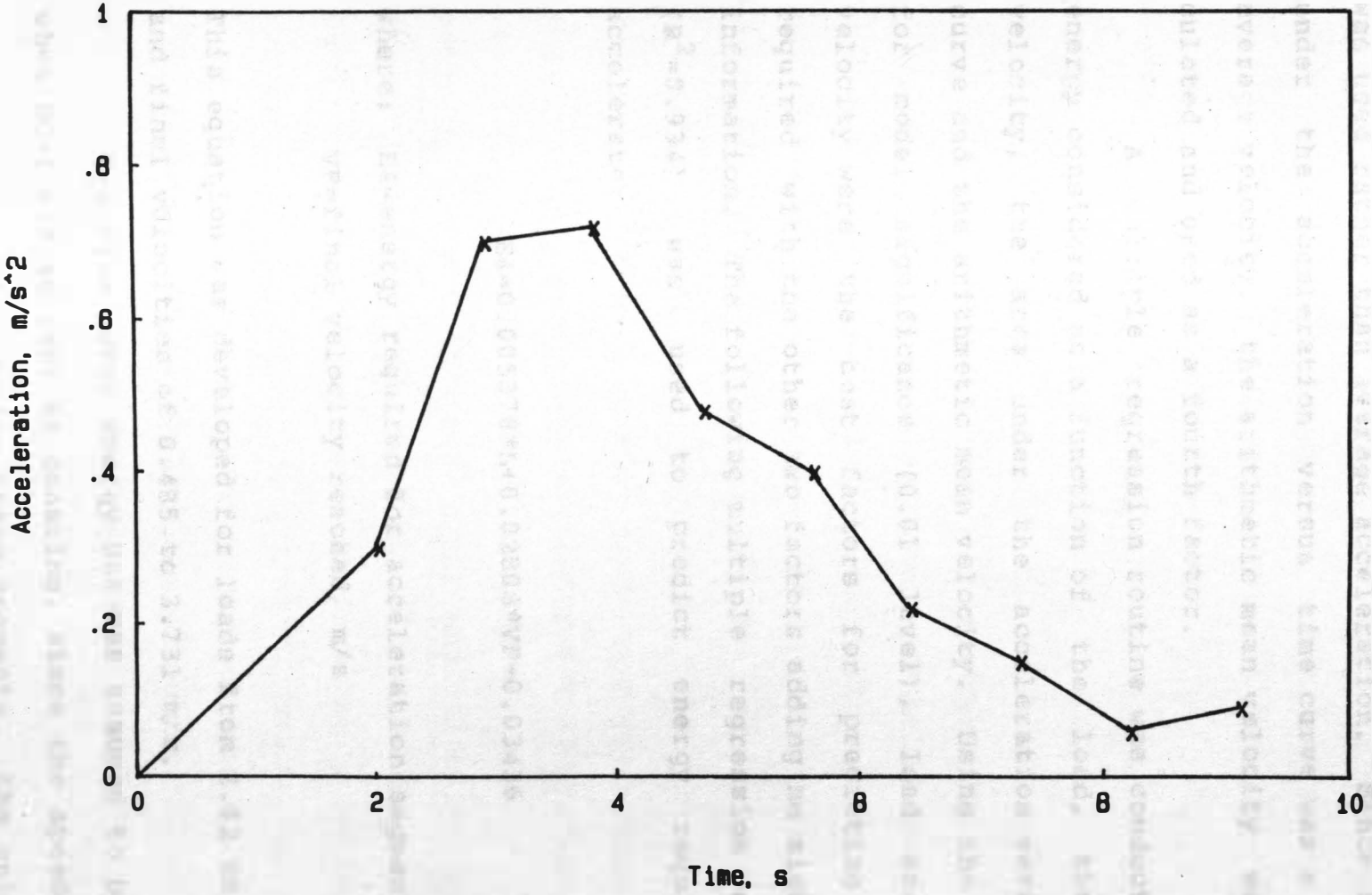

Figure 36. Acceleration changes during acceleration segment.

was used rather than average acceleration. Since the area under the acceleration versus time curve was a form of average velocity, the arithmetic mean velocity was calculated and used as a fourth factor.

A multiple regression routine was conducted with energy considered as a function of the load, the final velocity, the area under the acceleration versus time curve and the arithmetic mean velocity. Using the F-test for model significance (0.01 level), load and final velocity were the best factors for predicting energy required with the other two factors adding no significant information. The following multiple regression equation (R^2=0.934) was used to predict energy required to accelerate:

$$E4=0.005378*L+0.02808*VF-0.03436$$

where: E4=energy required for acceleration segment, kWh
VF=final velocity reached, m/s

This equation was developed for loads from 2.62 to 9.84 kN and final velocities of 0.485 to 3.731 m/s.

Traction motor energy use was assumed to be zero, when EC-I was at rest or coasting, since the speed control was in neutral. During these segments, the only energy

used operated the PTO/HYD motor at 800 r/min. The energy used to operate the PTO/HYD motor at 800 r/min was included in the prediction equations for the constant velocity and acceleration segments.

Evaluation of Model Performance

Standard cycles, with independent data to examine the model, were defined and data were collected for model examination after the prediction equations were developed. The data from each cycle were divided into segments using velocity and current criteria. The acceleration segment was defined using the same criteria that were used to define the segment for the prediction equation. The parameters required to predict energy for that segment were calculated from the data collected. For a constant velocity segment, the mean draft and velocity parameters required in the prediction equation were calculated from data collected during the cycle. An adjustment was required in the average velocity during the constant velocity segments due to radar gun inaccuracy. This inaccuracy may have been caused by tractor vibrations during use. A linear regression (R^2=0.997) was used to predict the timed velocity given radar gun velocity:

$$VA=0.9412*VR-0.0014$$

where: VA=timed velocity over course, m/s

VR=radar gun velocity over course, m/s

The acceleration segment used the mean draft from the constant velocity segment in the prediction equation and the final velocity reached. No method of energy use prediction was found for one segment. This segment (creep) occurred when EC-I was started from rest during a cycle, and the operator had to creep ahead to prevent a jolt when accelerating by tightening the load cable.

When the energy for each segment had been predicted, the actual energy for each segment was calculated by using Simpson's Rule to find the area under the power versus time curve. Segments without an even number of intervals had one data point either added or subtracted depending on which affected the results least. Actual energy for the cycle was found by using Simpson's Rule for the entire power versus time curve, and subtracting the energy used for the creep segment. Percent error was calculated using the following equation:

$$ER=((PE-AE)/AE)*100$$

where: ER=error, percent

PE=predicted energy, Wh

AE=actual energy, Wh

The model predicted the energy use within 6.8 percent, 240.7 Wh compared to the actual energy use of 258.3 Wh (Table 14) for cycle I (Table 3). The percent error for each segment was higher due to the small amount of actual energy used in each segment (Figure 37). The assumption of zero energy for coasting and resting was verified as the actual energy for the resting segments was nearly zero and for the coasting segment was only slightly greater than that predicted as required for PTO/HYD motor operation. All acceleration and constant speed segments had a predicted energy use within 15 Wh of the actual.

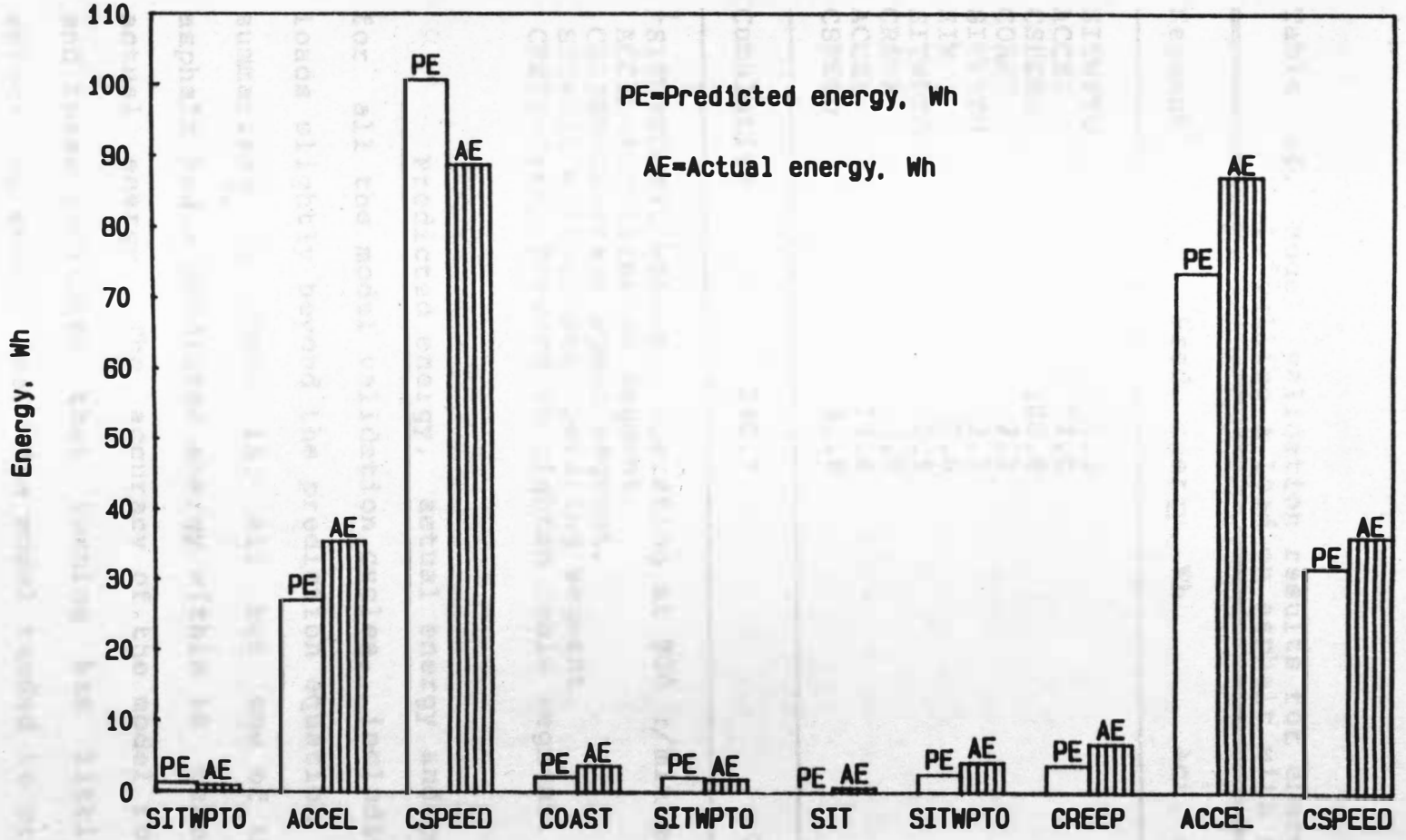

Figure 37. Comparison of predicted versus actual energy for each segment of energy use cycle I, pulling a load on asphalt.

Table 14. Model validation results for energy use cycle I, pulling a load on asphalt with no turns.

Segment[1]	Pred. energy, Wh	Act. energy, Wh
SITWPTO	1.3	0.9
ACCEL	27.0	35.4
CSPEED	100.6	88.7
COAST	2.1	3.7
SITWPTO	2.1	1.8
SIT	0.0	0.6
SITWPTO	2.5	4.2
CREEP	3.8	6.8
ACCEL	73.6	87.1
CSPEED	31.6	36.0
Cumulative	240.7	258.3

[1]SITWPTO=Sit with pto operating at 800 r/min segment.
ACCEL=Acceleration segment.
CSPEED=Constant speed segment.
SIT=Sit without pto operating segment.
CREEP=Creep forward to tighten cable segment.

Predicted energy, actual energy and percent error for all the model validation cycles, including four with loads slightly beyond the prediction equation range, are summarized in Table 15. All but one of the cycles on asphalt had a predicted energy within 10 percent of the actual energy. The accuracy of the model for cycles two and three indicates that turning has little, if any, effect on energy use. The model tended to predict energy

use low more often than high. The cycle unloading the feed wagon on a gravel surface was not analyzed due to instrumentation problems. Cycles on dirt were out of the range of the prediction equations, and the model was not adequate to predict the energy use on a dirt surface.

Table 15. Total predicted compared to actual energy used for all model validation cycles.

Cycle[1]	Load[2]	Total pred. energy, Wh	Total act. energy, Wh	Error, %
I	1	171.0	184.2	- 7.2
I	1	198.5	215.1	- 7.7
I	2	240.7	258.3	- 6.8
I	2	231.3	276.2	-16.2
II	1	568.3	518.8	9.5
II	1	577.4	552.5	4.5
II	2	664.6	710.3	- 6.4
II	2	668.4	685.1	- 2.4
III	1	503.6	472.7	6.5
III	1	477.9	447.9	6.7
III	2	547.6	547.2	0.1
III	2	581.0	582.1	- 0.2
IV	3	53.8	186.9	-71.2
IV	4	64.2	180.1	-64.3

[1] See tables 3 to 7 for cycle definitions.
[2] Load one was one tractor towed.
Load two was two tractors towed.
Load three was a partially loaded feed wagon.
Load four was a partially loaded feed wagon.

This work established the energy use model as a valid concept, and indicated that a model can accurately predict energy use for certain task segments. For the model to become a valuable tool, it must be extended to include different surfaces and more segments.

Suggestions for Future Research

This research has suggested the following areas for future research:

1. Design an electronic control system to prevent coasting.
2. Extend the energy use model to soil surfaces with wider ranges for the prediction equations.
3. Conduct extensive on-farm tests.
4. Perform an economic analysis utilizing performance results.
5. Continue to explore the effect of DOD on performance.
6. Conduct periodic capacity tests to examine changes in battery capacity as the battery ages.

The design of an electronic control system is suggested as a top priority to improve vehicle safety. The extension of the energy use model is needed to better relate the model to operating conditions, thereby, increasing its value for design. Extensive on-farm tests would complement the controlled test information presented in this thesis. To further explore the economic feasibility of an agricultural EV, economic analysis utilizing performance results would be valuable. The effect of DOD on performance and changes in battery capacity as the battery ages have been explored to a limited extent in this analysis, but need further definition.

SUMMARY AND CONCLUSIONS

A test procedure that quantifies performance capabilities has been devised for electric tractors and was used to determine the performance of EC-I. The test procedure consists of standardized component and vehicle testing; and subjective on-farm tests.

The maximum continuous pto power was 12.2 kW in the present configuration, and the maximum drawbar power was 34.73 kW in third gear. Loader tests indicated increasing temperatures from 3 to 24 degrees C caused current requirements to decrease 20 to 30 percent due to temperature effects on the vehicle components, rather than on the battery. The following pto and traction operating characteristics were demonstrated:

1. Pto power slowly decreased when the operator set the speed control and did not reset it.

2. The maximum continuous pto power of 12.2 kW drained the battery in 1.5 to 2 h.

3. The SCR must be cooled to maintain maximum continuous power output.

4. Potential problems for on-farm pto use at high power included: (a) SCR overheating, (b) electrolyte overheating, (c) possible motor shutdown due to thermal overload and (d) reduced power at low SoC.

5. Peak drawbar powers on asphalt in first, second and third gear were 25.4 kW at 0.8 m/s, 31.3 kW at 1.7 m/s and 32.0 kW at 2.6 m/s, respectively.

6. Peak efficiencies on asphalt in first, second and third gear were 75 percent at 1.2 m/s, 76 percent at 2.5 m/s and 73 percent at 3.6 m/s, respectively.

7. Soil surfaces increased battery power required 3.12 to 8.68 kW compared to asphalt and dry soil.

8. Forward tire tread decreased battery power required 2.65 kW compared to reverse tread.

9. EC-I had an average rolling resistance of 2.03 and 5.85 kN on asphalt and dry soil, respectively.

A model has been developed and examined that predicts EC-I energy use within 10 percent for standardized farm chore tasks. Developed for second gear, the model predicts energy for standard task segments on asphalt and adds the results for each segment to obtain energy required for the task. The model was unable to accurately predict energy use on soil and needs to be extended to predict energy use for chore tasks.

Specific design improvements recommended for EC-I included:

1. The pto and hydraulic pump should be powered by separate motors.

2. The transmission and axles should be designed to withstand the maximum torque output by the dc motor-battery combination, or an overload protection system should be installed.

3. An electronic control system needs to be added to prevent unwanted coasting.

4. A conventional brake should be added for safety in emergency situations.

5. A switch should automatically open when the controller covering is removed to prevent high voltage shocks.

REFERENCES

Agricultural Engineers Standards. 1985. Agricultural Tractor Test Code (S209.5). ASAE, St. Joseph, MI 49085.

Agricultural Engineers Standards. 1985. Agricultural Machinery Management Data (D230.4). ASAE, St. Joseph, MI 49085.

Alcock, R. 1983. Battery powered vehicles for field work. TRANSACTIONS of the ASAE 26(1):10-13.

Alcock, R. 1984. F.O. Butler Faculty Development Award Report on Travel to United Kingdom. Agricultural Engineering Department, South Dakota State University, Brookings, SD 57007.

Alcock, R.; N. Buck and H. Hughes. 1981. Electric vehicles: assessment of potential for south eastern United States farm operations. ASAE Paper No. 81-1548, ASAE, St. Joseph, MI 49085.

Bandy, S.M.; W.A. Babcz; J. Grogan; S.W. Searcy and B.A. Stout. 1985. Monitoring tractor performance with a three-point dynamometer and an on-board microcomputer. ASAE Paper No. 85-1078, ASAE, St. Joseph, MI 49085.

Berg, M.R.; M.J. Converse and D.H. Hill. 1984. Electric vehicles in commercial sectors applications. Electric Power Research Institute project 1569-3. Institute for Social Research. The University of Michigan.

Bish, J.R. and G.P. Tietmeyer. 1983. Electric vehicle field test experience. IEEE Transactions of Vehicle Technology 32(1):81-89.

Blickwedel, T.W. and C.G. Hand. 1983. Field testing of electric vehicle batteries. Proceedings of the EV Expo 83, EVC Paper No. 8314, Electric Vehicle Development Council, Washington, D.C. 20011.

Blom, W.G.; C.E. Dare; D.W. Deane; L.L. Ogborn and A.T. McDonald. 1981. High speed digital data acquisition system for electric vehicles. Proceedings of the EV Expo 81, EVC Paper No. 8125, Electric Vehicle Development Council, Washington, D.C. 20011.

Booth, G.D. 1977. Some aspects of modeling. Unpublished seminar presentation at the University of Missouri, Columbia in April, 1977.

Brodbeck, K. 1985. Personal telephone interview with K. Brodbeck, Engineer. Firestone Tire Company, Akron, OH 44317.

Bryant, J. 1983. Recommended changes to SAE J227a electric vehicle test procedure for the SAE electrical vehicle technical committee. Jet Propulsion Laboratory, California Institute of Technology, Pasadena, CA.

Carter, C.L. and D.E. Todd. 1983. Electric vehicle test facility capabilities. Proceedings of the EV Expo 83, EVC Paper No. 8320, Electric Vehicle Development Council, Washington, D.C. 20011.

Christianson, L.L.; R. Alcock; G. Jahns and K.L. Seshasai. 1985. Electric vehicles in agriculture. Vol. V, Ch. XI, Energy in Agriculture Handbook. Farm Electrification and Electricity Use Systems (in editing).

Ewashinka, J.G. 1984. Results of electric vehicle propulsion system performance on lead-acid battery systems. NASA Tech Memo-83657. Lewis Research Center, Cleveland, OH.

Fenton, J.F. and J.M. Olsen. 1983. Testing of electric cars as a function of lead-acid battery life. Proceedings of the EV Expo 83, EVC Paper No. 8314, Electric Vehicle Development Council, Washington, D.C. 20011.

GBC-Industrial Battery Service Manual. 1980. Product Manual. General Battery Corporation. Reading, PA 19603.

Giese, R.F. and W.J. Walsh. 1983. A least-cost method for prioritizing battery research. In: Batteries for Electric Vehicles--Research, Development, Testing, and Evaluation. Paper no. 830221 SAE SP-541, SAE, Warrendale, PA 15096.

Green, M.K.; B.A. Stout and S.W. Searcy. 1983. Instrumentaion package for monitoring tractor performance. ASAE Paper No. 83-1562, ASAE, St. Joseph, MI 49085.

Grevis-James, I.W.; D.R. DeVoe; P.D. Bloome, D.G. Batchelder and B.W. Lambert. Microcomputer-based data acquisition for tractors. TRANSACTIONS of the ASAE 26(3):692-695.

Hamilton, W.F. and O.M. Bevilacqua. 1985. Analysis of specifications for an electric fleet van. SAE Paper No. 850224, SAE, Warrendale, PA 15096.

Helder, D. 1985. Control and instrumentation for an electric farm tractor. Unpublished M.S. Thesis, South Dakota State University, Brookings, SD 57007.

Hewitt, R. and J. Bryant. 1982. Testing of the Eagle-Picher nickel-iron, the Globe ISOA lead-acid, and the Westinghouse nickel-iron battery subsystems in a electric vehicle environment. Prepared by Jet Propulsion Laboratory for U.S. Department of Energy, Washington, D.C. 20011.

Hornstra, F. 1985. Personal telephone interview with F. Hornstra, Manager. National Battery Test Laboratory, Chemical Engineering Division, Argonne National Laboratory, Argonne, IL 60439.

Hornstra F. and N.P. Yao. 1982. Standard test procedures for electric vehicle batteries at the national battery test laboratory. In: Developments in Electric and Hybrid Vehicles, SAE, Warrendale, PA 15096.

Hunt, D. 1977. FARM POWER AND MACHINERY MANAGEMENT. Iowa State University Press, Ames, IA.

Johnson, C.E. and W.B. Voorhees. 1979. A force dynamometer for three-point hitches. TRANSACTIONS of the ASAE 22(2):226-228, 232.

JPL. 1981. Electric vehicle test report Cuttler-Hammer corvette. Prepared by Jet Propulsion Laboratory for U.S. Department of Energy, Washington, D.C. 20011.

Kalhammer, F.; J. Mader and O. Bevilacqua. 1984. Electric vehicle R+D activities at the Electric Power Research Institute. Proceedings, Seventh International Electric Vehicle Symposium, Paris, France.

Latif, N. 1985. Vehicle configuration design for a battery-powered chore tractor including human factors considerations. Unpublished M.S. Thesis, South Dakota State University, Brookings, SD 57007.

Leviticus, L.F. 1985. Personal telephone interview with L.F. Leviticus, Engineer. Nebraska Tractor Testing Laboratory, University of Nebraska, Lincoln, NE 68583.

Marsh, K., ed. 1981. Battery book one: lead acid traction batteries. Curtis Instruments, Inc., Mt. Kisco, NY 10549.

Marte, J. and J. Bryant. 1983. Electric vehicle chassis dynamometer test methods at JPL and their correlation to track tests. Prepared by Jet Propulsion Laboratory for U.S. Department of Energy, Washington, D.C. 20011.

McKinney, B.L.; G.L. Wierschen and E.N. Mrotek. 1983. Thermal management of lead-acid batteries for electric vehicles. Proceedings, 1983 SAE International Congress and Exposition, Detroit, MI.

Menga, P.; V. Arcidiacono; S. Cattaneo; G. Drera and F. Russo. 1981. ENEL research on EVs: assessment scheme and instrumentation for on-board data acquisition. Proceedings of the EV Expo 81, EVC Paper No. 8160, Electric Vehicle Development Council, Washington, D.C. 20011.

Miller, E.G. 1984. Personal telephone interview with E.G. Miller, National Service Manager. Motive Power Products, General Battery Corporation, Reading, PA 19603.

National Electric Manufacturers Association Standards. 1983. Cycle life testing of lead-acid industrial storage batteries for motive power service (IB 3). NEMA, Washington D.C. 20037.

National Electric Manufacturers Association Standards. 1982. Definitions and precautionary labels for lead-acid industrial storage batteries (IB 1). NEMA Washington, D.C. 20037.

National Electric Manufacturers Association Standards. 1974. Determination of capacity of lead-acid industrial storage batteries for motive power service (IB 2) (R 1980). NEMA, Washington, D.C. 20037.

National Electric Manufacturers Association Standards. 1984. Safety recommendations for lead-acid industrial storage batteries used for motive power service (IB 10). NEMA, Washington, D.C. 20037.

Nowak, D. 1983. Methods to improve electric vehicle performance at low temperatures, based on an analysis of battery tests. Proceedings of the EV Expo 83, EVC Paper No. 8338, Electric Vehicle Development Council, Washington, D.C. 20011.

Nowak, D. 1981. User testing of electric vehicles at the University of Alabama in Huntsville. Proceedings of the EV Expo 81, EVC Paper No. 8122, Electric Vehicle Development Council, Washington, D.C. 20011.

Perone, S.P. and W.C. Spindler. 1984. Battery lifetime prediction by pattern recognition. Application to lead-acid battery life-cycling data. Journal of Power Sources. 13(1984):23-38.

Ponsford, J.M. 1979. Life testing of lead-acid batteries for electric vehicle duties. SAE Paper No. 790157. SAE, Warrendale, PA 15096.

Popeck, R.A.; J.M. Olsen and M.L. Veillette. 1983. Improve EV reliability through battery discharge tests. Proceedings of the EV Expo 83, EVC Paper No. 8330, Electric Vehicle Development Council, Washington, D.C. 20011.

Reese, R. 1983. EV battery charger testing in the EPRI/TVA program. Proceedings of the EV Expo 83, EVC Paper No. 8339, Electric Vehicle Development Council, Washington, D.C. 20011.

Resen, M.; P. Caulkins and L.L. Christianson. 1981. Electric vehicles: assessment of potential for north central regional farm operations. ASAE Paper No. 81-1547, ASAE, St. Joseph, MI 49085.

Sampson, B. 1985. Personal telephone interview with B. Sampson, Engineer. Nebraska Tractor Testing Laboratory, University of Nebraska, Lincoln, NE 68583.

Schober, W. 1984. Personal telephone interview with W. Schober, Chief Engineer. Hertner Division, General Battery Corporation, Cleveland, OH 44111.

Society of Automotive Engineers Standards. 1976. Electric vehicle test procedure (J227a). SAE, Warrendale, PA 15096.

Stange, K.; L.L. Christianson; B. Thoreson; B. Vik and R. Alcock. 1982. Portable instrumentation package for measuring tractor work. ASAE Paper No. 82-5516, ASAE, St. Joseph, MI 49085.

Tompkins, F.D.; W.E. Hart; R.S. Freeland; J.B. Wilkerson and L.R. Wilhelm. 1985. Comparison of tractor ground speed measurement techniques. ASAE Paper No. 85-1082, ASAE, St. Joseph, MI 49085.

Tompkins, F.D. and L.R. Wilhelm. 1982. Microcomputer-based, tractor data acquisition system. TRANSACTIONS of the ASAE 25(6):1540-1543.

Unnewehr, L.E. and S.A. Nasar. 1982. ELECTRIC VEHICLE TECHNOLOGY. John Wiley and Sons. New York, NY 65211.

USDOD. 1963. Test and inspection of trucks, lift, fork. Military Standard MIL-STD-268C. Department of Defense, Washington, D.C.

Vik, B. 1985. The electric choremaster: design and performance of an agricultural electric tractor. Unpublished M.S. Thesis, South Dakota State University, Brookings, SD 57007.

Vinal, G.W. 1955. STORAGE BATTERIES. John Wiley and Sons, New York, NY 65211.

Vincent, C.A.; F. Bonino; M. Lazzari and B. Scrosati. 1984. MODERN BATTERIES AN INTRODUCTION TO ELECTROCHEMICAL POWER SOURCES. Edward Arnold Ltd., London.

Vivian, H.C. and J.A. Bryant. 1984. Performance of the Lester battery charger in electric vehicles. Prepared by Jet Propulsion Laboratory for U.S. Department of Energy, Washington, D.C. 20011.

Von Courbiere, R. and F.H. Klein. 1983. Requirements for traction batteries for sufficient application in electric road vehicles and ways for solutions. Proceedings of the EV Expo 83, EVC Paper No. 8304, Electric Vehicle Development Council, Washington, D.C. 20011.

Walker, K. 1985. Personal telephone interview with K. Walker, Design Engineer. Versatile Manufacturing Co. Ltd., Winnipeg, Manitoba, Canada R3T1T3.

APPENDICES

Appendix A:
List of Abbreviations

Abbreviation	Explanation
A	ampere
ac	alternating current
Ah	ampere-hour
ANL	Argonne National Laboratory
ASAE	American Society of Agricultural Enginneers
C	Celsius
cm	centimeter
dc	direct current
DOD	depth-of-discharge
EC-I	Electric Choremaster I
EPRI	Electric Power Research Institute
EV	electric vehicle
EVDC	Electric Vehicle Development Corporation
FUDS	Federal Urban Driving Schedule
g	gram
GBC	General Battery Corporation
h	hours
JPL	Jet Propulsion Laboratory
kg	kilogram
km	kilometer
kN	kilonewton
kPa	kilopascal
kW	kilowatt

Abbreviation	Explanation
kWh	kilowatt-hour
m	meter
min	minute
ml	milliliter
m/s	meter per second
mV	millivolt
NBTL	National Battery Testing Laboratory
NEMA	National Electrical Manufacturers Association
Nm	newton-meter
NRECA	National Rural Electric Cooperative Association
pto	power take-off
PTO/HYD	pto and hydraulic motor on Electric Choremaster I
r/min	revolutions per minute
rms	root mean square
s	second
SAE	Society of Automotive Engineers
SCR	silicon-controlled-rectifier
SDSU	South Dakota State University
SoC	state-of-charge
TVA	Tennessee Valley Authority
V	volt
Wh	watt-hour

Appendix B:

List of Symbols

Symbol	Explanation	Units
A	acceleration	m/s^2
ABP	average battery power over course	kW
ACE	total ac energy to charger	kW
ADJT	adjusted tachometer reading	r/min
AE	actual energy	Wh
BP	instantaneous battery power	kW
BP1	battery power for pto operation segment	kW
BP2	battery power for constant speed segment	kW
Ct	five-hour rate battery capacity at t degrees C	Ah
C1	average battery current over course	A
C30	five-hour rate battery capacity at 30 degrees C	Ah
D	draft	kN
DBD	average drawbar draft over course	kN
DBP	average drawbar power over course	kW
DCD	total dc energy discharged from battery	kWh
DCE	total dc energy to battery	kWh
DOD	depth-of-discharge	percent
EA	total energy available (capacity) at a specified rate	kWh

Symbol	Explanation	Units
ED	energy discharged at a specified rate	kWh
EFF	efficiency	percent
EI	strain gage bridge power supply	V
EO	strain gage bridge output	V
ER	error	percent
E1	energy for PTO/HYD motor operation at 800 r/min	kWh
E2	energy required for pto operation	kWh
E3	energy required for constant speed segment	kWh
E4	energy required for acceleration segment	kWh
GR	gear reduction from traction motor to wheel	dimensionless
GS	speed	m/s
L	average load	kN
NR	number of wheel revolutions	dimensionless
P	power	W, kW
PE	predicted energy	Wh
PP	instantaneous pto power	kW
PS	pto rotational speed	r/min
PT	pto torque	Nm
RPM	rotational speed of traction motor	r/min

Symbol	Explanation	Units
RR	average rolling radius of the four wheels	m
SE	weight of syringe empty	g
SF	weight of syringe and 10 ml of electrolyte	g
SL	average slip over course	percent
SP	specific gravity	dimensionless
SW	weight of syringe and 10 ml of water at 25 degrees C	g
T	time of operation	h
t	battery electrolyte temperature	degrees C
TACH	original tachometer reading	r/min
TT	time to traverse course	s
T1	time of first data point	s
T2	time of second data point	s
V	voltage read by voltmeter or multimeter	V
VA	average timed velocity over course	m/s
VF	final velocity reached	m/s
VR	radar gun velocity over course	m/s
VT	theoretical velocity over course	m/s
V1	average battery voltage over course	V
VA1	velocity at first data point	m/s
VA2	velocity at second data point	m/s

Appendix C:

Summary of Analysis Equations

Table C.1 Equations describing battery DOD and capacity changes with temperature.

1. Battery DOD

$$DOD=(ED/EA)*100$$

where: DOD=depth-of-discharge, percent
ED=energy discharged at a specified rate, kilowatt-hour (kWh)
EA=total energy available (capacity) at a specified rate, kWh

2. Capacity changes with temperature for temperatures below 30 degrees C

$$Ct=C30*(1+0.009(t-30))$$

where: C30=five-hour rate battery capacity at 30 degrees C, Ah
Ct=five-hour rate battery capacity at t degrees C, Ah
t=electrolyte temperature, degrees C

Table C.2 Instrumentation calibration equations.

1. Ac power transducer

$$P=19500*V$$

where: P=power, W
V=voltage read by multimeter, V

2. Torque transducer

Torque

$$PT=1074.4*(EO/EI)+2.1$$

where: PT=pto torque, Nm
EO=torque sensor strain gage bridge output, V
EI=torque sensor strain gage bridge power supply, V

Speed

$$PS=200*V$$

where: PS=pto rotational speed, r/min

3. Three-point hitch dynamometer

$$D=23.70*(EO/EI)$$

where: D=draft, kN
EO=drawbar dynamometer strain gage bridge output, V
EI=drawbar dynamometer strain gage bridge power supply, V

range: 0 to 50 kN

4. Radar gun

$$GS=2.02*V-0.01$$

where: GS=speed, m/s

range: 0.43 to 4.3 m/s

Table C.2 (continued)

5. Adjustment to EC-I tachometer measurement

$$ADJT=0.986*TACH+41.591 \qquad R^2=0.999$$

where: ADJT=adjusted tachometer reading, r/min
TACH=original tachometer reading, r/min

6. Adjustment to radar gun velocity measurement

$$VA=0.9412*VR-0.0014 \qquad R^2=0.997$$

where: VA=timed velocity over course, m/s
VR=radar gun velocity over course, m/s

Table C.3 Data analysis equations.

1. Specific gravity of electrolyte

$$SP=(SF-SE)/(SW-SE)$$

where: SP=specific gravity, dimensionless
SF=weight of the syringe and 10 ml of electrolyte, g
SE=weight of the syringe empty, g
SW=weight of the syringe and 10 ml of water at 25 degrees C, g

2. Charger efficiency

$$EFF=(DCE/ACE)*100$$

where: EFF=efficincy, percent
DCE=total dc energy to battery, kWh
ACE=total ac energy to charger, kWh

3. Battery efficiency

$$EFF=(DCD/DCE)*100$$

where: DCD=total dc energy discharged from battery, kWh

4. Pto efficiency

$$EFF=(PP/BP)*100$$

where: EFF=efficiency, percent
PP=instantaneous pto power, kW
BP=instantaneous battery power, kW

5. Drawbar power

$$DBP=DBD*VA$$

where: DBP=average drawbar power over course, kW
DBD=average drawbar draft over course, kN
VA=average timed velocity over course, m/s

Table C.3 (continued)

6. Velocity

$$VA=91/T1$$

where: T1=time to traverse the course, s

7. Drawbar efficiency

$$EFF=(DBP/ABP)*100$$

where: EFF=efficiency, percent
ABP=average battery power over course, kW

8. Battery power

$$ABP=(C1*V1)/1000$$

where: C1=average battery current over course, A
V1=average battery voltage over course, V

9. Slip

$$SL=1-(VA/VT)$$

where: SL=average slip over course, percent
VT=theoretical velocity over course, m/s

10. Theoretical velocity

$$VT=(NR*RR)/T1$$

where: NR=number of wheel revolutions, dimensionless
RR=average rolling radius of the four wheels, m
RR=3.46 m

Table C.3 (continued)

11. Number of wheel revolutions

$$NR=(RPM*T1)/(GR*60)$$

where: RPM=rotational speed of traction motor, r/min
GR=gear reduction from traction motor to wheel, dimensionless

12. Acceleration

$$A=(VA2-VA1)/(T2-T1)$$

where: A=acceleration, m/s^2
VA2=velocity at second data point, m/s
VA1=velocity at first data point, m/s
T2=time of second data point, s
T1=time of first data point, s

13. Percent error in model prediction of energy use

$$ER=((PE-AE)/AE)*100$$

where: ER=error, percent
PE=predicted energy, Wh
AE=actual energy, Wh

Table C.4 Prediction equations.

1. Specific gravity reduction versus time during a constant-current discharge at the six-hour rate.

$$SP=-0.00043*T+1.30047 \qquad R^2=0.983$$

where: SP=specific gravity, dimensionless
T=time, min

ranges: 0 to 389 min
1.125 to 1.295

2. Vehicle draft available at different levels of current flow.

$$D=0.0643*Cl-7.1221 \qquad R^2=0.999$$

where: D=draft, kN
Cl=current, A

ranges: 3.82 to 34.8 kN
170.4 to 649.5 A

3. Battery power required to operate in second gear with no load

$$BP=2.24*VA+2.74 \qquad R^2=0.980$$

where: BP=battery power, kW
VA=average velocity, m/s

ranges: 0.69 to 3.03 m/s
4.27 to 9.11 kW

Appendix D:

Summary of Model Energy Prediction Equations

Table D.1 Summary of prediction equations for energy use of standard task segments.

1. Energy to operate the PTO/HYD motor at 800 r/min

$$E1=1732.4*T/1000$$

where: E1=energy for PTO/HYD motor operation at 800 r/min, kWh
T=time of operation, hours

2. Energy to operate the pto at a constant power

$$BP1=1.221*PP+0.004*PS+1.445 \qquad R^2=0.999$$

where: BP1=battery power for pto operation segment, kW
PP=pto power, kW
PS=pto speed, r/min

range: 1.5 to 11.5 kW

energy: $E2=BP1*T$

where: E2=energy required for pto operation, kWh

3. Energy to pull a constant load at a constant speed

$$BP2=2.248*L+4.671*VA-3.585 \qquad R^2=0.933$$

where: BP2=battery power for constant speed segment, kW
L=average load, kN
VA=average timed velocity, m/s

ranges: 2.62 to 9.84 kN
0.84 to 3.66 m/s.

energy: $E3=BP2*T$

where: E3=energy required for constant speed segment, kWh

Table D.1 (continued)

4. Energy to accelerate a load to a final speed

$E4=0.005378*L+0.02808*VF-0.03436$ $\quad R^2=0.934$

where: E4=energy required for acceleration segment, kWh
VF=final velocity reached, m/s

ranges: 2.62 to 9.84 kN
0.485 to 3.731 m/s.

Appendix E:

Data File Locations on Disk

Test	Data File	Disk
capacity	CAP03-CAP05	ET-DATA-85-1
charger	CHR02-CHR06	ET-DATA-85-1 ET-DATA-85-2
loader	ET03#-ET15#	ET-DATA-85-2 ET-DATA-85-3 ET-DATA-85-4
pto	SPTO1-SPTO9	ET-DATA-85-4 ET-DATA-85-5
draft	ET18#-ET32#	ET-DATA-85-5 ET-DATA-85-6
	ET57#	ET-DATA-85-9
field	ET01#-ET02#	ET-DATA-85-2
	ET16#-ET17#	ET-DATA-85-4
model development	ET34#-ET35#	ET-DATA-85-6
	ET47#-ET53#	ET-DATA-85-7
model evaluation	ET54#-ET56#	ET-DATA-85-7
	ET58#-ET60#	ET-DATA-85-8
		ET-DATA-85-9

Test	Program name	Disk
capacity	BATCAP	ET-PROG-85
charger	CHRBAT	ET-PROG-85
loader	ETRACB	ET-PROG-85
pto	ETPTOT	ET-PROG-85
draft	ETRACB	ET-PROG-85
field	ETRACB	ET-PROG-85
model development	ETRACB	ET-PROG-85
model evaluation	ETRACB	ET-PROG-85